third international conference

materials science and nanotechnology

msn 2025

Ekaterinburg, Russia
24–27 August 2025

Ural Federal University
named after the first President of Russia B.N.Yeltsin

> Abstract book

УДК **538.9**
ББК 22.37
С-423

Materials Science and Nanotechnology (MSN-2025). Abstract Book of the Third International Conference (Ekaterinburg, August 24-27, 2025) Ekaterinburg, Ural Federal University, 2025 - 117 с.
ISBN 978-5-9500624-8-3

Organizers

School of Natural Sciences and Mathematics, Ural Federal University named after the first President of Russia B.N. Yeltsin (UrFU)
http://www.urfu.ru

Ural Center for Shared Use “Modern Nanotechnology” UrFU
http://nanocenter.urfu.ru

Labfer Ltd.
http://www.labfer.com

Ferroelectric Laboratory, INSM UrFU
http://labfer.ins.urfu.ru

General chair

Prof. Vladimir Shur

Organizing committee

Vladimir Kruzhaev, Ural Federal University, Ekaterinburg, Russia
Alexander Sigov, MIREA - Russian Technological University, Moscow, Russia
Nikolai Mushnikov, M. N. Mikheev Institute of Metal Physics, Ekaterinburg, Russia
Leonid Korotkov, Voronezh State Technical University, Voronezh, Russia
Sergey Vakhrushev, Ioffe Institute, Saint-Petersburg, Russia
Alexander Vtyurin, Kirensky Institute of Physics, Krasnoyarsk, Russia
Xiaoyong Wei, Xi'an Jiaotong University, Xi'an, China
Le He, Soochow University, Jiangsu, China

Local organizing committee

Prof. Vladimir Shur	Ekaterinburg, Russia
Mrs. Elena Pelegova	Ekaterinburg, Russia
Mrs. Yana Mayorova	Ekaterinburg, Russia
Dr. Ekaterina Shishkina	Ekaterinburg, Russia
Mr. Eduard Linker	Ekaterinburg, Russia
Dr. Andrei Ushakov	Ekaterinburg, Russia
Dr. Victoria Pryakhina	Ekaterinburg, Russia

ISBN 978-5-9500624-8-3
9 785950 062483

ББК 22.37

Ural Federal University
named after the first President
of Russia B.N. Yeltsin

MSN-2025 sponsors

Ostec-ArtTool Ltd.
https://www.arttool.ru

SINTEZ Ltd.
https://sintez-lab.ru/

MTEON Ltd.
https://www.mteon.ru/

Cryotrade Engineering Ltd.
https://www.cryotrade.ru/

Avesta Ltd.
https://avesta.ru/

TUTORIAL LECTURES

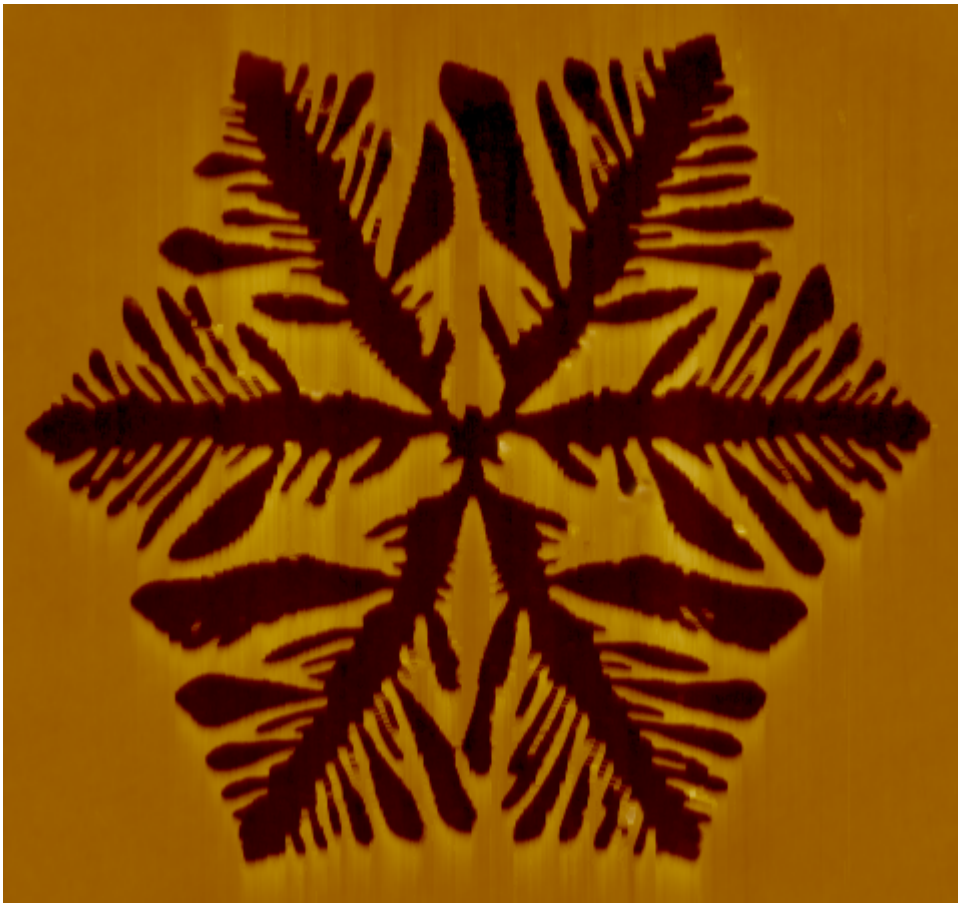

L1

Light-only domain switching in ferroelectrics

V.Ya. Shur

School of Natural Sciences and Mathematics, Ural Federal University, 620000 Ekaterinburg, Russia
vladimir.shur@urfu.ru

A brief review of the unexpected effect which contradicts the classical definition of the ferroelectrics will be presented. It looks impossible, but the ferroelectric domains can be switched without application of external electric field. The temperature change of any ferroelectric leads to appearance of the pyroelectric field. It was shown that fast local heating by pulse laser irradiation and subsequent cooling leads to the creation of the pyroelectric field which is strong enough for domain switching [1]. In this way the all-optical domain switching can be realized in ferroelectrics without application of the external electric field. This trend of domain engineering has been developed recently for manufacturing nonlinear photonic crystals (NPCs) with tailored periodical domain structure [1]. The created stable structures allow to realize frequency conversions of laser beams by means of quasi-phase matching, which opens opportunities for second harmonic generation and optical parametric oscillators with record efficiency [2]. The tailored periodical domain structures with modulation of the $\chi(2)$ sign can be produced in ferroelectrics. The most popular method for domain patterning is electrical field poling using the electrodes with proper geometry for field application [2] is inable to create 3D domain structures in the crystal bulk.

The all-optical poling of ferroelectric crystals by pulse laser irradiation is considered now as a promising alternative to electrical field poling. Two variants of these approaches have been realized using strongly absorbable and non-absorbable light. The first method was based on UV and far IR irradiation strongly absorbed in the surface layer. The absorbed energy stimulates nonuniform heating and subsequent cooling thus stimulating appearance of pyroelectric field strong enough for domain switching [3-5]. The spatial distribution of the pyroelectric field leads to domain nucleation only at the surface and domain growth in polar direction. Thus, this method doesn't allow creating 3D domain structures in the crystal bulk. This drawback has been overcome recently using tightly focused irradiation of the femtosecond laser with wavelength in the near IR range. The main idea of this method is based on the high enough multiphoton absorption of the light from the transparent spectral range due to the extremely high light intensity in the focusing region. In 2015 for the first time such domain switching was demonstrated in ferroelectric lithium niobate ($LiNbO_3$, LN) crystals [6]. The further works widely expended the number of ferroelectrics used for 2D and 3D domain patterning [1].

We study formation of the domain structures in the single crystals of uniaxial high-quality lithium niobate $LiNbO_3$ and lithium tantalate $LiTaO_3$ family as the most frequently used nonlinear optical materials by local irradiation and linear scanning [7,8]. The created domain structure has been imaged in the bulk by Cherenkov-type confocal Second Harmonic Generation. We suppose that the domain formation near the focus point is caused by depolarization field appearing at the phase boundaries of nonpolar microtracks and subsequent domain growth is caused by pyroelectric field occurring during nonuniform temperature change [8]. The creation of the three-dimensional nonlinear photonic crystals and periodical domain structures in the bulk was demonstrated [7,8].

The equipment of the Ural Center for Shared Use "Modern nanotechnology" Ural Federal University (Reg.№ 2968) was used. The research was made possible by Russian Science Foundation (Project № № 24-12-00302).

1. Y. Sheng, X. Chen, T. Xu, S. Liu, R. Zhao, W. Krolikowski, *Photonics* **11**, 447 (2024).
2. V.Ya. Shur, A.R. Akhmatkhanov, I.S. Baturin, *Applied Physics Review*, **2**, 040604 (2015).
3. V.Ya. Shur, D.K. Kuznetsov, E.A. Mingaliev, et al., *Appl. Phys. Lett.* **99**, 082901 (2011).
4. V.Ya. Shur, E.A. Mingaliev, M.S. Kosobokov, et al., *J. Appl. Phys.* **127**, 094103 (2020).
5. V.Ya. Shur, M.S. Kosobokov, A.V. Makaev, et al., *Acta Materialia*, **219**, 117270 (2021).
6. X. Chen, P. Karpinski, V. Shvedov, et al., *Appl. Phys. Lett.* **107**, 141102 (2015).
7. B.I. Lisjikh, M.S. Kosobokov, A.P. Turygin, A.V. Efimov, V.Ya. Shur, *Photonics*, **10**, 1211 (2023).
8. B.I. Lisjikh, M.S. Kosobokov, V.Ya. Shur, *Photonics*, **11**, 928 (2024).

L2

Ferroelectricity in the world of 2D materials

A.Yu. Kuntsevich

National Research University Higher School of Economics, 101000 Moscow, Russia
akuntsevich@hse.ru

2D materials and Van der Waals heterostructures directions were sparkled by discovery of graphene. Graphene monolayer itself is a pretty symmetric material: it has inversion center and 6th order rotational axis, prohibiting any possibility of piezo- or ferroelecricity, moreover, it has metallic conductivity, that screens electric fields.

Monolayers of the other popular two-dimensional materials (hexagonal bron nitride - hBN and transition metal dichalcogenides - TMDCs) are usually insulating and less symmetric (have no inversion symmetry) and, therefore, may demonstrate in-plane piezoelectricity [1]. Importantly, this piezoelectricity emerges only in mono- or few-odd-number of layers form, whereas the bulk crystals are not piezoelectric, because they are stacks of alternating-sign monolayers. TMDCs and hBN are symmetric enough to prohibit spontaneous polarization. Numerous less symmetric 2D materials from the other classes are mostly unstable under ambient conditions.

Nevertheless, ferroelectricity in the field of 2D materials is possible and is now intensively developing direction. The first and the most evident direction is taking pretty asymmetric 2D materials and layers, for example $CuBiP_2Se_6$ or In_2Se_3 [2]. More interestingly, TMDCs have low symmetry politypes, 1T` with different from standard hexagonal arrangements of atoms inside layers [3].

The second direction is dealing with hetero interfaces; those are always less symmetric than isolated layers. For example, two layers of different TMDCs may produce ferroelecricity [4]. There are examples of assymmetric environment driven ferroelectricity in symmentric TMDC [5]. Ferroelecricty could be developed in TMDCs by proximity effect and such functionalization of 2D materials is very promissing for electronic applications [6].

The third and the most promising direction in 2D ferroelecricity is symmetry breaking at homointerfaces in marginally twisted structures [7, 8]. We assume by marginal twist a mutual rotation of two adjacent layers by extremely small angle. Thus, arranged structure forms switchable ferroelectric domains which were unstable or impossible in bilayers exfoliated from stable bulk crystals.

The work is supported by Basic Research Program of the HSE University.

1. W. Wu, et al, *Nature* **514**, 470 (2014).
2. Y. Zhou, et al, *Nano Letters* **17**, 5508 (2017).
3. A. Lipatov, et al, *npj 2D Materials and Applications,* **6**, 18 (2022).
4. L Rogee, et al, *Science* **376**, 973 (2022).
5. Z. Fei, et al, *Nature* **560**, 336 (2018).
6. H. Ryu, et al, *Appl. Phys. Lett.,* **117**, 080503 (2020).
7. K. Yasuda, et al, *Science* **372**, 1458 (2021).

L3

Magnetic functional materials produced by selective laser melting

A.S. Volegov

Ural Federal University, 620002 Ekaterinburg, Russia
alexey.volegov@urfu.ru

The talk will describe the approaches to additive manufacturing of permanent magnets and magnetically soft elements with and without organic binder used worldwide including specific structures which minimize sharp change in magnetic fields, protect the material from eddy currents etc.

The development of power engineering, robotics, and miniaturized high-tech devices with electric motors and actuators as well as electric transport, including personal mobility devices, requires an increase in production of magnetic systems and a simultaneous improvement or optimization of specific technical tasks related to the intensity and distribution of magnetic fields. Traditional and subtractive technologies are widely used to create functional materials and devices. Due to AC magnetic fields, the temperature of permanent magnets used in generators and electric motors often exceeds room temperature, reaching 400 - 450 K in most devices. Further development requires improvement of the functionality and miniaturization, as well as improvement of functional properties (in particular magnetic) of materials and products derived from them. Magnetic materials have almost reached their theoretical limits. Further development in consumer electronics, robotics etc. The functionality of a device can be changed by changing its form and tuning the local properties inside the device. The only way to do this is through additive manufacturing, as this technology allows us to vary both process parameters and the composition of added material. So far, there are technologies for additive manufacturing of construction materials and their products. Functional properties are usually extremely dependent on the microstructural properties of the material.

The most difficult task in the creation of functional materials is the reproduction of the microstructure. This is usually an unsolvable problem, but it can be worked around by changing the design of devices. Let's take a look at some problems with magnetic materials. As the useful magnetic properties of these materials deteriorate when the temperature increases, it is necessary to create specific structures that suppress eddy currents and heat in the magnetic system. One way to suppress these eddy currents is by creating a layered structure made of materials with high resistivity. This method is well known in traditional electric steel production, but selective laser melting does not allow for the creation of a thin layer (1 - 5 μm) of electrical insulation. This problem can be solved by creating a structure with areas arranged in a specific manner with different electrical properties, while maintaining similar magnetic properties. In particular, the Curie temperature of Nd2Fe14B compounds is relatively low. Their coercivity depends on temperature in the range from room temperature up, and the main way to improve the properties of magnets for motors and generators is to increase coercivity over the entire temperature range below the Curie point.

The work was financially supported by the Ministry of Science and Higher Education of Russian Federation (FEUZ-2024-0060).

L4

X-ray photoelectron spectroscopy: surface study

I.M. Zhukov

Exiton Analytic Ltd., 194021 Saint-Petersburg, Russia
ZYM@exiton-analytic.ru

X-ray photoelectron spectroscopy (XPS) is a powerful analytical technique widely used for studying the chemical and electronic properties of surfaces. Based on the photoelectric effect, XPS measures the kinetic energy of electrons emitted from a material under X-ray irradiation, providing detailed information about elemental composition, chemical states, and electronic structure. Due to its high surface sensitivity (probing depths of ~3–8 monolayers), XPS is indispensable in materials science, nanotechnology, catalysis, and surface chemistry.

One of the key advantages of XPS is its non-destructive nature, allowing for repeated measurements on the same sample. The technique is applicable to a broad range of materials, including metals, semiconductors, and insulators. Additionally, XPS provides quantitative data on elemental concentrations and identifies chemical bonding states through precise analysis of binding energy shifts.

A critical requirement for XPS is an ultra-high vacuum (UHV) environment (~10^{-10}–10^{-9} Torr) to minimize surface contamination and ensure accurate measurements. When combined with ion beam sputtering (depth profiling), XPS enables three-dimensional chemical mapping with nanometer-scale resolution, making it essential for thin-film analysis and interface studies.

This presentation will discuss the fundamental principles of XPS, its experimental setup, and key applications in modern physics and materials science. Special attention will be given to case studies in semiconductor device characterization, catalytic surface analysis, and emerging biomedical applications. The talk will also address recent advancements in high-resolution XPS, angle-resolved measurements, and synchrotron-based techniques, which further expand the capabilities of this method.

In conclusion, XPS remains a cornerstone technique in surface science, offering unparalleled insights into material properties at the atomic and molecular levels. Its continued development ensures its relevance in cutting-edge research across multiple disciplines.

INVITED
PRESENTATIONS

I1

Achievements and development prospects of nanodomain engineering in ferroelectrics

V.Ya. Shur

School of Natural Sciences and Mathematics, Ural Federal University, 620002 Ekaterinburg, Russia
vladimir.shur@urfu.ru

The recent progress in fabrication of nonlinear photonic crystals based on quasi-phase matching effect realized by creation of the stable periodic ferroelectric domain structures with nanoscale period reproducibility will be presented. The second harmonic generation and optical parametric oscillation have been realized with record efficiency in periodically poled lithium niobate and lithium tantalate bulk crystals, thin films and waveguides [1,2]. The recently discovered abilities of all-optical domain switching in the crystal bulk by IR pulse laser irradiation for creation of the three-dimensional nonlinear photonic crystals will be demonstrated [3-6].

All obtained achievements are based on complex study of the domain structure evolution in uniaxial ferroelectric crystals using complimentary domain imaging methods with high spatial and temporal resolution by example of MgO doping lithium niobate and lithium tantalate. The conventional methods of domain engineering are based on application of the nonuniform electric field using: (1) periodical stripe electrodes [1], (2) biased tip of scanning probe microscope [2], (3) focused electron and ion beams [7].

The produced stable tailored domain structures allowed us to realize the out-of-cavity second harmonics generation with record efficiency and mid-infrared optical parametric amplifier (OPA) [8]. It was shown that the fan-out periodical domain structures allowed us to obtain super-wide OPA tuning range from 2.5 to 4.5 μm in one element [8].

It was shown recently that the tightly focused irradiation by femtosecond near-IR laser allowed to realize the domain nucleation in the crystal bulk. The subsequent in-bulk domain growth can be achieved under the action of the pyroelectric field that appeared during crystal cooling [4-6]. The creation of the three-dimensional nonlinear photonic crystals and tailored domain structures in the crystal bulk was demonstrated by us in the single-domain plates of MgO doped lithium niobate and lithium tantalate using femtosecond laser emitting at the 1030 nm wavelength [4-6].

The generating of entangled photon pairs for application in quantum communication and photonic quantum technologies has been realized by spontaneous parametric down conversion in periodically poled lithium niobate channel waveguides [9].

The research was made possible by Russian Science Foundation (Grant No. 24-12-00302). The equipment of the Ural Center for Shared Use “Modern nanotechnology” Ural Federal University (Reg. № 2968) was used.

1. V.Ya. Shur, A.R. Akhmatkhanov, I.S. Baturin, *Appl. Phys. Rev*. **2**, 040604 (2015).

2. B.N. Slautin, H. Zhu, V.Ya. Shur, *Ceramics International*, **47**, 32900 (2021).

3. V.Ya. Shur, M.S. Kosobokov, A.V. Makaev, D.K. Kuznetsov, M.S. Nebogatikov, D.S. Chezganov, E.A. Mingaliev, *Acta Materialia* **219**, 117270 (2021).

4. B. Lisjikh, M. Kosobokov, A. Turygin A. Efimov, V. Shur, *Photonics*, **10**, 1211 (2023).

5. B.I. Lisjikh, M.S. Kosobokov, A.V. Efimov, D.K. Kuznetsov, V.Ya. Shur, *Ferroelectrics* **604**, 47 (2023).

6. B. Lisjikh, M. Kosobokov, V. Shur, *Photonics* **11**, 928 (2024).

7. D.S. Chezganov, E.O. Vlasov, E.A. Pashnina, M.A. Chuvakova, A.A. Esin, E.D. Greshnyakov, V.Ya. Shur, *Appl. Phys. Lett.* **115**, 092903 (2019).

8. E. Erushin, B. Nyushkov, A. Ivanenko, A. Akhmathanov, V. Shur, A. Boyko, N. Kostyukova, D. Kolker, *Laser Phys. Lett.* **18**, 116201 (2021).

9. T. B. Gäbler, P. Hendra, N. Jain, M. Gräfe, *Adv. Physics Res*. **3**, 2300037 (2024).

I2

Demonstration of ferroelectric $Hf_{0.5}Zr_{0.5}O_2$-based 1T-1C FeFET integrated with 350 nm CMOS technology

A.A. Chouprik[1], P.S. Zakharov[2], V.S. Konstantinov[2], I.A. Mutaev[1], S.V. Ilyev[1], A.A. Scherbakov[1]

[1]*Moscow Institute of Physics and Technology, 141700 Dolgoprudny, Russia*

[2]*Molecular Electronic Research Institute, 124460 Zelenograd, Moscow, Russia*

chouprik.aa@mipt.ru

Among the next-generation non-volatile memory concepts alternative to Flash memory, ferroelectric memory is a special case because it has been on the market for a long time: ferroelectric random-access memory (FRAM) has nanosecond write/read times, very low power consumption and almost unlimited endurance. FRAM devices based on traditional perovskite ferroelectrics have been produced worldwide for the last 20 years in technologies up to 90 nm. However, scalability and technology compatibility issues have limited the scope of these devices to niche markets. As a result, research and development toward FRAM was halted in the mid-2000s, ending the ferroelectric memory boom. Meanwhile, the discovery in 2011 of ferroelectric properties in doped HfO_2-based thin-film layers [1] and, in particular, HfO_2-ZrO_2 alloyed films, has revived the interest of researchers and engineers, as these materials are used in modern CMOS technology as gate dielectrics in field-effect transistors and capacitors, and ferroelectric materials based on them are automatically compatible with it. Therefore, the development of a ferroelectric memory based on this class of materials could potentially overcome the above problems.

In addition to the above advantages of ferroelectric memory, ferroelectric field-effect transistors (FeFETs) are highly scalable, i.e., they have the major advantage of Flash memory, which allows the industry to continuously increase the capacity of memory chips. Thus, FeFETs combine the advantages of ferroelectric and Flash memory. This work presents FeFET memory chips based on the alternative 1T-1C topology (1 transistor - 1 capacitor) and $Hf_{0.5}Zr_{0.5}O_2$ (HZO) ferroelectric film manufactured at foundry of NIIIS by Sedakov (Nizhny Novgorod, Russia) using 350 nm technology. In contrast to the classical FeFET of 1T (1 transistor) topology, when the gate dielectric is replaced by a ferroelectric, in 1T-1C topology a metal-ferroelectric-metal capacitor is connected in series with the gate of the field-effect transistor. An important advantage of the chosen approach is the absence of the Si-HZO interface, which inevitably contains the SiO_2 interlayer. This low-*k* layer causes a giant charge injection from the electrodes, which significantly limits the information storage time (due to the strong imprint effect) and switching endurance (due to electrical breakdown). FeFETs exhibit excellent memory properties (Fig. 1) and good reliability characteristics, including a storage time of more than 10 years and an endurance of than 10^7 switching cycles.

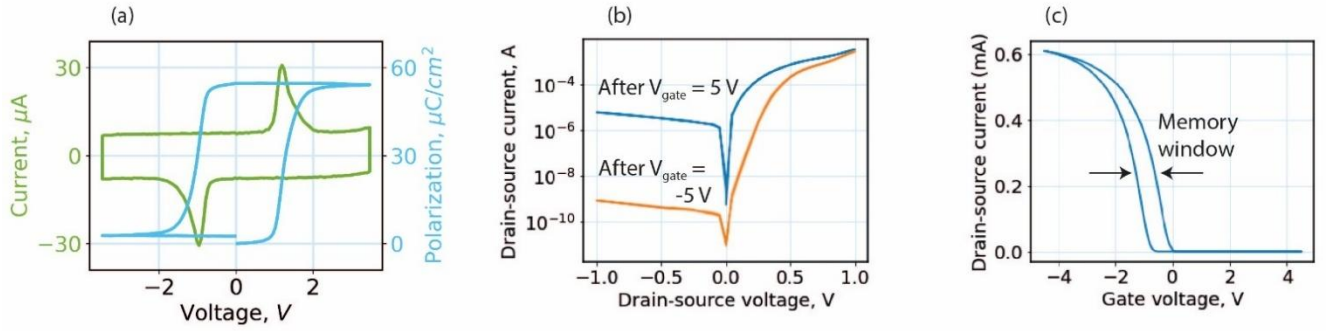

Figure 1. (a) Switching *I-V* and *P-V* curves, (b) output and (c) transfer characteristics of 1T-1C FeFETs.

The work was supported by the Ministry of Science and Higher Education (Agreement № 075-03-2025-662, Project FSMG-2025-0025).

1. T.S. Böscke, J. Müller, D. Brauhaus, U. Schröder, U. Böttger, *Appl. Phys. Lett.* **99**, 102903 (2011).

I3

Functional micro- and nanostructures for photonics of optical and terahertz ranges

V.S. Pavelyev

Samara National Research University, 443086 Samara, Russia
nano@ssau.ru

The talk is devoted to developing of photonics elements on the base of micro- and nanostructured materials. Technologies for silicon and diamond transmission diffractive microoptics have been developed [1,2]. Diamond diffractive optical elements (DOEs) for focusing infrared [1] and terahertz [2] laser beams as well for formation of terahertz laser beam with predetermined mode composition and polarization state [2] have been manufactured and experimentally investigated. Developed technologies [1,2] are based on lithographic etching and laser ablation. The generation of terahertz beams with pre-given characteristics paves the way for the development of new applications. One of such applications was demonstrated in [3], where beams with orbital angular momentum generated by the DOEs described in [2] were used to excite vortex surface plasmon polaritons propagating along a cylindrical conductor.

The organization of multichannel optical communication system based on transversal mode selection (MDM) by elements of microoptics is discussed in [4]. However, to realize such system one would need elements for fast modulation of laser beam transversal mode spectrum. Tunable diffractive optical elements for fast modulation of orbital angular momentum spectrum are proposed in [5,6]. The results of experimental investigation of realized elements [5,6] are closed to theoretical expectations. The development of tunable elements [5,6] open up possibility to develop MDM communication systems.

1. T.V. Kononenko, D.N. Sovyk, P.A. Pivovarov, Pavelyev V.S., et al., *Diamond & Related Materials* **101**, 107656 (2020).

2. Yu. Choporova, B. Knyazev, V. Pavelyev, *Light: Advanced Manufacturing* **3**, 31 (2022).

3. V.V. Gerasimov, O.E. Kameshkov, B.A. Knyazev, N.D. Osintseva, V.S. Pavelyev, *Journal of Optics* **23**(10), 10LT01 (2021).

4. V.A. Soifer, L.L. Doskolovich, N.L. Kazanskiy, V.V. Kotlyar, D.L. Golovashkin, V.S. Pavelyev, S.N. Khonina, R.V. Skidanov, *Computer Design of Diffractive Optics* (Woodhead Publishing Limited, Cambridge) (2012).

5. A. Esin, A. Akhmatkhanov, V. Pavelyev, V. Shur, *Optical Materials* **157**(3), 116401 (2024).

6. V. Shikhova, A. Akhmatkhanov, M. Chuvakova, L. Ivleva, V. Pavelyev, M. Nebogatikov, V. Shur, *Journal of Advanced Dielectrics* **15**(3), 2450036 (2025).

I4

1D and 2D peptide nanostructures for green energy harvesting and storage

P. Zelenovskii, R. Ferreira, F. Hagiwara, F. Figueiredo

Department of Physics and CICECO – Aveiro Institute of Materials, University of Aveiro, Aveiro, Portugal
zelenovskiy@urfu.ru

Functional elements based on supramolecular peptide materials are actively integrated into various biomedical devices, such as biosensors, drug delivery systems, etc., due to their inherent eco-friendliness, biocompatibility, and remarkable chemical diversity [1,2]. However, peptide nanostructures demonstrate a variety of other unique physical properties, which allow them to be used in less obvious areas, such as energy harvesting and energy storage devices.

In this work, we demonstrate the formation of one-dimensional (1D) nanotubes and two-dimensional (2D) layered crystals based on diphenylalanine (FF) and phenylalanyl-glutamic acid (FE), studied their structure and morphology, and evaluated their cathodic and anodic properties. Estimations show an outstanding Li capacity of FF nanotubes about 375 mAh/g comparable with the capacity of graphite (372 mAh/g). Moreover, large-area (c.a. 500 mm^2) crystalline films of dileucine (LL) with a thickness below 400 nm created by the spin-coating technique, demonstrate high piezoelectric coefficient d_{33} c.a. 18 pm/V comparable to that of other organic materials. The films have been tested in triboelectric and piezoelectric energy harvesting devices. The obtained results demonstrate the potential of peptide-based nanomaterials for energy applications.

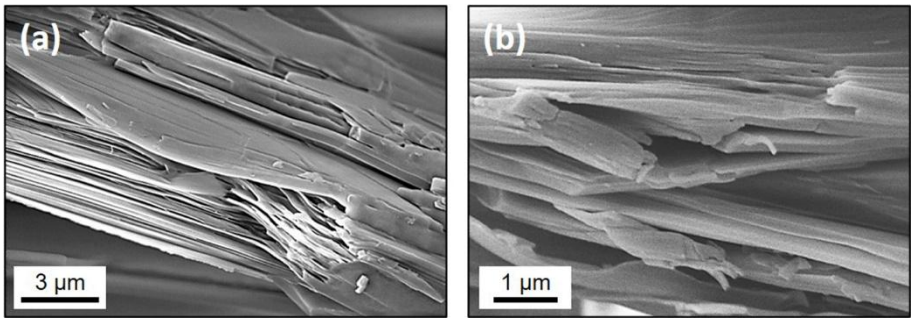

Figure 1. Self-assembling 2D layered crystals of (a) FF and (b) FE.

This work was developed within the projects CICECO-Aveiro Institute of Materials (UIDB/50011/2020, UIDP/50011/2020, LA/P/0006/2020) and “BioPiezoSensor” (2022.03781.PTDC, DOI 10.54499/2022.03781.PTDC) financed by national funds through the FCT and FCT/MEC (PIDDAC). The authors are grateful for the financial support granted by the Recovery and Resilience Plan (PRR) and by the Next Generation European Funds to Universidade de Aveiro, through the Agenda for Business Innovation “NGS - Next Generation Storage” (Project nº2 with the application C05-i01.01/2022).

1. J. Zhao, Q. Liu, X. Tong, et al., *Adv. Funct. Mater.* **34**, 2401466 (2024).
2. P. Zelenovskii, K. Romanyuk, et al., *Adv. Funct. Mater.* **31**, 2102524 (2021).
3. K. Romanyuk, V. Slabov, et al., *Appl. Mater. Today* **26**, 101261 (2022).
4. D. Alikin, V. Yuzhakov, et al., *ACS Biomater. Sci. Eng.* **9**, 6715 (2023).

I5

Raman scattering in relaxor ferroelectrics with phase charge separation

S.G. Lushnikov[1], N.K. Derets[1], A.I. Fedoseev[1], R.S. Katiyar[2], J.-H. Ko[3]

[1]*Ioffe institute, 194021 St. Petersburg, Russia*
sergey.lushnikov@mail.ioffe.ru

[2]*University of Puerto Rico, San Juan, PR 110007, USA*

[3]*Hallym University, Chuncheon 24252, Korea*

Relaxor ferroelectrics (relaxors) with the perovskite structure and the general formula AB'B"O3 demonstrate unique dielectric and piezoelectric properties, which are widely used in industry. These unique properties of relaxors are largely determined by the dynamics of polar nanoregions that arise due to chemical and charge disorder in the B-sublattice of perovskite [1]. In recent years, relaxor crystals with magnetic ions of variable valence in the B-sublattice of perovskite have been grown. The results of studying the properties of these crystals make it possible to distinguish AB'B"O3 compounds (where B' is Co, Ni, Mn; B" is Nb, Ta) into a separate group. A characteristic feature of this group of compounds is the variable valence of ions in the B sublattice, which changes the dynamics of polar nanoregions and leads to the appearance of phase charge separation [2]. In detail, the process of phase separation was considered in the $PbCo_{1/3}Nb_{2/3}O_3$ (PCN) crystal. The existence of a continuous, correlated change in the dielectric properties and electric polarization in the temperature range of 5 – 350 K was shown. These changes are induced by local polar regions in which continuous switching of the valence of Co and Nb ions occurs. The existence of continuous, correlated changes in the dielectric properties and electric polarization in the temperature range of 5 – 350 K was shown. These changes are induced by local polar regions in which continuous switching of the valence of Co and Nb ions occurs. At temperatures below 150 K, these are phase separation regions with barriers of 0.3 eV, caused by the finite probability of tunneling e_g electrons between Co^{2+} and Co^{3+} ions. In the temperature range from 225 K to 300 K, there are local polar regions with barriers of 0.77 eV, formed near Pb^{2+} ions that locally distort the lattice. In the intermediate temperature range of 125 K – 225 K, the recharging of Nb^{5+}-Nb^{4+} ions by e_g electrons causes a connection between pairs of these local polar regions. At a temperature of T > 300 K, the electrons recharging the ions overcome the 0.77 eV barrier and through conductivity prevails in the crystal. The proposed mechanism of phase separation is also applicable to other compounds from the discussed group of relaxors.

In this report, the phonon and relaxation dynamics in crystals with variable-valence magnetic ions (using PCN [3, 4] and $PbNi_{1/3}Nb_{2/3}O_3$ – PNN [5] as examples) will be considered. The results of Raman scattering experiments in PCN and PNN will be discussed and compared with the measurement data in the $PbMg_{1/3}Nb_{2/3}O_3$ – PMN crystal. A comparative analysis of the temperature behavior of the phonon and relaxation subsystems in model relaxors and compounds from the group under consideration has made it possible to show the influence of variable-valence magnetic ions on the dynamics of polar nanoregions and phase transformations into the relaxor state.

1. R.A. Cowley, et.al. *Advance in Physics* **60**, 229 (2011).
2. B. X. Khannanov et al., *JETP* **130**, 439 (2020).
3. J.W. Lee, et al., *J.Phys.: Condensed Matter* **33**, 025402 (2021).
4. N.K. Derets, et al., *JETP Letters* **120**, 741 (2024).
5. N.K. Derets, et al., *JETP Letters* **121** (2025) in press.

I6

The influence of depolarizing field on the polarization modulation in ferroelectric by terahertz pulse

E.D. Mishina, K.A. Brekhov, N.E. Sherstyuk

MIREA-Russian Technological University, 119454 Moscow, Russia
mishina_elena57@mail.ru

Ultrafast polarization control in ferroelectric by electromagnetic pulses offers the prospect for the development of photoferroic devices whose operating speed is orders of magnitude shorter than that of voltage-controlled devices. Initiation of domain growth (or irreversible polarization switching) in polarized lithium niobate by femtosecond optical pulse was recently shown by V.Ya. Shur [1]. Over the last decade, dynamical modulation of ferroelectric polarization by a picosecond terahertz (THz) pulse has been studied experimentally and theoretically. In most experiments, the frequency of the THz pulse was close either to polar [2] or infrared (IR) [3] mode. However, only transient (dynamical) polarization switching was observed. Theoretically, both dynamical and permanent polarization switching was achieved. The modeling is usually based on the Landau-Khalatnikov equation (LKE) for the polar mode. For higher frequency considerations, LKE is coupled with the motion equation (ME) for IR mode. So far, only V. Abalmasov [4] has analyzed the role of the depolarizing field under THz excitation, studying ultrafast polarization switching in initially poled lithium niobate, and attributing the lack of permanent polarization reversal to that field. This study investigates ultrafast polarization switching in $Ba_{0.8}Sr_{0.2}TiO_3$ ferroelectric thin films with depolarizing field being considered. Both strong and week THz fields are considered. Additionally, for THz wave modulation we consider hybrid semiconductor/ferroelectric structures, in which ferroelectric gives additional tool for controlling parameters of THz waves [5].

At room temperature, BST-0.8 films are practically unpolarized, that means that they have, in halves, domains (unit cells) polarized in opposite directions. Therefore, we must write a system of four equations: a pair of LKE&ME for each group of domains. Landau-Khalatnikov equation is written for polarization, and the frequency of the polar mode Ω_p is determined by coefficients in Landau expansion, which were found in [4]. Motion equation is written for a generalized coordinate, and the frequency of the IR mode ω_{IR} is taken from [4]. Depolarizing field is unified for both types of domains. The system is excited by THz pulse with tunable frequency (Ω_{THz} = 0.5 ÷10 THz) with identical envelope with FWHM=0.7 ps, the resulting transient polarization simultaneously gives rise to the appearance of a depolarizing field.

In BST-0.8, for low ($\Omega_{THz}<\Omega_p$) and high ($\Omega_{THz}>\omega_{IR}$) frequencies, analogously to quasi-static (<GHz) regimes, depolarizing field decreases the internal field in ferroelectric, demanding stronger THz pulses for polarization modulation. In the intermediate frequency range, $\Omega_p <\Omega_{THz}<\omega_{IR}$, patterns are more complicated. In this range, depolarizing field gives acts as additional excitation field giving rise for high amplitude oscillations. An additional positive effect of the presence of a depolarizing field is the stabilization of the Landau-Khalatnikov equation (which is mathematically equivalent to the chaotic Duffing equation). In hybrid structures with transition metal dichalcogenide monolayers been taken as semiconductor, the influence of ferroelectric polarization on electric characteristics of TMD is shown. Ferroelectric switching promotes the transition of semiconductor to a metallic state, consequently, the concentration of charge carriers in the 2D semiconductor, and therefore change THz wave parameters. Finally, the obtained results facilitate the development of ultrafast photoferroic and hybrid optoelectronic devices.

The work is supported by Russian Science Foundation (Grant #25-19-00575).

1. B. Lisjikh, et al., *Photonics* **10**, 1211 (2023).
2. K. Grishunin et al., *Scientific Reports* **9**, 697 (2019).
3. R. Mankovsky et al., *Phys. Rev. Lett.* **118**, 197601 (2017).
4. V. Abalmasov, *Phys. Rev. B* **101**, 014102 (2020).
5. I.B. Misirlioglu et al., *Scientific Reports* **5**, 14740 (2015).

I7

Dielectric relaxation in some ferroelectrics with diffuse phase transition

L.N. Korotkov

Voronezh State Technical University, 394000 Voronezh, Russia
l_korotkov@mail.ru

A characteristic feature of diffuse phase transition ferroelectrics (FE DPTs), or relaxors, is a specific dielectric relaxation in the DPT region. The relaxation process is characterized by a wide distribution of relaxation times τ. The dependence of the average value of τ on temperature, unlike the case of conventional dielectrics, cannot be described using the Arrhenius law with a constant activation energy U. In various compounds and solid solutions, dielectric relaxation, along with general patterns, has specific features.

The purpose of this work was to perform a comparative analysis of relaxation processes in various FE DPTs.

The objects of the study were the $K_{1-x}(NH_4)_xH_2PO_4$ and the $(1-x)[0,7PbZrO_3\text{-}0,3(K_{0,5}Bi_{0,5})TiO_3]$ - $xSrTiO_3$ solid solutions, which demonstrate glass-like behavior, and some complex solid solutions based on $Pb(Zr_{0.52}Ti_{0.48})O_3$.

Analysis of the obtained results showed that in all cases, dielectric relaxation is characterized by a wide spectrum of relaxation times, expanding with temperature decreasing. For $K_{1-x}(NH_4)_xH_2PO_4$ crystals the τ distribution function is close to uniform, while in the case of the other two systems this function has a more complex form.

It was found that for all the systems under discussion, the temperature dependence of τ can be described by the Arrhenius law with an increase in activation energy with decreasing temperature. In this case, for each of the systems, a weakening of the dependence of U(T) is observed as the phase transition diffuseness increases. A possible reason for this is the decrease in interaction of polar microregions in ferroelectrics with a significantly diffuse phase transition.

This work was supported by Russian Scientific Foundation, research project No. 24-22-20054.

I8

Optically charged ferroelectric domain walls

P.V. Yudin[1,2], P.S. Bednyakov[1]

[1]*Institute of Physics of the Czech Academy of Science, 18200 Prague, Czech Republic*
yudin@fzu.cz

[2]*Kutateladze Institute of Thermophysics SB RAS, 630090 Novosibirsk, Russia*

Charged ferroelectric domain walls (CDW) attract important attention due to their unique properties promising for electronic applications [1]. Due to the screening of bound charge with free carriers CDWs may serve as reconfigurable conductive channels in otherwise insulating materials. Here we report on the creation of CDW by a simultaneous action of [110] (vertical) electric field and super bandgap illumination in tetragonal $BaTiO_3$ monocrystal. The obtained CDW are stable after removal of the electric field. Figure 1 shows the transition from polydomain structure with neutral (horizontal) 90-degree domain walls (NDW) to a structure with CDWs (vertical).

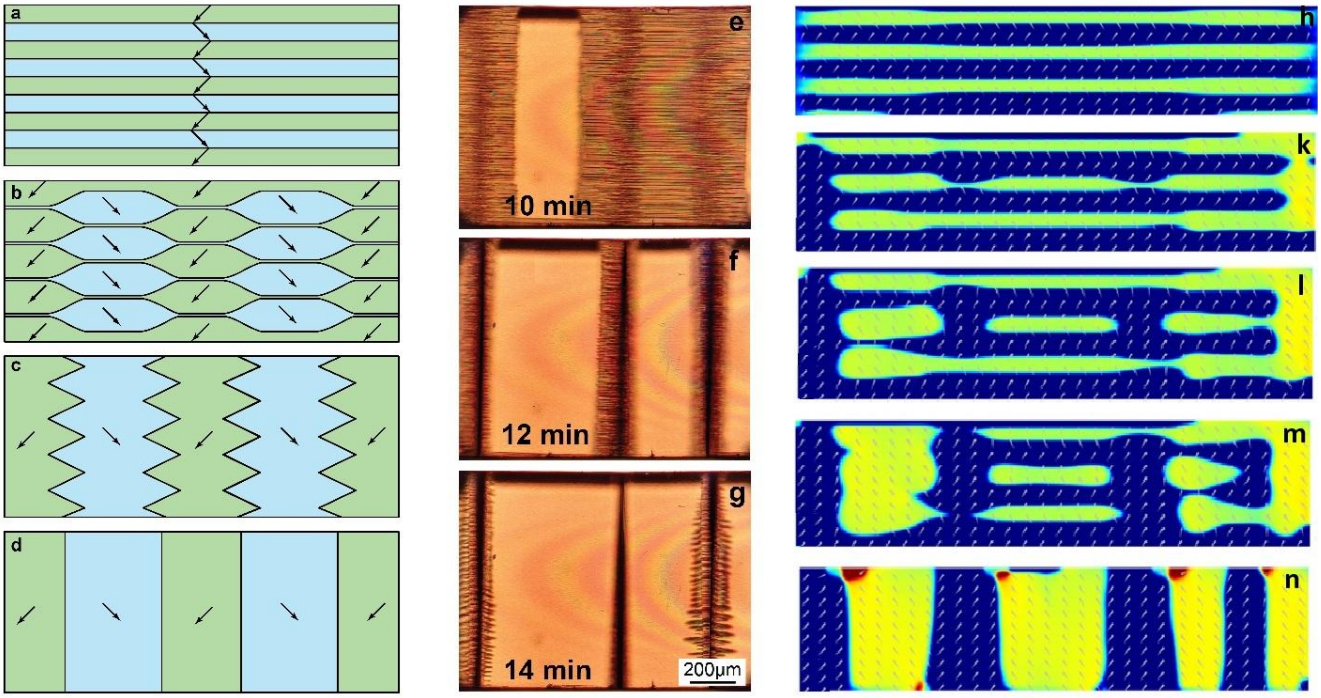

Figure 1. Creation of CDWs in tetragonal $BaTiO_3$ by application of vertical electric field of 3 kV/cm. (a)-(d) – schematics for the domain evolution, arrows show polarization direction; (e)-(f) – observations of ferroelastic NDW (horizontal) and CDW (vertical) in 1 mm thick sample by optical polarized light microscope, time after application of the UV light and electric field is shown; (h)-(n) – results of phase field modeling in samples with reduced size (thickness 40 nm).

The initial polydomain structure is routinely prepared by frustrative poling [2]. Our phase field model reveals that bulk photovoltaic effect plays the key role in the process, by pumping the free charge in the direction opposite to electric polarization, creating such conditions that CDWs are overcompensated, and thus apparently having negative energy. Electric field in turn selects two domain orientations out of four (in-plane of Figure 1) between which only vertical charged domain walls are possible. The presentation will focus on fundamental aspects of the domain evolution under UV light considering the processes of creation and recombination of electron-hole pairs, their interaction with electron donor defects and with the electric field induced by both applied voltage and ferroelectric polarization. Scaling laws will be discussed allowing modeling processes taking minutes and hours in mm-thick samples, using a nanometer-scale computational domain. Based on the same scaling principles nano-electronic devices may be designed. Results open new pathways for the use of ferroelectrics as photovoltaic elements and optically reconfigurable nano-electronics.

1. P.S. Bednyakov, *et al.*, *npj Computational Materials* **4**, 65 (2018).
2. P.S. Bednyakov, *et al.*, *Physical Review B* **110**, 214107 (2024).

I9

Twinning relationships in coexisting cubic and tetragonal phases of ferroelectrics

S. Gorfman[1], I. Biran[1], Nan Zhang[2], Zuo-Guang Ye[3]

[1]*Department of Materials Science and Engineering, Tel Aviv University, Israel*
gorfman@tau.ac.il

[2]*Electronic materials research laboratory, Xi'an Jiaotong University, Xi'an, China*

[3]*Department of Chemistry and 4D LABS, Simon Fraser University, Burnaby, V5A 1S6, Canada*

Many ferroelectric materials undergo phase transitions involving changes in crystal symmetry [1]. Despite decades of research, key questions remain unresolved, particularly the role of domains in the transition pathways. This is true even for well-studied systems, such as the cubic-to-tetragonal transition in $BaTiO_3$. It is widely believed that tetragonal domains accommodate mismatch-free coexistence with cubic regions, as proposed by the Wechsler–Lieberman–Read (WLR) crystallographic theory [2]. However, experimental characterization of such domain arrangements remains rare, since conventional microscopy techniques have limited capabilities for probing domain microstructures.

The goal of the presented work is to advance single-crystal X-ray diffraction to investigate domains during cubic-tetragonal phase transition. We developed formalism which helps investigate coherent twin relationships in single-phase tetragonal, rhombohedral or monoclinic ferroelectrics symmetry using X-ray diffraction [3-5]. Next, we derived formulas for the orientation relationships between the lattice basis vectors of coexisting tetragonal domains and cubic phase. These derivations allowed prediction of Bragg peaks splitting for 24 possible variants of coexistence (one is demonstrated in the figure). We applied this technique for the investigation of cubic-tetragonal phase transition in PMN-35PT [6] at the phase coexistence temperatures.

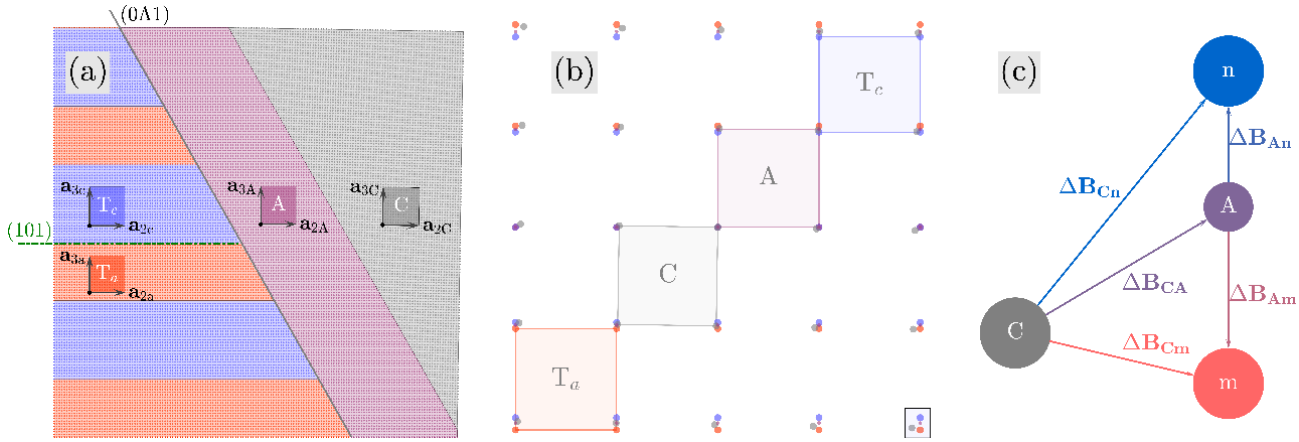

Figure 1. Schematic of a tetragonal–cubic coexistence variant. (a) Real space: cross-section of coexisting lattices. (b) Reciprocal space: cross-section of reciprocal lattices. (c) Bragg peak splitting.

Our results expand the capability of X-ray diffraction as a bulk-penetrating, non-destructive technique for domain microstructure characterization, and provide new tools for understanding the behavior of ferroelectric materials.

1. C.J. Howard, H.T. Stokes, *Acta Cryst.* **A61**, 93 (2004).
2. D.S. Lieberman, M. Wechsler, T. Read, *Journal of Applied Physics* **26**, 473 (1955).
3. S. Gorfman, D. Spirito, G. Zhang, C. Detlefs, N. Zhang, *Acta Cryst.* **A78**, 158 (2022).
4. I. Biran, S. Gorfman, *Acta Cryst.* **A80**, 112 (2024).
5. I. Biran, S. Gorfman, *Acta Cryst.* **A80**, 293 (2024).
6. I. Biran, A. Bosak, Z.-G. Ye, I. Levin, S. Gorfman, *Appl. Phys. Lett.* **124**, 242901 (2024)

I10

Study of electric charge quantization of Au nanoparticles using Kelvin Probe Force Microscopy

A.V. Ankudinov[1], A.C. Vlasov[1], M.S. Dunaevskiy[1], V.Yu. Axenov[1], I.V. Ilkiv[2], A.V. Malevskaya[1], V.D. Rodin[1], A.S. Schenin[1], A.M. Mintairov[1]

[1]*Ioffe Institute, 194021 Saint-Petersburg, Russia*
alexander.ankudinov@mail.ioffe.ru
[2]*Alferov University, 194021 Saint-Petersburg, Russia*

The value of the electron charge, very close to the modern one, was determined more the hundred years ago by Millikan [1], who analyzed the fall of micron-sized oil droplets applying vertical electric field. Quantization of electric charge is an empirical law, and half a century later [2] the possibility to detect the fractional charge of a free quark was discussed. Experiments [3] were also conducted: sub millimeter diamagnetic particles suspended in a magnetic field were studied, which, as was discovered, occupied discrete equilibrium positions when the electric field was turned on, corresponding to elementary charge jumps. Following Millikan, the authors changed the charge of the particles in jumps using a flow of air ions created by X −ray radiation and an electric field.

We investigated the values of the electric potential of metal nanoparticles on an insulator. Colloidal Au particles with characteristic diameters of 20, 40 and $80nm$ were studied. The method of Kelvin probe Force microscopy (KPFM) was used under atmospheric and moderate vacuum conditions. Amplitude and phase modulation modes (AM and PM KPFM) were used. Compared to AM mode, FM mode had approximately twice worse than signal-to-noise ratio. However, using PM KPFM, potential differences between submicron surface areas were determined more correctly. A special sample (Fig. 1a) in the form of a silicon-based capacitor with a thick, $d \cong 1.4\mu m$, thermal oxide as an insulating gap (2) and a perforated upper Au −electrode (1), was used to control the charge state of particles (5). By changing the potential of the lower solid $GaIn$ −electrode (4) with the upper one grounded, the total surface charge of micron-diameter apertures could be smoothly regulated at the level of hundredths of an elementary charge. When a voltage sweep was applied, enhanced temporal oscillations of the potential were observed over a gold particle isolated inside such an aperture. In particular, the $10mV$ peak-to-peak oscillations measured in the AM KPFM mode at a height of $20nm$ above a $40nm - Au$ −particle (Fig. 1c) may reflect elementary charge jumps on it.

Let us estimate the experimental signal, considering the shape of the $40nm$ −particle to be spherical and accounting for the potential was measured at the probe-sample distance $h = 20nm$. One electron on a metal ball, $R = 20nm$, lying on SiO_2, $\varepsilon = 4$, changes the electrostatic potential at a height h above it by the value [4]:

$$\varphi = \frac{q_e}{4\pi\varepsilon_0(R+h)} - \frac{(\varepsilon-1)q_e}{4\pi(\varepsilon+1)\varepsilon_0(3R+h)} \cong 25mV. \quad (1)$$

In the measurements, the characteristic oscillation range, $\Delta SP = 10mV$, is two and a half times smaller than the obtained estimate (1). Since the AM KPFM mode was used, the actual potential changes may be underestimated. As mentioned above, the PM KPFM mode, having a signal-to-noise ratio that is twice as bad, more accurately determined the SP signal drops over submicron sections of the sample. Taking this into account, the actual changes in potential above the particle in Figure 1c will be at least 2 times greater: $\cong 20mV$.

The dipole contribution to potential due to particle polarization in the electric field outside the aperture $\boldsymbol{E}$ is significantly less than the discussed values. An isolated metal ball with a diameter of $2R$ placed in such a field creates a potential of $\varphi_d = (\boldsymbol{E}, \boldsymbol{r})R^3/r^3$ at a point with a vector $\boldsymbol{r}$, [4]. Outside the aperture the field is smaller than inside the capacitor: $E < \Delta V/d$. Therefore, on the ball top $\varphi_d < \Delta VR/d$. In particular, for the particle in Figire 1: $\varphi_d < \Delta V/70$.

In sum, the above allows us to connect those $10mV$-oscillations with single-electron charge jumps on the $40nm$ particle. The presented data also demonstrate the high sensitivity of elementary charge detection by the KPFM method.

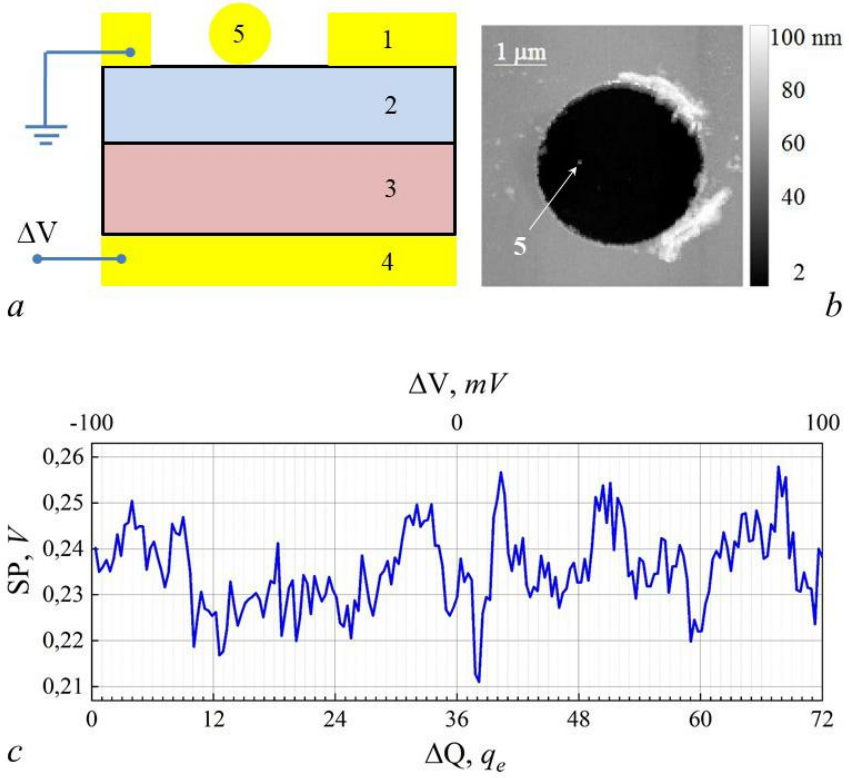

Figure 1. Circuit diagram for smooth regulation of the charge of a metal particle (5): a flat capacitor made of *p-Si* (3) with SiO_2 insulator (2). (a) AFM image of the top contact region (1) with an aperture, $D \cong 3.4\mu m$, with a solitary $40nm - Au -$particle inside (5). (b) Time scan of the surface potential (SP) signal at a height of $20nm$ above the particle, measured in the AM KPFM mode when applying a sweep of $200mV$ at a speed of $0.5mV/s$ to the lower contact (4). (c) $\Delta Q = \varepsilon_0 \pi D^2 \Delta V / 4 q_e d$, the charge of the aperture, corresponding to ΔV, is shown at the bottom (neglecting the electric field outside). CSG30/Pt cantilever was used.

The work was supported by the grant of the Russian Science Foundation 24-22-20014 and the grant of the St. Petersburg Scientific Foundation 24-22-20014 (A.V. Ankudinov, V.D. Rodin, A.M. Mintairov).

1. R.A. Millikan, *Electrons (+ And -) Protons Photons Neutrons Mesotrons And Cosmic Rays* (The Univ. of Chicago press, Chicago IL), 674 (1947).

2. Ya.B. Zel'dovich, *Sov. Phys. Usp.* **9**, 60 (1967).

3. V.B. Braginsky, *Physical Experiments with Test Bodies* (NASA Technical translation, Washington DC), 130 (1972).

4. D.V. Sivukhin, *The general course of physics, vol. 3, Electricity* (Moskva: "Nauka"), 656 (2004).

I11

Mapping local structural and charge inhomogeneities in ferroelectric thin-film hafnia using 4D Transmission Electron Microscopy

D.V. Pelegov[1,2], F. Wunderwald[3], U. Schroeder[3], Y. Ivry[1,2]

[1]*Department of Materials Science and Engineering, Technion-Israel Institute of Technology, 3200003 Haifa, Israel*
dpelegov@technion.ac.il

[2]*Solid State Institute, Technion-Israel Institute of Technology, 3200003 Haifa, Israel*

[3]*NaMLab gGmbH, 01187 Dresden, Germany*

Hafnia thin films were recently found as a ferroelectric platform, which is promising for semiconducting silicon industry. Contrary to conventional ferroelectrics, hafnia-based thin films exhibit ferroelectric ordering only at a narrow film-thickness, stoichiometry, and bias wake-up ranges. While ferroelectricity is a consequence of long-range ordering, local structure and charge inhomogeneities, inherent for thin-film hafnia, impose a competing action. The fundamental ferroelectric mechanism in such limited and heterogeneous materials is still not fully understood, and a major reason for this knowledge gap is the lack of observations of short-range ordering. Here, we used novel electron-microscopy techniques, namely ASTAR and 4D-STEM (Fig. 1), for revealing and mapping intrinsic inhomogeneities of a different origin – local variations in structure, orientation, charge/bias field, strain, etc. We found that the electric-field variations are substantial near the interface, paving the way to interface-engineered hafnia samples with augmented functional properties.

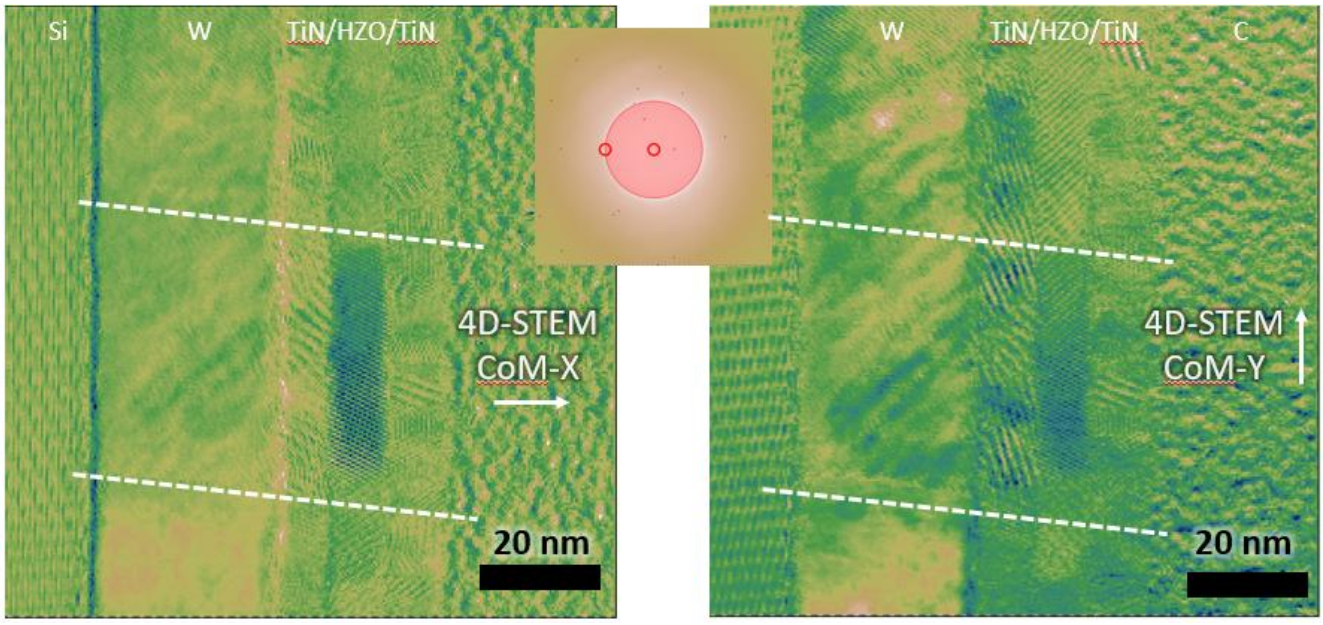

Figure 1. The example of spatial inhomogeneity of local electric fields (charges) in Si/W/TiN/HZO/TiN stacks, revealed by Center-Of-Mass analysis of 4D-STEM data. Brighter and darker colors correspond to negative and positive shifts of non-diffracted electron beam in X (left image) and Y (right image) directions. Inset between images shows an averaged diffraction pattern with a disk-mask for CoM analysis. Images were obtained using converged beam (21.7 mrad).

I12

A hybrid of photonics and optoacoustics in the visible part of the spectrum

N.A. Inogamov[1-3]

[1]*Landau Institute for Theoretical Physics of Russian Academy of Sciences, 142432 Chernogolovka, Russia nailinogamov@gmail.com*

[2]*Dukhov All-Russia Research Institute of Automatics, 127055 Moscow, Russia*

[3]*Joint Institute for High Temperatures of Russian Academy of Sciences, 125412 Moscow, Russia*

The report provides a brief description of the results obtained in papers 1-3. Structured optically thick films (metasurfaces) are considered for applications in telecommunications and nanosensing. Thanks to structure, these films transmit light [1,2] thus acting as a photonic device. At the same time, in our case the film remains an effective transducer of terahertz sound generators in the film and substrate [1]. Thus, our device combines the properties of photonic and optoacoustic devices. The Nickel films are created by magnetron sputtering inside a few Pa Argon atmosphere.

Sub-picosecond optical laser processing of metals is actively utilized for modification of a heated surface layer. But for deeper modification of different materials a laser in the hard X-ray range is required. Here [3], we demonstrate that a single 9-keV X-ray pulse from a free-electron laser (XFEL) can form a μm-diameter cylindrical cavity with a length of ~1 mm in LiF surrounded by shock-transformed material [3]. In our case the plasma-generated shock wave with TPa-level pressure results in damage, melting and polymorphic transformations of any material, including transparent and non-transparent to conventional optical lasers.

Moreover, cylindrical shocks can be utilized to obtain a considerable amount of exotic high-pressure polymorphs. Indeed, due to the cylindrical geometry and the large length of the cavity shown in Figure 1e, the amount of matter that has passed through strong compression is much higher than the same amount when an optical laser is sharply focused (Fig. 1b,c). In the case of optics, the geometry of the shock wave divergence shown in Figure 1b,c is quasi-spherical [4,5]. In such a geometry, the amount of matter that has passed through a solid-solid phase transition is in the order of magnitude of a femtogram.

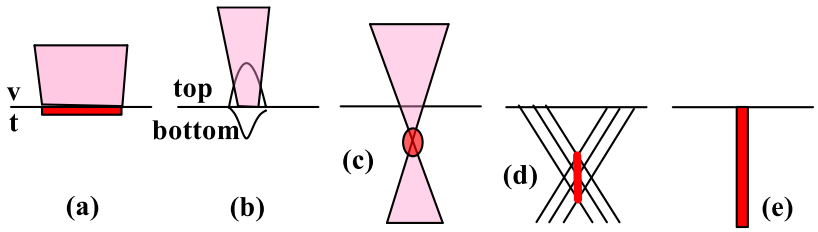

Figure 1. Geometry of the currently available options for femtosecond laser exposure to matter. Different laser impacts are in the different interests of scientific and technological applications.

(a) The most standard situation. Optical action, a spot with a diameter of 10-100 and more wavelengths while heating depth is less than 1 μm. This is a “shallow water” heating region. The region is shown as red rectangular. Notations: v - vacuum, t - target. The same situation with v-t applies to irradiation of a condensed medium through vacuum or gas in the examples (Fig. 1c,d,e).

(b) Optical irradiation of a target (bottom) covered with a liquid or solid medium transparent in optics (top). See [4,5] with example in Figure 5a in [5]. Here curved closed contours mark the boundaries of the cavities in the transparent lid (semi space top) and the nontransparent target (semi space bottom).

(c) Irradiation through vacuum with focusing in the volume of the target. The target is transparent in optics. With sufficient energy and ultra-short exposure, an empty cavity forms around the focus area. The mechanism of cavity formation is similar to the one shown in Figure 1e. But geometry is different: spherical versus cylindrical.

(d) Optical irradiation through an axicon. The formation of a quasi-cylindrical channel is a red vertical segment [6-9]. In versions of optical irradiation of optically transparent media with a Bessel beam, the length of the cylindrical cavity can be as large as in our case (Fig. 1e). But an energy density

comparable to our own inside the cavity has not yet been achieved. Our energy concentration [3] (Fig. 1e) is 2-3 orders of magnitude higher than that achieved in the case (Fig. 1d) [6-9]. Nevertheless, it seems that in cases [6-9], radial extrusion of the substance from cylindrical axis takes place. Similar to our case (Fig. 1e) [3]. In paper [6], the pulse energy at the input to the optical system SLM is E = 60 μJ. Let's divide this energy by the volume of the focus area by the axicon. We will determine the energy density per unit volume. This volume density is equal in order of magnitude to the initial pressure in the focus area:

$P \sim E/(L\ \pi\ R^2) = 60\ \mu J/(500\ \mu m\ 3.14\ (1\ \mu m)^2) = 60\ \mu J/(1500\ \mu m^3) = \alpha_{opt}\ \alpha_{plasm}\ 40\ GPa \sim 2\ GPa.$ where L is length of a cylindrical cavity in [6], R is the radius of cylindrical focal beam, $\alpha_{opt} \sim 0.2$-0.3 is energy losses in the optical system from E = 60 μJ to final incident into illuminated column inside PMMA, $\alpha_{plasm} \sim 0.2$ is anergy absorbed by plasma column inside PMMA.

PMMA is polymethylmethacrylate (acrylic glass or plexiglass}. It is rather weak mechanically. Thus 2 GPa is enough for its radial extrusion because its yield stress is low ~ 0.1 GPa.

(e) Our situation [3] with hard X-rays at high attenuation depth (D_{att}=475 μm for LiF and 9 keV), high energy density (up to 0.9 MJ/cm^3 ~ p ~ 1 TPa), and state-of-the-art focusing with a long Rayleigh length z_R~1 mm is shown. We see how far this case is from the usual hallow case shown in Figure 1a. There are papers with extremely tight focusing of hard XFEL beam. The record for today is 7*7 nm^2 waist at a target surface and huge intensity 10^{22} W/cm2 (similar to the petaWatt optical lasers) [10]. But in this case, the length $z_R \sim (R/\lambda)\ R$ is greatly reduced. The length z_R becomes less than the attenuation length D_{att}. Then the length L of the cylindrical cavity will be limited by the value of z_R, and not by the attenuation length D_{att} due to absorption. In our case [3], these lengths are of the same order $z_R \sim D_{att}$, because our beam radius R the surface of target is 200 nm. This is an optimal value. Due to this, the maximum L is achieved. In our case [3], the beam waist is located on the target surface.

A tempting future possibility is to focus the hard XFEL beam inside the volume. In this case, the waist is located below the surface of the target at the depth of one or few Rayleigh length z_R.

Pressure wave propagation in LiF, radial material flow, formation of cracks and voids are analyzed via continuum and atomistic simulations [3] revealing a sequence of processes leading to the final structure with the long cavity [3] shown in Figure 1e. Similar results can be produced with semiconductors and ceramics, which opens a new pathway for development of laser material processing with hard X-ray pulses.

1. Yu.V. Petrov, et al., *ZhTEF* **167**, 645 (2025). In Russian.
2. A. Dyshlyuk, et al., *Bulletin of the Russian Academy of Sciences: Physics* **88**(3), S450 (2024).
3. S. Makarov, et al., 2024 arXiv:2409.03625 [physics.plasm-ph].
4. V.P. Veiko, V.I. Konov (ed.), *Fundamentals of laser-assisted micro- and nanotechnologies* (Springer Verlag), (2014).
5. L.A. Smillie, et al., *Phys. Rev. Mat.* **4,** 093803 (2020).
6. Z. Yao, et al., *Optics Express* **26**(17), 21960 (2018).
7. R. Meyer, et al., *Appl. Phys. Lett.* **114**, 201105 (2019).
8. H.D. Nguyen, et al., *Ultrafast Science* **4**, 0056 (2024).
9. G. Zhang, et al., *Ultrafast Science* **5**, 0103 (2025).
10. J. Yamada, et al., *Nature Photonics* **18**, 685 (2024).

I13

Forward growth of ferroelectric domains created by femtosecond laser irradiation in lithium niobate single crystals

A.R. Akhmatkhanov, I.A. Kipenko, B.I. Lisjikh, M.S. Kosobokov, A.U. Ushakov, V.Ya. Shur

School of Natural Sciences and Mathematics, Ural Federal University, 620000 Ekaterinburg, Russia
andrey.akhmatkhanov@urfu.ru

Femtosecond-laser-induced modification of materials has become nowadays one of the most promising techniques for in-bulk modification of various materials [1]. The underlying mechanism of light-matter interaction consisting in two-/multi-photon absorption provides two main advantages of this method: the possibility to achieve sub-wavelength resolution by breaking the diffraction limit while leaving the surrounding material unaffected and the possibility of modification of the materials with low linear absorption coefficients at the utilized laser wavelength [1]. Recently it was shown that this method is applicable for in-bulk modification of ferroelectric domain structures thus opening the possibilities of creation of 1D, 2D and 3D periodical domain structures for nonlinear frequency conversion of coherent light. Despite the strong potential of the method, its application to creation of periodical domain structures on the large areas can be a challenging task. That's why it is important to develop the combined methods of periodical poling including creation of seed domains by fs-laser irradiation and application of uniform electric field for their further forward growth.

Two types of samples have been studied: congruent lithium niobate cut at 36° to Y axis (CLN36Y) and MgO doped congruent lithium niobate cut perpendicular to the polar axis (MgOLN). The initial in-bulk domains were created by local fs-laser irradiation by femtosecond regenerative amplifier (TETA-10, Avesta Project, Russia) based on a Yb-solid state laser delivering 250-fs laser pulses with wavelength 1030 nm, frequency 100 kHz, and energy from 2 to 10 μJ. Laser irradiation was focused approximately at the center of the sample by the objective with numerical aperture 0.65. The positioning of the focus spot was realized by 3D-motorized table (Zolix Instruments, China).

The second harmonics generation microscopy (SHGM) imaging has revealed the formation of spindle-like domains at the spots of fs-laser irradiation with the length about 60-100 μm. These domains were elongated along the irradiation direction. It was shown that the application of uniform electric field with polar component 20.6 kV/mm for CLN36Y and 5 kV/mm for MgOLN leads to forward growth of the created spindle-like domains which starts from their vertexes. The shape changes of the domains during forward growth and after touching the sample's surfaces are discussed. The forward growth velocities in both directions were extracted and analyzed.

Obtained results are important for further development of fa-laser assisted domain engineering methods in ferroelectrics.

The research was made possible by Russian Science Foundation (Project № 24-12-00302). The equipment of the Ural Center for Shared Use "Modern nanotechnology" Ural Federal University (Reg.№ 2968) was used.

1. Y. Sheng, X. Chen, T. Xu, et al., *Photonics* **11**, 447 (2024).
2. T. Xu, K. Switkowski, X. Chen, et al., *Nature Photon.* **12**, 591 (2018).

I14

Fabrication of electro-optic deflectors and modulators based on domain engineered ferroelectrics

A.D. Ushakov[1], W. Huang[2], M.A. Chuvakova[1], I.A. Kipenko[1], X. Liu[2], H. Zheng[2], X. Wei[2], V.Ya. Shur[1]

[1]*School of Natural Sciences and Mathematics, Ural Federal University, 620000 Ekaterinburg, Russia bddah@ya.ru*

[2]*Electronic Materials Research Laboratory, Key Laboratory of the Ministry of Education and International Center for Dielectric Research, Xi'an Jiaotong University, 710049 Xi'an, China*

We introduce the study on two distinct electro-optic applications of relaxor ferroelectric single crystals with tailored domain structures: the deflector based on PMN-PT and the electro-optic modulator employing PIN-PMN-PT.

The first part of our research focuses on developing an advanced beam steering apparatus using [001]-oriented $Pb(Mg_{1/3}Nb_{2/3})O_3$-$PbTiO_3$ single crystals. The operational mechanism of this device exploits voltage-controlled birefringence modifications $\Delta n(E)$ to achieve beam steering. Motivated by the high electro-optic coefficient of PMN-PT family crystals, approximately 100 pm/V [2,3], we developed a prototype of electro-optic deflector using [001]-cut PMN-PT crystals possessing tetragonal symmetry. Following the establishment of a single-domain state, a stable cascaded domain structure was created using a surface fixation technique. The quality of the domain structure within the crystal bulk was verified using the second-harmonic generation microscopy. The achieved deflection efficiency of $2.5 \cdot 10^{-4}$ deg/V/mm is comparable to previous results obtained with CLN [1].

The second part of our research introduces an innovative approach for preparation of the [110]-cut rhombohedral PIN-PMN-PT crystals for electro-optic modulators. In contrast to previous studies [4] established that field-cooling technique could enhance optical clarity by inducing the domain structure of specific type thus eliminating light-scattering boundaries, it suffers from the long processing time. Our solution implements a room-temperature protocol combined with real-time domain imaging, yielding a simplified and more reliable procedure that maintains both excellent electro-optic characteristics and optical transparency.

These findings collectively demonstrate the significant opportunities presented by tailored domain configurations in PMN-PT-based ferroelectric materials for next-generation photonic systems.

The authors are grateful for financial support of the Ministry of Science and Higher Education of the Russian Federation (state task FEUZ-2023-0017). The work was performed using the equipment of the Ural Center for Shared Use "Modern Nanotechnologies" UrFU (reg. No. 2968).

1. J. Li, et al., *Appl. Phys. Rev.* **10**, 031413 (2023).
2. X. Wan, et al., *Appl. Phys. Lett.* **85**, 5233 (2004).
3. Q. Hu, et al., *Appl. Phys. Lett.* **115**, 222901 (2019).
4. X. Liu, et al., *Science*, **376**, 371 (2022).

I15

Spectroscopic investigations of dipole moment in $BaSrTiO_3$ thin films

A.M. Pugachev[1], A.V. Tumarkin[2]

[1]*Institute of authomation and electrometry RAS, 630090 Novosibirsk, Russia*
apg@iae.nsk.su

[2]*St. Petersburg State Electrotechnical University "LETI", 197376 St. Petersburg, Russia*

Thin ferroelectric films of $Ba_{0.5}Sr_{0.5}TiO_3$ grown on various substrates (Sp, $LaAlO_3$ polycor) using Rf spattering technology were studied using spectroscopic methods (IR absorption, Raman scattering, second harmonic generation). The samples were synthesized at the St. Petersburg State Electrotechnical University. The actual properties of these films were obtained.

The thickness of the films (in the vicinity of 500 nm) was determined by the IR spectroscopy method during the analysis of the interference interaction of the IR radiation reflected from the film and the substrate, and the growth rates at different deposition temperatures were compared.

In the Raman spectroscopy experiments, a uniformly broadened component in the vicinity of 300 cm^{-1} (E (TO) phonon), similar to the peak described in [1] was investigated. It was shown that, just as in the crystal and ceramics of barium titanate [2], the relative integral value of this component is proportional to the magnitude of spontaneous polarization. Test measurements showed that the temperature dependence of this line in barium titanate ceramic [3] demonstrated the presence of phase transitions between the rhombohedral, orthorhombic, tetragonal and cubic phases.

Second optical harmonic generation (SHG) experiments demonstrated the temperature evolution of the dipole moment in the mentioned above films when the transition from the tetragonal to the cubic phase occurred. The results of the SHG experiments, describing the temperature dependence of spontaneous polarization, correspond to the temperature dependence of the integrated intensity of the E(TO) phonon line.

The study was supported by the Russian Science Foundation No. 25-22-20030.

1. A.S. Anokhin, A.G. Razumnaya, Yu.I. Yuzyuk, Yu.I. Golovko, V.M. Mukhortov*, Physics of the Solid State,* **58**(10), 1956 (2016).

2. A.M. Pugachev, I.V. Zaytseva, N.V. Surovtsev, A.S. Krylov, *Ceramics International* **46**, 22619 (2020).

3. L. Gimadeeva, A. Ushakov, A. Pugachev, A. Turygin, R. Jing, X. Wei, Z. Hu, V. Shur, L. Jin, D. Alikin, *Journal of Materiomics*, **11**(5), 101014 (2025).

I16

Custom functionalization of monolayers and ultrathin films

X. Chang[1], A. Nashchekin[2], L. Chi[1,3], Y. Fang[1,4], O. Ivasenko[1,3]

[1]*State Key Laboratory of Bioinspired Interfacial Materials Science, Institute of Functional Nano & Soft Materials (FUNSOM), Soochow University, 215123 Suzhou, China*
ivasenko@suda.edu.cn

[2]*Characterization of Materials and Structures of Solid State Electronics Laboratory, Ioffe Institute, 194021 St. Petersburg, Russia*

[3]*Jiangsu Key Laboratory of Advanced Negative Carbon Technologies, Soochow University, Suzhou, 215123 Jiangsu, PR China*

[4]*Jiangsu Key Laboratory for Carbon-Based Functional Materials & Devices, Soochow University, Suzhou, 215123 Jiangsu, PR China*

Precisely engineering and characterizing interfacial layers on carbon-based materials is crucial for optimizing their performance in diverse applications, particularly sensing and electronics. Developing well-defined functional platforms allows for fundamental insights into surface processes and the rational design of advanced materials. Our research focuses on achieving custom functionalization of graphene and graphite surfaces with controlled nanoscale precision.

We have explored the controlled direct covalent grafting of heterocycles onto carbon substrates, focusing on achieving ultrathin adlayers (<1 nm). Beyond the initial grafting, we have studied the reactivity of these surface-bound grafts through on-surface reactions. This allows for post-modification and fine-tuning of the surface functional groups. Examples include N-alkylation and nucleophilic aromatic substitution reactions on grafted pyridine-based adlayers. These reactions confirm the accessibility of the surface-bound heterocycles and highlight the potential for creating complex surface functionalities in a modular fashion. Furthermore, such modifications can lead to responsive interfaces, where properties like charge transport can be reversibly modulated, for example, via changes in pH.

The utility of these custom-engineered interfaces has been showcased in model applications, particularly in the design and testing of biosensor interfaces. By controlling the nanoscale architecture and functional group presentation, we can significantly enhance the sensitivity and selectivity of detection. For example, an ultrathin monolayer of carboxy-functionalized groups grafted via controlled diazonium chemistry dramatically improved the electrochemical detection of epinephrine at sub-micromolar concentrations, facilitated by favorable electrostatic interactions. This work underscores how molecular-level surface engineering on high-quality carbon substrates provides a powerful platform for the rational design of advanced electrochemical sensing interfaces, contributing significantly to the characterization and application of functional micro- and nano-materials.

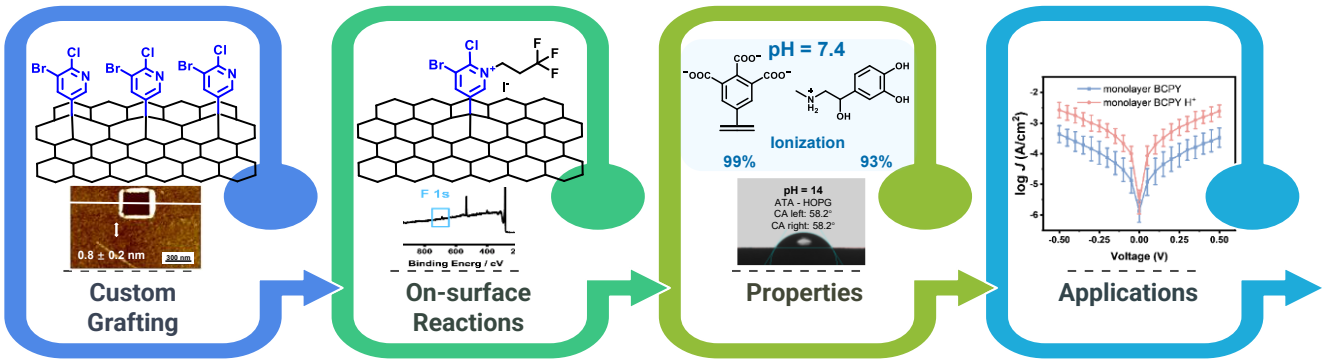

Figure 1. Design, grafting, and reactivity of covalent adlayers for the construction of custom functional interfaces.

1. J. Wekalao, L. Hao, I. Ul Haq, *et al.*, *Plasmonics* (2025), https://doi.org/10.1007/s11468-025-02946-0
2. X. Xie, X. Chang, S. Kang, Y. Fang, O. Ivasenko, *Chem. Commun.* **60**, 8375 (2024).
3. X. Chang, Y. Fang, O. Ivasenko, Molecules, *under revision*.

I17

Advanced design and polarization regulation strategies in relaxor ferroelectric ceramics for enhanced energy storage performance

Li Jin

Electronic Materials Research Laboratory, Key Laboratory of the Ministry of Education, School of Electronic Science and Engineering, Xi'an Jiaotong University, Xi'an 710049, China
ljin@mail.xjtu.edu.cn

Relaxor ferroelectric ceramics have garnered significant attention for their potential in energy storage applications due to their unique polarization characteristics. However, achieving high energy-storage density (W_{rec}) and energy-storage efficiency (η) while maintaining material reliability remains a key challenge. This study consolidates three innovative approaches to design and optimize relaxor ferroelectricity and polarization regulation in $(Bi_{0.5}Na_{0.5})TiO_3$ (BNT)-based ceramics, leading to exceptional energy storage performance.

The first approach introduces a cooperative optimization strategy involving a nonergodic-to-ergodic phase transformation in $0.85(Bi_{0.5}Na_{0.5})_{0.7}Sr_{0.3}TiO_3$-$0.15NaNbO_3$ ceramics. The implementation of a viscous polymer process (VPP) significantly reduces porosity and enhances material compactness, resulting in an impressive W_{rec} of 7.6 J/cm^3 and η of 90% under 410 kV/cm. This method also ensures reliable temperature adaptability across a broad range (20–120 °C).

The second approach employs entropy engineering, leveraging local polar fluctuations and high-entropy design to regulate the energy storage performance of BNT-based dielectrics. By optimizing the atomic configurational entropy in $0.85(Bi_{0.375}Na_{0.3}Sr_{0.25}K_{0.075})TiO_3$-0.15 $Bi(Mg_{0.5}Sn_{0.5})O_3$ ceramics, the study achieves an outstanding W_{rec} of 11.24 J/cm³ and η of 88.3% under 610 kV/cm. The high-entropy ceramics exhibit remarkable discharge characteristics and temperature stability, demonstrating the efficacy of entropy manipulation in enhancing dielectric performance.

The third strategy focuses on mitigating polarization-strain coupling in multilayer ceramic capacitors (MLCCs) to address fatigue and ultrasonic damage in pulse power systems. By designing a composition with ultra-low electrostrictive coefficient (Q_{33}) of 0.012 m^4/C^2 in $0.55(Bi_{0.5}Na_{0.5})TiO_3$-$0.45Pb(Mg_{1/3}Nb_{2/3})O_3$, the study achieves a minimal strain of 0.118% at 330 kV/cm. This approach enables a significant ESP of 7.6 J/cm^3 and an ultrahigh η of 93% under 720 kV/cm, ensuring excellent fatigue resistance and temperature stability.

Collectively, these advanced design strategies underscore the potential of tailored relaxor ferroelectric ceramics in next-generation energy storage applications, offering a path forward for achieving high-performance, reliable, and efficient dielectric materials.

I18

Energy storage performance and bandgap tuning in $BaTiO_3$ and $Bi_4Ti_3O_{12}$ based ceramics

J.A. Eiras[1], M.S. Alkathy[1], F.L. Zabotto[1], M.H. Lente[2], E.B. Araujo[3], I.A. dos Santos[4]

[1]*Depto. de Física, Universidade Federal de São Carlos, São Carlos, SP CEP 13565-905, Brazil*
eiras@df.ufscar.br

[2]*Instituto de Ciência e Tecnologia, Universidade Federal de São Paulo, São José dos Campos, SP, Brazil*

[3]*Depto. Física, Universidade Estadual de São Paulo, Ilha Solteira, SP, Brazil*

[4]*Depto. Física, Universidade Estadual de Maringá, Maringá, PR, Brazil*

Ferroelectric materials due to their multifunctionality become increasingly important as promising materials to address energy challenges and exhibiting potentially improved energy storage and photovoltaic performance. In light of this, doped ferroelectric (FE) oxides are being investigated through compositional engineering (e.g., doping with transition metals) viewing to the influence that defects dipoles can promote as well on the spontaneous polarization and domains switching dynamics as on optical properties. This talk will cover recent investigations into acceptor doping of $BaTi_{0.95}Zr_{0.05}O_3$ (BZT) and $Bi_{3.25}Sm_{0.75}Ti_3O_{12}$ (BSmT) based ceramics. Lithium ions were selected as acceptor ions substituting in Ba site of BZT perovskite, while (Co/Fe) were used substituting Ti on three perovskites layers BSmT ceramics. A systematic investigation of its effect on the structural, dielectric, ferroelectric, optical and energy storage properties has been performed. The obtained results indicate that acceptor doping, inducing the formation of oxygen vacancies (VO) plays an essential role in changing the ferroelectric hysteresis loops. Pinched hysteresis loops with high maximum polarization and small remnant polarization were acquired in the BZT based ceramics when the doping content was raised, increasing the recoverable energy density. On the other side, unsaturated leaky but wide P-E hysteresis loops (characteristic from strong domain switching), caused by Co-VO or Fe-VO dipoles defects resulted in lower recoverable energy density for the BSmT ceramics, compared with BZT based ceramics. Optical studies, viewing to tune the band gap for solar radiation absorption, showed that the BSmT band gap was reduced from 3.22 eV to 2.02 eV with Co/Fe co-doping, which can be attributed to the modulation of orbital overlaps and compensation mechanisms. The experimental results will be correlated with the crystallographic structure, structural distortions, grain morphology and dipole defects caused by doping.

I19

Improving the stability of halide perovskites by mixed cation substitutions

E.B. Araújo, R.M. Silva Jr, F.B. Minussi, M.A.M. Teixeira

Department of Physics and Chemistry, São Paulo State University, 15385-000 Ilha Solteira, Brazil
eudes.borges@unesp.br

Hybrid halide perovskites have been intensively studied recently due to their exceptional properties and potential for optoelectronic and photovoltaic applications. Despite unprecedented success in low-cost laboratory applications, the low stability of materials and devices based on halide perovskites is one of the main bottlenecks for their commercial applications. The degradation of the physical properties of halide perovskites is a complex problem whose degradation mechanisms have not yet been satisfactorily understood and is a real challenge to overcome. Humidity, intense illumination, high temperatures, thermal stresses, and interfacial reactions are possible events that trigger degradation processes in photovoltaic devices based on halide perovskites. Mixed-component formulation has emerged as a promising engineering strategy to control degradation processes and design high-performance halide perovskite compositions. The present work reports a systematic study of the thermal degradation of methylammonium lead iodide ($MAPbI_3$) compositions partially substituted with guanidinium (GA^+), formamidinium (FA^+), and acetamidinium (AC^+) cations, prepared under different thermal treatment conditions to investigate the evolution of their structural, microstructural, electrical, dielectric, thermal and optical properties. The results show that mixed-cation halide perovskites exhibit higher thermal stability with lower degradation rate constants. However, guanidinium-rich compositions show increased rate constants due to $GAPbI_3$ segregation triggered by the volatilization of MA^+ and related molecules. The ionic conductivity and electronic charge carrier mobility are reduced in solid solutions, while the electronic charge carrier density is slightly larger. Ionic conductivities are lower in equimolar solid solutions, while substituting MA^+ greatly reduces electronic charge carrier mobilities. Light-accelerated degradation tracked with X-ray diffraction and scanning electron microscopy coupled with energy dispersive X-ray spectroscopy shows that AC^+ incorporation does not significantly enhance the materials' stability. The work advances the understanding of thermal degradation processes and how to increase the thermal stability of halide perovskites.

I20

Magnetogalvanic effect in metallic tetragonal antiferromagnets

Z.V. Gareeva[1], A.I. Popov[2], A.K. Zvezdin[3]

[1]*Institute of Molecule and Crystal Physics, 450054 Ufa, Russia*
zukhragzv@yandex.ru

[2]*National Research University of Electronic Technology MIET, 124498 Moscow, Russia*

[3]*Prokhorov General Physics Institute of the Russian Academy of Sciences, 119991 Moscow, Russia*

In recent years, metallic antiferromagnets have attracted significant attention due to their potential for spintronic applications. Among these, CuMnAs and Mn_2Au are particularly notable for their high Néel temperatures (~480 K and ~1351 K, respectively), excellent conductivity, and demonstrated capability for current-induced switching of antiferromagnetic order [1, 2].

In this report, we consider a mechanism of spin dynamics in antiferromagnets based on general symmetry consideration. By employing group - theoretical analysis, we derive invariant combinations of magnetic and electric order parameters and demonstrate that the magnetoelectric effect is intrinsic to tetragonal antiferromagnets such as CuMnAs and Mn_2Au

$$\Phi_{me} = g_1 L_z \left(M_x P_y + M_y P_x \right) + g_2 M_z \left(L_x P_y + L_y P_x \right) + g_3 P_z \left(L_y M_x + L_x M_y \right) \quad (1)$$

where $\boldsymbol{L}=\boldsymbol{M}_1-\boldsymbol{M}_2$ is antiferromagnetic vector, $\boldsymbol{M}_1$, $\boldsymbol{M}_2$ are the Mn^{3+} ions sublattice magnetizations, $\boldsymbol{P}$ is the magnetically induced electric polarization.

We show that the presence of the magnetoelectric invariant (1) naturally leads to electrically induced torques, including Neel spin orbit torque [3], which are crucial for understanding various aspects of current-driven spin dynamics.

Another key phenomenon we investigate is the magnetogalvanic effect, which arises in tetragonal antiferromagnets under the application of a time-varying magnetic field $\boldsymbol{H}(t)$. We explore the generation of electric currents in response to external magnetic fields, considering different field orientations and profiles to clarify the underlying mechanisms of current emergence and dynamic behaviour. By examining the electric response to alternating magnetic fields, we identify key features, including current stabilization and harmonic responses. Figure 1 shows the electrical response to a field $\boldsymbol{H}$||[001]. These findings deepen our understanding of the interplay between symmetry, magnetization dynamics, and electric current generation in antiferromagnetic materials, offering new insights for the development of advanced spintronic technologies.

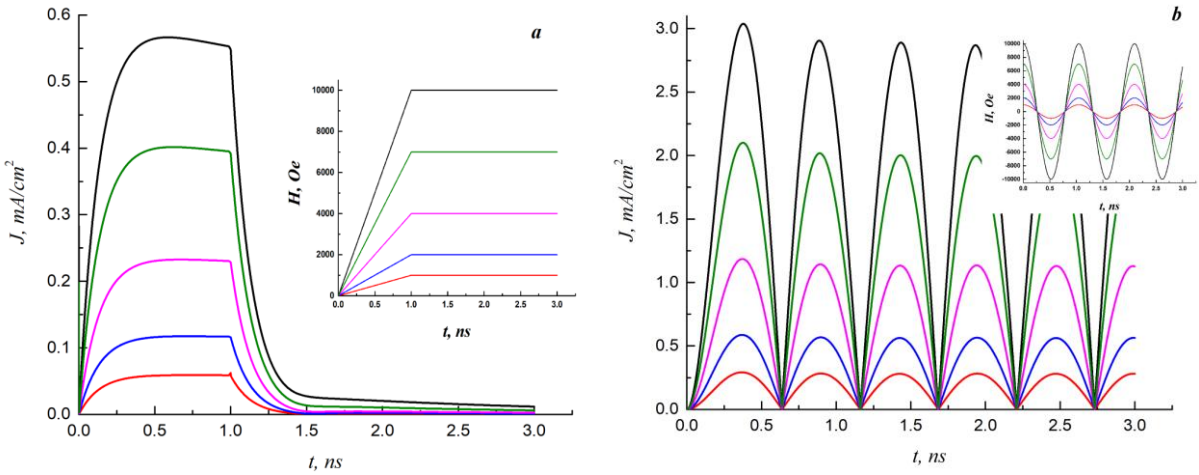

Figure 1. Temporal dependences of the amplitude of electric current induced by a magnetic field $\boldsymbol{H}(t)$||[001] (a) linear $\boldsymbol{H}(t)$, (b) harmonic $\boldsymbol{H}(t)$. The form of $H(t)$ is shown in the figures inset. Material parameters used in our calculations are consistent with experimental data [2].

1. S. Reimers et al., *Phys. Rev. Appl.* **21**, 064030 (2024).
2. V. Barthem, et al., *Nat. Commun.* **4**, 2892 (2013).
3. J. Železný et al., *Phys. Rev. Lett.* **113**, 157201 (2014).

I21

Raman spectroscopy to study magnetic transitions in borate crystals

A.S. Krylov, A.N. Vtyurin, S.N. Krylova, S.N. Sofronova

Kirensky Institute of Physics Federal Research Center KSC Siberian Branch Russian Academy of Sciences, 660036 Krasnoyarsk, Russia
shusy@iph.krasn.ru

Raman spectroscopy has long been widely used to study structural phase transitions. The study of magnetic phase transitions of samples in an external magnetic field is also widely presented in the literature. In this paper, we want to present the results of studying magnetic transitions without an external magnetic field.

Here we will consider two classes of crystals with huntite and kotoite structure. These crystals belong to different families of borates. They contain magnetic and rare earth ions.

The ferroborates with the huntite structure with the general formula of $ReMe_3(BO_3)_4$ (Re = rare-earth cation, Me = Fe, Ga) are the objects of many studies due to the wide range of promising physical properties. They are multiferroic, combining the mutual influence of magnetic and electrical subsystems, where transition points may be varied by substituting as rare earth element as a magnetic ion [1]. We present the Raman spectroscopy result of the investigation of single crystals and a solid solution.

Temperature measurements were performed in the temperature range 10–150 K. This study aims to investigate the possible interaction of a soft mode related to structural order parameter and effects of magnetic transitions on Raman spectra. Analysis of the experimental Raman spectra, temperature dependences of the provisions of the centers of lines, their width and relative intensity was carried out, as well as theoretical temperature approximation for some lines. Some anomalies in the temperature dependences of the spectral lines associated with the occurrence of magnetic order. It was found that significant changes are observed in the spectrum of low-frequency range (below 100 cm^{-1}) - there is a mode corresponding to two-magnon scattering. The structural phase transition accompanied condensation of soft mode [2, 3].

The oxyborates $Ni_{3-x}Co_xB_2O_6$ oxyborates with the kotoite structure are known as antiferromagnetic materials and are of interest for optical applications and as promising battery anode materials. The evidence of spin-phonon interaction was found for some specific phonons below T_N. The anomalies in the behavior of these phonon modes as a function of the nickel concentration in the crystal have been presented. The position and intensity of the Raman modes decrease when the Ni atoms are replaced by Co atoms [4].

Russian Science Foundation and Krasnoyarsk Regional Science Foundationfunded the reported study according to the research project № 23-12-20012.

1. A.S. Krylov, et al. *Solid State Commun*. **174**, 26 (2013).
2. E. Moshkina, et al. *Cryst. Growth. Des.* **16**, 6915 (2016).
3. E. Moshkina, et al. *Cryst. Growth. Des.* **20**, 1058 (2020).
4. S.N. Sofronova, et al. *J. Raman Spectrosc.* **56**, 435 (2025).

I22

Long-lived photoinduced nonthermal coercivity reduction of $L1_0$-FePt and FePtRh epitaxial thin films

R.V. Yusupov[1], A.V. Petrov[1], S.I. Nikitin[1], L.R. Tagirov[1,2], A.S. Kamzin[3]

[1]*Kazan Federal University, 420008 Kazan, Russia*
Roman.Yusupov@kpfu.ru

[2]*Zavoisky Physical-Technical Institute, Kazan, Russia*

[3]*Ioffe Institute, St.-Petersburg, Russia*

Intermetallic compounds like FePt and FePd as well as their solid solutions with some nonmagnetic metals are capable of self-arrangement to the tetragonal $L1_0$ atomic layer-by-layer structure in which they possess strong uniaxial magnetic anisotropy. Properly prepared epitaxial thin films of FePt-based materials on, e.g., MgO (001) substrates manifest perpendicular magnetic anisotropy of the order of 10^7 erg/cm^3 therefore are promising for high-capacity magnetic storage devices. Several-nanometer large grain is enough to satisfy the superparamagnetic limit. The drawback however is a strong coercivity that cannot be overcome by writing heads in modern hard disks. One way to release this constraint is the heat-assisted magnetic recording [1] that assumes a temporary local heating up the material close to the Curie temperature thus reducing the coercivity value. It, however, induces a strong mechanical strain at the interface of the film and a substrate thus reducing durability of a device based on such a medium. Here, we demonstrate another approach for coercivity reduction not involving a significant heating up though still based on optical pumping.

The time-resolved magneto-optical Kerr effect in epitaxial thin films of the FePt compound and the $FePt_{0.84}Rh_{0.16}$ solid solution with perpendicular magnetic anisotropy on the MgO (001) substrates was studied. The evolution of hysteresis loops on fast (100 fs – 1 ns) and slow (1 – 20 ms) time scales after the excitation with a femtosecond light pulse was studied. The effect of long-lived non-thermal magnetic softening was discovered. The value of the coercive field is restored on a time scale of milliseconds. A hypothesis relating the observed phenomenon to the excitation of high-Q acoustic resonances in the substrate/film system and strong magnetoelastic interaction in FePt and $FePt_{0.84}Rh_{0.16}$ films is proposed [2].

Comparison of the hysteresis loops under ultrashort pulse laser excitation with the data of static magnetometry indicates the nonthermal origin of the decrease in coercivity, since the temperature is restored after approximately 2 ns from the pump pulse.

The process of magnetization reversal of a continuous thin film with perpendicular magnetic anisotropy includes two necessary stages, namely, the nucleation of domains with the opposite direction of magnetization and their growth via the domain wall motion. Since both nucleation and the motion of domain walls are of an activation origin, we suggest that a broadband hypersonic wave induced by a femtosecond laser pulse in a film excites the high-Q (therefore slowly decaying) acoustic resonances in the single-crystal MgO substrate with near-ideal parallel faces. Standing acoustic waves promote a mechanical strain in epitaxial magnetic films, which increase the energy of the magnetic subsystem via the inverse magnetostriction. The latter promotes domain nucleation and facilitates overcoming potential barriers by domain walls arising from the pinning on defects [3]. We note also a known for many decades strong magnetoelastic coupling in FePt compound [4].

Support by the Kazan Federal University Strategic Academic Leadership Program (PRIORITY-2030) is acknowledged.

1. M.H. Kryder, E.C. Gage, T.W. McDaniel, *Proceedings of the IEEE* **96**, 1810 (2008).
2. A.V. Petrov, et al., *JETP Letters* **118**, 117 (2023).
3. L. Thevenard, et al., *Physical Review B* **93**, 140405 (2016).
4. N.S. Akulov, Z.I. Alizade, K.P. Belov, *Doklady Akademii Nauk SSSR* **65**, 815 **(**1949).

I23

Specific heat behavior in real ferroelectric crystals

I.V. Shnaidshtein, S.V. Grabovsky, A.A. Zilbert

Faculty of Physics, Lomonosov Moscow State University, 119991 Moscow, Russia
shnaidshtein@physics.msu.ru

The study of temperature-dependent heat capacity near ferroelectric phase transitions provides insights into the nature and type of these transitions, forming the basis for the thermodynamic classification of ferroelectrics. Imperfections in the crystal structure – such as defects, impurities, domains, and interphase boundaries—can influence the shape of heat capacity anomalies in various ways. Consequently, analyzing these anomalies helps clarify the nature of structural defects.

The experimentally measured heat capacity comprises contributions both related and unrelated to the phase transition. The latter, referred to as the background heat capacity, typically exhibits weak dependence on lattice inhomogeneities. For this reason, data analysis begins with calculating the background heat capacity, the accuracy of which determines the reliability of anomaly determination.

Notably, defects can distort heat capacity anomalies in a manner resembling the effects of order parameter fluctuations near the phase transition temperature in ideal crystals, as described by the Levanyuk–Sigov theory. Distinguishing between these two sources of distortion requires precise determination of the critical indexis of heat capacity within the phase transition region.

An additional complication in the temperature dependence of heat capacity arises from the superposition of anomalies in crystals undergoing sequential phase transitions. Analyzing such cases necessitates consideration of the material's phase diagram.

This review outlines the current understanding of the relationship between the shape of heat capacity anomalies in ferroelectric crystals and the types of structural inhomogeneities responsible for deviations from the "ideal" behavior expected in a perfect crystal.

The key distinction between this work and the eponymous review [1] lies in the detailed examination of multiaxial ferroelectrics, which was not covered in [1]. Particular focus is given to barium titanate crystals and lead magnoniobate-based compounds. The discussion incorporates both previously published data [2,3] and new results obtained in our study. These findings are compared with small available literature on the influence of domain switching processes on the thermal properties of ferroelectrics.

The study was conducted under the state assignment of Lomonosov Moscow State University.

1. B. Strukov, I. Shnaidshtein, A. Onodera, *Ferroelectrics* **363**, 27 (2008).

2. S.V. Grabovsky, I.V. Shnaidshtein, M. Takesada, A. Onodera, B.A. Strukov, *J. Adv. Diel.* **3**, 1350032 (2013).

3. S. Grabovsky, I. Shnaidshtein, J. Przeslawski, Zhenrong Li, Zhuo Xu, B. Strukov, *J. Adv. Diel.* **7**, 1750032 (2017).

I24

Disorder effects and line shapes in Raman spectra of multiferroic crystals

A.N. Vtyurin, A.S. Krylov, S.N. Krylova

Kirensky Institute of Physics, 660036 Krasnoyarsk, Russia
vtyurin@iph.krasn.ru

Anomalies of low frequency lattice vibrations, especially condensations of soft phonon modes corresponding to fluctuations of the order parameter of phase transitions are the most striking physical effects, that in many cases determine mechanisms of instability of a crystal lattice. Dependences of such modes on external parameters (temperature, pressure, electric or magnetic fields) allow us to establish many characteristics of the crystals under study that are important both for solving problems of fundamental solid-state physics and for practical applications. The technique of Raman spectroscopy is widely used for such investigations.

To improve the accuracy of determining the frequencies of the Raman spectrum lines, computer processing of the spectrum is currently generally used. In this case, dispersion or Gaussian contours, or a combination of both, are used to describe the shape of the spectral lines.

It is known that the shape of the Raman scattering line in an ideal crystal in the case of small damping is described by the dispersion contour, therefore it is used in many standard programs for processing spectra. At the same time, when studying low-frequency oscillations, when the line frequency becomes comparable to its width and approaches the elastic scattering wing or approach each other, the line contour becomes obviously asymmetric, which makes determining the Raman scattering line frequency problematic. To solve this problem, various approximate approaches were previously proposed (see, for example, [1]), but the shape of the spectral line contour was still assumed to be dispersive. At the same time, it was shown in [2] that when the frequency of the soft mode is reduced near the phase transition, the contour of the corresponding line becomes asymmetric and differs significantly from the dispersion one. Additional distortions in spectral contours can be introduced by mode interactions with quasi-elastic scattering on structural defects and non-critical low-frequency lattice vibrations.

The report will present examples of processing low-frequency Raman scattering spectra taking these factors into account.

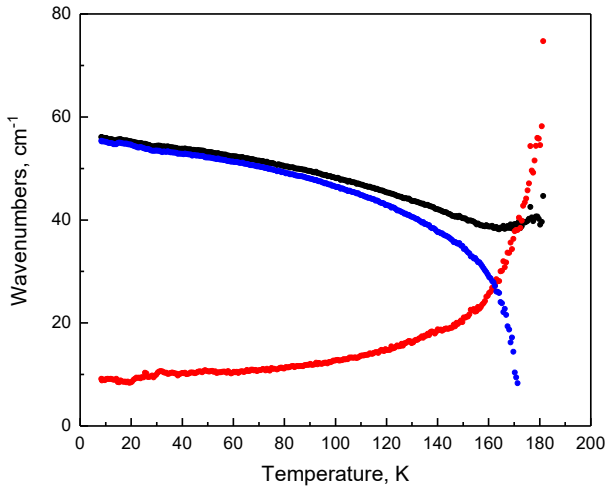

Figure 1. Results of processing the temperature dependence of the low-frequency spectrum of the $HoFe_2Ga(BO_3)_4$ crystal. The black curve is the soft mode frequency obtained using the dispersion contour, the blue curve is its frequency obtained using [2], and the red one is the damping parameter.

Low-frequency Raman spectra of some ferroborate crystals and complex oxides are used as examples.

1. H. Taniguchi, M. Itoh, D. Fu, *J. Raman Spectroscopy* **42**, 706 (2010).
2. V.L. Ginzburg, A.P. Levanyuk, A.A. Sobyanin, *Physics Reports* **57**, 151 (1980).

ORAL
PRESENTATIONS

O1

Quantum dots in nanowires for sources of non-classical light

S.V. Mikushev, V.G. Dubrovskii, E.D. Leshchenko, R.R. Reznik

Faculty of Physics, St. Petersburg State University, 199034 St. Petersburg, Russia
s.mikushev@spbu.ru

Nanostructured materials based on III-V compound semiconductors are poised to transform scalable quantum photonics and secure communication systems. III-V quantum dots (QDs) in nanowires (NWs) in different material systems including (In)GaAs/AlGaAs, InAsP/InP and InGaN/GaN are one of the most promising candidates for efficient sources of non-classical light, with a possibility for on-demand generation, detection, and manipulation with single and entangled photons, photonic cluster states and electron spins. Here, we review our recent achievements in the design, synthesis and characterization of III-V QDs in the body of freestanding III-V NWs. We show how the advanced modeling of the vapor-liquid-solid (VLS) and vapor-solid (VS) growth of III-V ternary NWs and heterostructures of different types based on such NWs enables precise design and control of the NW composition and interfacial abruptness in NW heterostructures by the growth parameter tuning (material fluxes, total V/III ratio, growth temperature) during molecular beam epitaxy (MBE) and related technologies [1-3]. Very importantly, these structures can be synthesized on Si substrates, which allows for monolithic integration of III-V nanophotonics with the Si electronic platform [2]. Furthermore, we show that III-V NW heterostructures provide almost unlimited opportunities for the bandgap engineering and material combinations that are unattainable in epi-layers due to the lattice-mismatch issues [1-5].

We then demonstrate the suppression of the thermodynamically forbidden miscibility gaps in highly mismatched InGaAs [2,5] and InGaN [6] material systems with strong interactions between dissimilar III-V pairs. This effect originates from the specific features of the VLS or VS NW growth, including fast kinetics and quasi-instantaneous formation of III-V ternary monolayers on top of NWs. The latter feature is shown to yield spontaneous core-shell heterostructures in MBE-grown InGaN NWs [6], where In-rich $In_xGa_{1-x}N$ cores (with $x\sim0.4$) demonstrate efficient red emission at 650 nm. We consider the formation mechanisms and electronic structure of wurtzite (WZ) AlGaAs NWs [4], which become direct bandgap in the WZ phase. It is emphasized that the WZ phase formation in zincblende (ZB) III-V semiconductors, the controlled WZ/ZB polytypism and WZ/ZB heterostructures with extremely abrupt interfaces are possible only in NWs. Finally, we discuss optical properties of (In)GaAs QDs in WZ AlGaAs NWs, accessed by spatially and time-resolved photoluminescence techniques [4,5,7], single-photon emission from GaAs QDs in AlGaAs NWs, fine-tuning of the NW QD emission to atomic resonances, manipulations with quantum optical states, and possible implications of these structures in quantum information technologies.

1. V.G. Dubrovskii, E.D. Leshchenko, *Phys. Rev. Mater*. **7**, 074603 (2023).
2. E.D. Leshchenko, V.G. Dubrovskii, *Nanomaterials* **13**, 1659 (2023).
3. V.G. Dubrovskii, *Phys. Rev. Mater*. **9**, 016002 (2025).
4. D. Barettin, I.V. Shtrom, R.R. Reznik, S.V. Mikushev, G.E. Cirlin, M. Aufder Maur, N. Akopian, *Nano Lett*. **23**, 895 (2023).
5. R.R. Reznik, V.O. Gridchin, K.P. Kotlyar, et al., *Semiconductors* **56**, 492 (2022).
6. V.G. Dubrovskii, G.E. Cirlin, D.A. Kirilenko, et al., *Nanoscale Horiz*. **9**, 2360 (2024).
7. L. Leandro, J. Hastrup, R. Reznik, G. Cirlin, N. Akopian, *NPJ Quantum Inform*. **6**, 93 (2020).

O2

Superparamagnetic γ-Fe_2O_3 nanoparticles influence the differentiation of dendritic cells from human blood monocytes

F.A. Fadeyev[1,2], A.P. Safronov[3,4], G.V. Kurlyandskaya[3], F.A. Blyakhman[1,3]

[1]*Ural State Medical University, 620028 Ekaterinburg, Russia*
fdf79@mail.ru

[2]*Institute of Medical Cell Technologies, 620026 Ekaterinburg, Russia*

[3]*Institute of Natural Sciences and Mathematics, Ural Federal University, 620002 Ekaterinburg, Russia*

[4]*Institute of Electrophysics UB RAS, 620016 Ekaterinburg, Russia*

Magnetic nanoparticles (MNPs) of the iron oxides (Fe_3O_4 and γ-Fe_2O_3) attract special attention of researchers and practitioners of many nanoscience areas representing multidisciplinary research involving material science, physics of magnetic phenomenon, chemistry and biomedicine [1,2]. In particular, the processes in the course of interaction of living cells and magnetic nanoparticles are very important to understand. Magnetic nanoparticles for biomedical applications are mainly requested in the superparamagnetic state and prepared as stabilized suspensions [3]. Their "professions" in the biomedical treatments can be different: supporting imaging, drug delivery, magnetic biosensing, hyperthermia/thermal ablation and others. Present day trend is the development of multifunctional materials supporting more than one function. For example, for the iron oxides it can be magnetic field assisted delivery of primary drugs toward the point of the therapy combined with magnetic biodetection of the MNPs concentration for correct determination of the minimum therapeutic dose. Dendritic cells (DCs) uploaded with MNPs, is one of promising areas of immunotherapy for the needs of cancer treatment.

DCs are a group of antigen-presenting cells, which engulf necrotic tumor cells, process them and present the epitopes of tumor-associated antigens to naive T-cells in lymph nodes. Low migration rate of *ex vivo* generated DCs to lymph nodes after injection into patient is presumably one of the most important challenges, that limits the clinical efficacy of DCs [3]. Meanwhile, MNPs-loaded DCs can be traced in patient's tissues after administration by magnetic-resonanse imaging (MRI) or magnetic biodetection. Besides, their migration to lymph nodes can be guided by application of the external magnetic field. Loading DCs with MNPs for immunotherapy requires assession of the biological effect of nanoparticles. In our previous work, the moderate cytotoxicity of MNPs on DCs was demonstrated [4]. The aim of this study is to estimate the impact of MNPs on the differentiation of monocyte-derived DCs.

γ-Fe_2O_3 MNPs were obtained by laser target evaporation technique [2] using the laboratory installation with Ytterbium fiber laser with 1.07 mm wavelength. Condensation of MNPs took place in a mixture of N_2 and O_2 gases in the volume ratio 0.79:0.21. Transmission electron microscopy (TEM) was done using JEOL JEM2100 microscope operated at 200 kV. The X-ray diffraction analysis (XRD) was performed using D8 DISCOVER diffractometer operated at 40 kV at Cu-K*a* radiation (wavelength l = 1.5418 Å. The field dependences of magnetization M(H) of MNPs were measured using an MPMS-XL7 EC equipment operating with the external fields up to ±70 kOe.

DCs were derived from human blood monocytes by cultivation in differentiation medium supplemented with GM-CSF and interleukin-4. Monocytes were differentiating to DCs in the presence of MNPs at final concentrations 250 and 1000 ng/mL. Immunophenotype of DCs was analyzed by flow cytometry. Secretory activity of cells was measured by enzyme-linked immunosorbent assay (ELISA).

Figure 1 shows typical images of MNPs and dendritic cells. Particle size distribution was calculated based on the graphical analysis of 2160 particle images. It was found lognormal with median 11.4 nm and logarithmic dispersion 0.42. According to XRD crystalline structure of iron oxide MNPs corresponded to maghemite γ-Fe_2O_3 which is typical for this sort of MNPs [2]. To confirm the MNPs internalization by DCs, the nanoparticles were stained by Prussian blue.

DCs differentiated in the presence of MNPs preserved the typical, though slightly modified, shape. Cells also retained the basic surface receptor signatures of immature dendritic cells (CD11c+ HLA-DR+ CD40+ CD86+), though the receptors' expression was significantly affected. The expression of the

antigen-presenting receptor HLA-DR at both MNPs concentrations did not differ from control. At high concentration (1000 ng/mL) of nanoparticles, DCs increased the quantity of costimulatory molecule CD40, though reduced to presence of other receptors, necessary for interaction with T-cells, CD86. MNPs greatly reduced the expression of CD1a (MFI = 32,02 ± 5,07 for DCs without MNPs and 5,46 ± 0,95 for DCs in medium with 1000 ng/mL MNPs), the other antigen-presenting molecule, that presents lipid antigens.

(a) 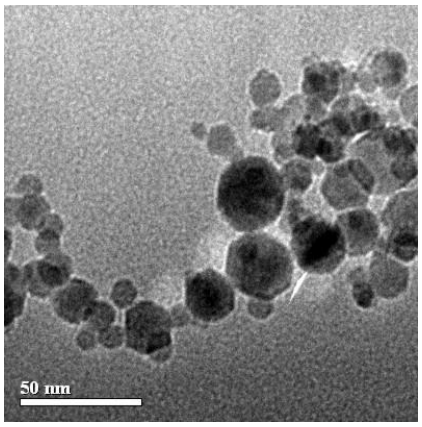

(b) 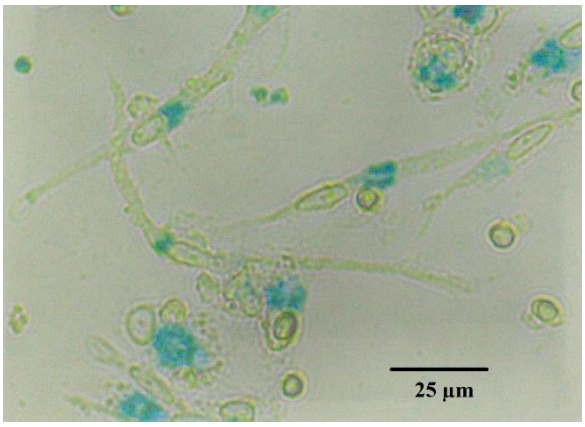

Figure 1. (a) TEM image of LTE MNPs. (b) Dendritic cells differentiated with MNPs in medium, day 4. MNPs concentration in medium is 250 ng/mL. Iron-containing MNPs gave the blue staining of cells.

Interestingly, DCs differentiated in the presence of MNPs, preserved the expression of CD14, the marker of monocytes (the proportion of CD14+ cells were 4,97 ± 0,27% for control and 32,78 ± 3,82% for 1000 ng/mL MNPs). This receptor is typically lost by cells during differentiation from monocytes to DCs. At the same time, the level of expression of chemokine receptor CCR7 was significantly increased in the presense of MNPs in a dose-dependent manner (MFI = 0,71 ± 0,12 for DCs in control, 1,21 ± 0,19 for DCs with 250 ng/mL MNPs and 2,92 ± 0,62 for DCs with 1000 ng/mL MNPs). This fact is rather important, because CCR7 is a marker of maturation of DCs, and it plays key role in attraction of DCs to lymph nodes. Meanwhile, the expression of other markers of DCs maturation, CD83, was not elevated by the presense of nanoparticles.

MNPs also significantly increased the production of pro-inflammatory cytokines, such as TNFα, IL-1β, IL-6, IL-8. The increased secretion of IL-6 (from 1079 ± 235 pg/mL in control to 3011 ± 703 pg/mL for DCs with MNPs in high concentration) is remarkable, because the secretion of this cytokine is increased in mature DCs. At the same time, nanoparticles stimulated the secretion of tolerogenic IL-10 (from 84,11 ± 16,57 pg/mL to 754,04 ± 27,96 pg/mL, respectively), the inhibitor of T-cell mediated immune response.

It can be concluded that MNPs do not prevent the induced differentiation of blood monocytes into immature DCs. At the same time, nanoparticles substantially affect the expression of receptors necessary for migration and interaction with T-cells, as well as the secretion profile of differentiated DCs. The influence of these modifications of DCs on their maturation and T-cells stimulation activity is the theme for our future research.

This research was funded by the Russian Science Foundation, grant # 25-24-00175 (https://rscf.ru/en/project/25-24-00175/).

1. Q.A. Pankhurst, J. Connolly, S.K. Jones, J. Dobson, *J. Phys. D Appl. Phys.* **36**, R167 (2003)

2. A.P. Safronov, I.V. Beketov, S.V. Komogortsev, G.V. Kurlyandskaya, A.I. Medvedev, D.V. Leiman, A. Larranaga, S.M. Bhagat, *AIP Adv.* **3**, 052135 (2013).

3. R.L. Sabado, N. Bhardwaj, *Immunotherapy* **2**, 37 (2010).

4. F. Blyakhman, F. Fadeyev, A. Safronov, T. Terziyan, E. Burban, T. Shklyar, G. Kurlyandskaya, *Materials* **18**, 2142 (2025).

O3

Laser hyperdoping of silicon by transition metals for enhanced NIR absorption

V.I. Pryakhina[1], P.A. Paletskikh[1], D.E. Tkachuk[1], A.R. Akhmatkhanov[1], A.A. Sherstobitov[1], M.S. Kovalev[1,2], S.I. Kudryashov[1,2]

[1]*Institute of Natural Sciences and Mathematics, Ural Federal University, 620002 Ekaterinburg, Russia*
viktoria.pryahina@urfu.ru

[2]*Lebedev Physical Institute, 119991 Moscow, Russia*

Over the past few decades, efforts to enhance silicon's near-to-mid-IR response have been of interest because it eliminates the need for expensive hybrid integration methods and expands silicon-based optoelectronics [1,2]. To enable such sub-bandgap absorption laser hyperdoping is used to introduce shallow or deep-level defects into the material. The concentration of these impurities directly influences both the width of the impurity band and the carrier density in the hyperdoped layer, which in turn dictates its sub-bandgap sensitivity. Transition metals show potential as effective dopants for enhancing the performance of Si-based infrared photodetectors, as intermediate levels from such impurities in the Si closer to mid-gap.

In our research, we investigated the hyperdoping process of silicon using various transition metals (specifically Ti, Cr, Zn, Ag, Au) using fs- and ns- laser pulses. We used commercial Si (100) wafers (either nominally undoped or intentionally doped as p- or n-type) with pre-deposited metal film varying in thickness from 5 to 100 nm. The sample surface was irradiated with either 100-ns laser pulses at 1064-nm wavelength (Yb pulsed fiber laser within MiniMarker2-M20 laser marking system, equipped with galvanoscanner) or with 240-fs laser pulsed at 1030-nm wavelength (TETA-10, Avesta Project, combined with motorized tables). While shorter (ps-fs) pulses promote fast recrystallization, the longer (ns-ms) ones provide thicker melted regions and help restore crystal quality.

Laser parameters for optimal fluence values and total pulse exposure and the thickness of metal films were determined to provide more uniform profiles, deeper doped-layer thicknesses and higher total impurities content, and, as a result, enhanced impurity absorption characteristics [3]. Sample characterization included scanning electron microscopy (SEM), X-ray photoelectron spectroscopy (XPS) depth profiling, energy-dispersion X-ray spectroscopy (EDX) elemental analysis, Raman microspectroscopy, and visible−near-infrared (vis-NIR) reflectance/transmittance measurements.

The laser-hyperdoped Si samples have shown lower transmittance in the intra-gap spectral range (> 1.1 μm) comparing to the highly transmissive Si wafer. The change of sample's photoresponse from laser light irradiation at 1550 nm wavelength measured as dependence on radiation power. Laser light irradiation led to a decrease in sample resistivity and photocurrent increase at room temperature. These findings contribute toward enhancement of doping efficiency and pave the way towards reproducible development of silicon-based optoelectronics.

The work was supported by Russian Science Foundation (project 25-22-00326). The equipment of the Ural Center for Shared Use «Modern Nanotechnologies» Ural Federal University (Reg. № 2968) was used.

1. J.P. Mailoa, A.J. Akey, C.B. Simmons, D. Hutchinson, et al, *Nat. Commun.* **5**, 3011 (2014).
2. S.Q. Lim, J.S. Williams, *Micro* **2**, 1 (2022).
3. V. Pryakhina, S. Kudryashov, M. Kovalev, et al, *Opt. Laser Technol*. **188**, 112945 (2025).

O4

Application and tuning of high-temperature $BiScO_3$-$PbTiO_3$ piezoceramics for ITER

P.A. Pankratiev[1], E.G. Guk[1], E.P. Smirnova[1], V.N. Klimov[2], N.V. Zaitseva[1], A.V. Sotnikov[3], E.E. Mukhin[1]

[1]*Ioffe Institute, 194021 Saint-Petersburg, Russia*
pavel-pankratiev@yandex.ru

[2]*Central Research Institute of Structural Materials Prometey, National Research Centre Kurchatov Institute, 191015 Saint-Petersburg, Russia*

[3]*Emperor Alexander I St. Petersburg State Transport University (PGUPS), 190031 Saint- Petersburg, Russia*

$BiScO_3$-$PbTiO_3$ (BSPT) ceramics is a leading material for high-temperature piezoelectric applications, offering the combination of high Curie temperature (T_c > 450ºC) and large piezoelectric constant (d_{33} > 460 pC/N) [1]. Currently, these features and thermal stability make it unique for use in harsh environment conditions including aerospace, industrial sensors and even in the neutron harsh environment of fusion reactors. The International Thermonuclear Experimental Reactor (ITER) is a large-scale scientific project aimed to demonstrate the feasibility of controlled nuclear fusion as a sustainable energy source by reproducing processes occurring in stellar plasmas. Piezoelectric actuators have great potential for use in ITER, especially as drivers for shutters and optical mounts in diagnostic systems [2,3]. In particular, they are capable of operating in strong magnetic fields and withstand neutron/gamma irradiation [4,5]. Achieving optimum ceramic properties requires precise control over elemental composition, crystal structure and microstructure during processing.

The contribution presents studies of the elemental composition, crystal structure and microstructure as well as electromechanical properties of BSPT piezoelectric ceramics. Two variants of sintering processes are considered: conventional one-step and modified two-step techniques. The two-step process resulted in ceramics with a more diffused grain size distribution and a substantially smaller average grain size (0.8-1 μm) compared to those obtained through one-step synthesis (8-10 μm).

X-ray diffraction analysis confirmed the tetragonal structure of $0.36BiScO_3$-$0.64PbTiO_3$ (P4mm) and the location near the morphotropic phase boundary. Reduced tetragonality c/a = 1.017 is observed in fine-grained ceramics obtained by two-step technique, compared to c/a = 1.025 for the one-step technique. Dielectric measurements revealed a Curie Temperature T_c = 433ºC for two-step samples instead of 450ºC for one-step ones. Note, the decrease of dielectric losses for ceramics produced by two-step sintering. Enhanced piezoelectric properties, including a large piezoelectric constant d_{33} = 525 pC/N and strong anisotropy of the piezoelectric effect ($d_{33}/|d_{31}| \approx 5$) were observed.

The improvement of piezoelectric properties of fine-grained ceramics is caused by the reduction of domain size and increase the number of domains that leads to the increase of domain walls number and their mobility. Additionally, temperature dependences of dielectric, piezoelectric, and elastic constants are presented, providing further insights into the high-temperature application of BSPT ceramics.

These results highlight the potential of the two sintering techniques of BSPT ceramics for piezoelectric motors in harsh environments including high-temperature applications.

1. R.E. Eitel, C.A. Randall, T.R. Shrout, S.-E. Park, *Jpn. J. Appl. Phys.* **41**, 2099 (2002).

2. E.E. Mukhin, et al., *Fusion Engineering and Design* **123**, 686 (2017).

3. E.E. Mukhin, et al., *Fusion Engineering and Design* **176**, 113017 (2022).

4. E.P. Smirnova, V.N. Klimov, E.G. Guk, P.A. Pankratiev, N.V. Zaitseva, A.V. Sotnikov, E.E. Muhin, *Physics of the Solid State*, **65**, 1888 (2023).

5. E.P. Smirnova, V.N. Klimov, E.G. Guk, P.A. Pankratiev, N.V. Zaitseva, A.V. Sotnikov, E.E. Muhin, *Physics of the Solid State*, **66**, 95 (2024).

O5

Application of energy-conversion functional crystal fibers

Min Sun, Xu Lu, Xiaoyong Wei, Zhuo Xu

Electronic Materials Research Laboratory, Key Laboratory of the Ministry of Education & International Center for Dielectric Research, School of Electronic Science and Engineering, Xi'an Jiaotong University, 710049 Xi'an, China
jxsunmin@xjtu.edu.cn

With the development of optical fiber theory and multimaterial fabrication techniques, in the last three decades, multimaterial fibers have witnessed outstanding improvement. Many new multimaterial fibers with energy conversion function have been discovered, motivated by the novel concept of "Special functional fiber", fiber-drawing dissimilar core-clad composite technologies, and in-fiber crystallization mechanisms [1]. Although most of these fibers are used for "conventional" telecommunication applications, there is a growing need for multimaterial fibers relevant in other applications, such as light generation using fiber lasers, remote sensing, nonlinear optics, medicine and health, laser imaging, and so on. Aiming at the practical application of multimaterial fiber technology, more research has been undertaken in the design and fabrication of multimaterial fiber devices in recent years. However, many scientific and engineering problems still need to be solved. If the multifunctional materials, especially for functional crystals, can be integrated into multimaterial fibers and devices, the multifunction will be transmitted to thousands of homes [2]. It is high time to collect high-quality studies to highlight the cutting-edge development of multimaterial fibers with energy conversion function and discuss the device applications of multimaterial fiber technology. Multimaterial fibers and devices include but do not limite to the discovery of new fiber materials by preparing glass-clad/polymer multimaterial fibers [3,4] and designing fiber-based devices combining conductor, semiconductor, single crystal, polycrystal, nanocrystal, quantum dot, low-temperature glass, rare-earth ions doped core glass, and dissimilar core-clad materials. In this lecture, semiconductor optical fibers and microcrystal optical fibers are fabricated by an optical-fiber-template thermal drawing method, integrating a semiconductor/microcrystal into a silicate glass tube, being an optical-fiber preform [5,6]. We demonstrate the concept of "Special functional fiber", like laser, thermoelectric, and ferroelectric optical fibers, and they are developed being the advanced fiber devices with laser modulation, thermoelectric conversion, and ferroelectric optical doubling frequency functions, etc.

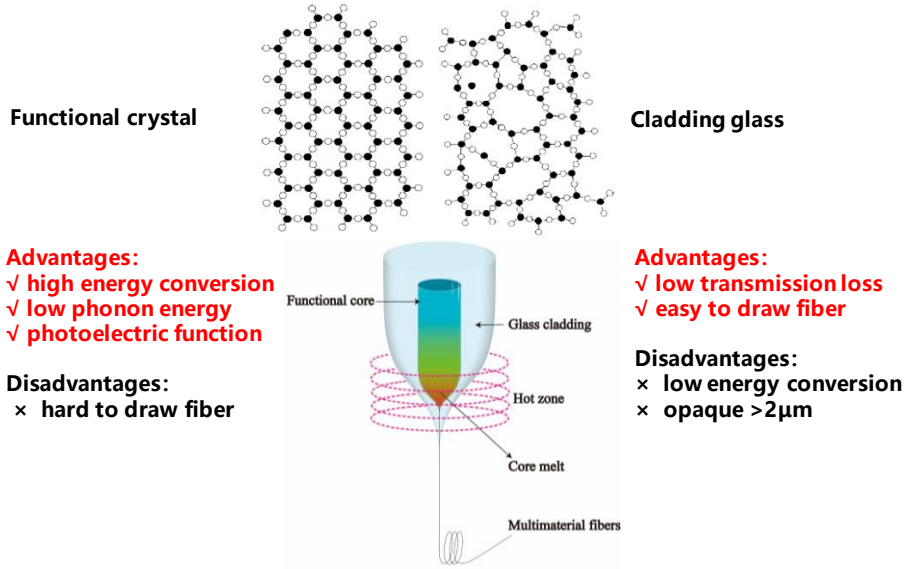

Figure 1. The research idea of functional optical fibers.

1. X. Liu, P. Tan, X. Ma, et al. *Science* **376**, 371 (2022).
2. J. Wang and Y. Tseng, *Optics Letters* **38**(4), 452 (2013).
3. B. Han, Q.H. Luo, P.Y. Zhang, et al. *Journal of the American Ceramic Society* **105**(3), 1640 (2021).
4. M. Sun, G.W. Tang, H.F. Wang, et al. *Advanced Materials* **34**(36), 2202942 (2022).
5. J.W. Cao, Lun, X.Z. Huang, et al. *Optics Express* **32**(10), 16712 (2024).
6. Y.S. Sun, M. Sun, Z.J. Lun, et al. *Advanced Materials* **37**(10), 2416861 (2025).

O6

New high resolution scanning electron microscope from Nanometric and Ostec

E. Lisov, A.B. Shubin, I.L. Prusakov

Ostec-ArtTool Ltd., Moscow
Lisov.E@ostec-group.ru, info@arttool.ru

Nanometric company supplies foreign analytical equipment to the territory of the Russian Federation and the CIS countries.

Today we would like to introduce a new high-resolution scanning electron microscope in our product line, Nanometric SemOn F-300. It can be used to obtain surface images with magnification from 10 to 2,000,000 times. Resolution up to 1.0 nm (at an accelerating voltage of 15 kV) and a minimum noise level are provided by using an electron gun with thermionic emission (Schottky cathode). The motorized five-axis stage is suitable for loading samples weighing up to 0.5 kg. The microscope is also equipped with all the necessary detectors: SE (intra-lens), SE (intra-chamber, Everhart-Thornley type), BSE; CCD camera for sample navigation, absorbed current detector, STEM detector, EDS. These detectors will allow to realize the maximum potential of the scanning electron microscope in laboratory experiments.

It is also important that the Nanometric SemOn F-300 microscope is developed and produced by our long-terms partners in China. They have 25 years experience of work in service and development divisions of Carl Zeiss, USA. And they created not only the analogue of one of the most powerful SEM tools, but also improved some bugs and inconveniences, that they found over the long years of development of these systems. Their team constantly works on updates of this product. Very soon we will announce the new model with the enhanced resolution down to 0.8 nm. Together with its partners, Nanometric provides an official warranty, post-warranty and methodological support to users of this and other products. When a number of foreign manufacturers left the Russian market, Nanometric SemOn F-300 may be of interest to many research organizations due to its attractive price-performance ratio and availability of official service department.

We would also like to highlight the IntoM OP100 optical profilometer in the Nanometric product line, which is designed on the basis of the optical scheme of the Mirau interferometer. This system is used for microtopography of samples, it allows you to evaluate the surface morphology and to measure the parameters of roughness, curvature, etc.

In 2024, a new model of the bench top scanning electron microscope (SEM) EM-40 from the Korean manufacturer COXEM Co., Ltd. became available for purchase. The new product is a logical continuation of the "bestseller" EM-30 (more than 60 installations in the Russian Federation and the CIS since 2018). It retains the advantages of EM-30: reliable construction of the main units, ease of maintenance, high image quality at the level of full-size thermal emission SEMs, user-friendly software with many adjustments and settings, the presence of options and specialized sample preparation systems for various user tasks. In the new, even more compact bench top SEM EM-40, the maximum magnification reached 250 thousand times (versus 150 thousand in EM-30). Motorization of the sample stage along the Z axis appeared, which makes positioning even more convenient for the operator. The device has been enhanced with the ability to adjust the pressure in the sample chamber in multiple stages, and the ultra-fast signal processing technology enables an image refresh rate of 13 frames per second.

O7

Influence of humidity on the domain evolution during local switching in strontium-barium niobate single crystals

V.A. Shikhova[1], A.S. Slautina[1], M.D. Kholodenko[1], A.R. Akhmatkhanov[1], A.P. Turygin[1], L.I. Ivleva[2], V.Ya. Shur[1]

[1]*School of Natural Sciences and Mathematics, Ural Federal University, 620002 Ekaterinburg, Russia*
vera@urfu.ru

[2]*Prokhorov General Physics Institute, Russian Academy of Sciences, 119991 Moscow, Russia*

The formation of a domain structure during local polarization switching in the field of the tip of a scanning probe microscope (SPM) at different humidity in single crystals of strontium-barium niobate (SBN) doped with Ni (0.05 wt. % Ni_2O_3) was investigated.

Polarization switching was performed both in samples with the initial maze nanodomain structure and in samples with single-domain state created by a medium-energy electron beam [1]. Domains were formed at room temperature, at a relative humidity (RH) of 20, 40, 60 and 80%. For local polarization switching rectangular pulses of an electric field with a duration (t_p) from 1 ms to 1000 s and an amplitude (U_p) from 10 to 300 V were used. The distance between points of field application was 20 μm. Domain structures were visualized on the crystal surface using piezoresponse force microscopy (PFM) and in the bulk of the crystal using Cherenkov-type second harmonic generation microscopy (SHGM) [2].

The domains formed as a result of local polarization reversal at low RH had circular shape and smooth walls, for higher RH the domain sizes increase, and the walls become rough (Fig. 1). Moreover, an additional irregular nanodomain ensembles were formed around the main domain at voltages above 200 V and RH above 40%.

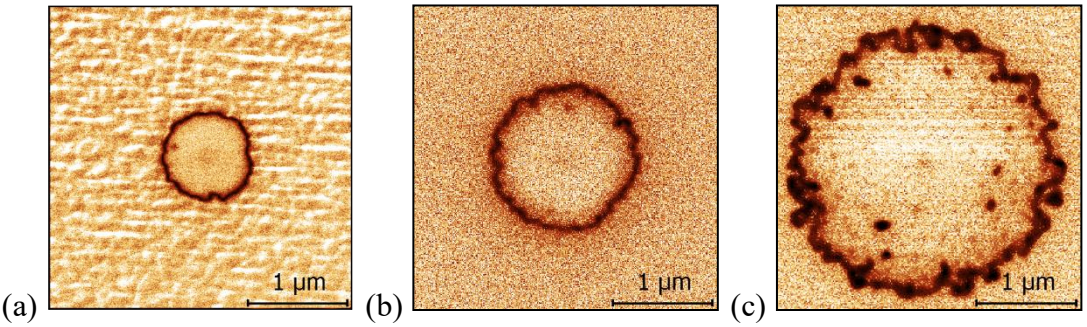

Figure 1. The PFM images of domains created by local switching in single-domain crystal. U_p = 60 V, t_p = 60 s. RH, %: (a) 20, (b) 40, (c) 60. Amplitude PFM signal.

The effective domain radius linearly increased with increasing of the pulse amplitude for all studied RH. From the slope of this graph, a value proportional to the domain wall mobility was determined, which depends linearly on RH.

The significant increase of the domain radius with RH can be attributed to the influence of a water meniscus appeared at the tip and a thin adsorbed water layer formed at the polar surface, which acts as an electrode with variable conductivity. The dependence of effective domain radius on the pulse duration was explained in terms of 2D current limited switching process with the surface water layer acting as a highly-resistive electrode with variable conductivity [3].

The domain radius decreased with depth in the bulk of the crystal. Thus, the domains were cones with an aspect ratio from 13 in polydomain crystal to 40 in single-domain one.

The work was supported by Russian Science Foundation (project 25-22-00231). The equipment of the Ural Center for Shared Use «Modern Nanotechnologies» UrFU (Reg. 2968) was used.

1. D.S. Chezganov, V.A. Shikhova, V.V. Fedorovyh, et al., *IEEE Trans. Ultrason. Ferroelectrics. Freq. Contr.* **67**, 191 (2020).

2. Y. Sheng, A. Best, H.-J. Butt, et al., *Opt. Express* **18** (16), 16539 (2010).

3. Y.M. Fomichov, P.V. Yudin, M. Tyunina, et al., *Nanotechnology* **35**, 04LT01 (2024).

O8

Analytical and technological equipment for research and small-scale production

Yu.E. Vysokikh, S.Yu. Krasnoborodko

MTEON, 124482 Moscow, Russia
info@mteon.ru

The MTEON team has been working in the field of scientific instrumentation for 20 years, the company specializes in the production and supply of analytical and technological equipment. Currently, the list of proposed solutions is quite wide: microscopy and spectroscopy, X-ray systems, maskless lithography, profilometry, systems for measuring a wide range of physical properties of materials under controlled conditions, etc.

We develop and manufacture small-sized and tabletop technological tools. These are tools for magnetron sputtering of metals and dielectrics, plasma-chemical etching and deposition from the gas phase, installations for sample preparation

Modern scanning electron microscopes allow morphology studies with a resolution of less than 1 nm, in addition, it is possible to measure elemental analysis, detect electron backscatter diffraction, cathodoluminescence. It is possible to work in low vacuum to minimize the charge on the surface of samples, use a second column with an ion source to modify samples, etc.

Atomic-force microscopy remains a popular method for studying a wide range of samples, including ferroelectrics. The devices allow measurements to be taken under controlled conditions and implement combined research methods, such as near-field optical microscopy [1] and a combination with Raman spectroscopy. For microelectronics tasks wafers up to 300 mm in diameter could be measured by special developed combine system. In addition to the AFM head this system can use a Raman probe, profilometer and ellipsometer in same tool.

X-ray diffractometry is based on the phenomenon of X-ray diffraction on the atomic planes of the crystal lattice. A single-crystal diffractometer requires a single crystal with a uniform structure and allows obtaining its complete atomic structure (atomic coordinates, interatomic distances, angles). A powder diffractometer can study polycrystalline material (powder, thin films, polycrystals) and allows identifying phases (for example, minerals in a mixture) and determining the parameters of the crystal lattice.

X-ray photoelectron spectroscopy is based on measuring the energy of photoelectrons knocked out of a sample by X-rays. The XPS spectrum is the dependence of the intensity of photoelectrons on their binding energy. each element has unique peaks corresponding to electrons of different orbitals.

For small-scale production tasks, maskless lithography is in high demand. Laser lithography systems are available in a desktop version for wafers up to 200 mm in diameter. It can use lasers with a wavelength of 365 nm or 405 nm, and a line width up to 450 nm. In the floor version, the sample size is up to 300x500 mm, laser 515 nm and line width up to 100 nm.

For magnetic characteristics studies, we offer Kerr microscopy systems and vibromagnetometers. Kerr microscopy is a method of visualizing magnetic domains in materials based on the magneto-optical Kerr effect (MOKE). A vibromagnetometer is a device for measuring the magnetic moment of samples based on recording the electromotive force (EMF) arising from mechanical vibrations of a sample or sensor in a magnetic field. The method combines vibration and electromagnetic induction to determine the magnetic characteristics of materials.

1. Yu.E. Vysokikh, T.V. Mikhailova, S.Yu. Krasnoborodko, et al., *J. Magnetism Magn. Mater.* **529**, 167837 (2021).

O9

Application of ferroelectric metal-organic frameworks in adsorption technologies

E.V. Aleksandrov[1], I.K. Shaikhutdinov[2], A.A. Shmelev[2], A.V. Sokolov[2]

[1]*Bauman Moscow State Technical University, 105005 Moscow, Russia*
aleksandrov_ev1@mail.ru

[2]*Samara State Medical University, 443099 Samara, Russia*

Metal-organic coordination polymers (MOCPs) and their porous subclass of metal-organic frameworks (MOFs) fill the gap between pure inorganic and organic ferroelectrics. MOF UiO-66 nanocrystals were previously believed to be piezo-/ferroelectrically inactive. However, via the nanoscale probing studies, it was demonstrateed that UiO-66 nanocrystals show certain piezo-/ferroelectric responses due to presence of a reduced symmetry form. In addition, UiO-66(Hf)-type MOF nanocrystals possess stronger piezoresponses and better ferroelectric switching. Gas transport through ZIF-8 membrane was switched in situ by applying an external electric field (E-field). The switching of gas permeation upon E-field polarization could be explained by the structural transformation of the zeolitic imidazolate framework ZIF-8 into polar polymorphs.

We synthesized new ferroelectric UiO-66 based MOFs Zr-UiO-66-2,5-PDC-BDC (1:1) and Zr-UiO-66-2,5-PDC-BDC (1:10) with different ratios of polar 2,5-pyridinedicarboxylate and non-polar terephthalate ligands. Drugs adsorption properties were studied for them and compared with ones of MIL-101(Fe), MIL-121, MIL-53(Al), MIL-88A [1,2]. Thus, the adsorption capacity of 1,94 mmol/g of 5-fluorouracil for Zr-UiO-66-2,5-PDC-BDC (1:1) for was reached. Nanosheets of the new compound $[Zn_4(THIP)(HCO_2)_3(H_2O)_4]\cdot DMF$ (H_5THIP = 4,5,6-trihydroxyisophthalic acid) were prepared for further use as drug delivery material [3]. We made *ab initio* simulations for perovskite-like ferroelectric MOCPs $C_3H_8N[Zn(HCO_2)_3]$ ($C_3H_8N^+$= azetidinium cation), $C_3H_8N[Mn(HCO_2)_3]$, $C_4H_{12}N[Mn(HCO_2)_3]$ ($C_4H_{12}N^+$ = tetramethylammonium cation), $N_2H_5[Mn(HCO_2)_3]$ ($N_2H_5^+$ = hydrazinium), $N_2H_5[Zn(HCO_2)_3]$, and analyzed their mechanical properties in relation with the composition, framework geometry and topology of H-bonds.

The work was supported by the Russian Science Foundation, project No. 24-23-00162.

1. I.Kh. Shaykhutdinov, I.M. Bairikov, A.A. Shmelev, A.V. Sokolov, *Research Journal of Pharmacy and Technology* **18**, 3 (2025).

2. I.Kh. Shaikhutdinov, T.K. Ryazanova, A.A. Shmelev, V.A. Kurkin, A.V. Sokolov, *Pharmaceutical Chemistry Journal*, Submitted (2025).

3. Y. Zhang, A.V. Sokolov, A.V. Vologzhanina, T.V. Sudakova, J. Wang, E.V. Alexandrov, *Materials Chemistry and Physics* **325**, 129804 (2024).

O10

Study of ^{3}He nuclear relaxation in contact with PrF_3 nanoscale powders

A.M. Garaeva, A.S. Makarchenko, G.A. Dolgorukov, I.V. Romanova, B.M. Mukhamadullin, E.I. Boltenkova, E.M. Alakshin

Kazan Federal University, Institute of Physics, 420008 Kazan, Russia
adeliagaraeva@gmail.com

Helium-3, due to its small molecular size, non-zero nuclear spin 1/2, and the ability to remain liquid at sufficiently low temperatures, is of great interest. ^{3}He has a number of advantages when used as a probe for studying porous media [1]. ^{3}He has a sufficiently large gyromagnetic ratio $\gamma/2\pi$ = -32.43 MHz/T and in most cases allows obtaining a sufficiently high signal-to-noise ratio in experiments. ^{3}He can be used as a model system for studying relaxation mechanisms [1,2] because it has more possibilities to change the parameters and experimental conditions. It is known that the longitudinal relaxation times T_1 of liquid ^{3}He in the case of a bulk liquid are 1000 seconds, but in an experimental NMR cell they can be significantly shorter due to wall relaxation and bounded diffusion [3], paramagnetic centers and non-uniform magnetic fields also affect relaxation [4,5]. Of particular interest is the relaxation of ^{3}He near paramagnetic centres, which create local magnetic fields, thereby affecting the rate of relaxation of the system. When considering a ^{3}He system in contact with paramagnetic particles, relaxation will also depend on the proximity of the paramagnetic particles to each other and on the particle size. The study of these processes is extremely important for understanding the mechanisms of relaxation near paramagnetic particles.

The PrF_3 crystal is a dielectric Van Vleck paramagnet. The Pr^{3+} ion has the electron structure $4f^2$. Due to the low symmetry of the PrF_3 crystal field, the ground multiplet $^3H_4$ is split into 9 singlets. The nucleus of the rare earth element has a non-zero nuclear spin 5/2 and this element compounds have nuclear magnetism. PrF_3 can be used for the dynamic polarization of ^{3}He nuclear spins [6]. The polarized system of nuclear spins of gaseous ^{3}He is widely used in medicine for NMR tomography of the lungs [7,8].

Particles of PrF_3 with a size of 56 × 34 nm were obtained by hydrothermal synthesis using a nitrate reaction [9]. Control of the chemical composition and confirmation of crystallinity was carried out by X-ray phase analysis on a Bruker D8 Advance Cu Kα diffractometer, λ=1.5418 Å. Based on photographs taken by transmission electron microscopy on a HitachiHT Exalens microscope, the shape and characteristic size of particles in the resulting powders were determined.

In this work, ^{141}Pr NMR in nanosized PrF_3 particles and ^{3}He NMR in contact with nanosized PrF_3 particles were studied. The measurements were carried out on the home-built NMR spectrometry [10]. The ^{141}Pr NMR spectra and spin-lattice and spin-spin relaxation times of the synthesized nanosized PrF_3 sample in contact with liquid ^{4}He and ^{3}He were measured at 6.63 MHz and 19.5 MHz. Based on the results obtained, a conclusion was made about the magnetic coupling of ^{141}Pr and ^{3}He nuclei. The effect of a powder of magnetic PrF_3 particles on the rate of longitudinal and transverse relaxation of helium-3 nuclei in the adsorbed layer, gas and liquid, and with adsorbed helium-4 was studied. The measurements were carried out at a temperature of 1.5 K in fields up to 800 mT. The mechanisms of magnetic nuclear relaxation are considered. A model that describing the nuclear magnetic relaxation of helium-3 in contact with PrF_3 nanoparticles is proposed.

This work was supported by the Russian Science Foundation (project no. 23-72-10039).

1. C.P. Lusher, M.F. Secca, M.G. Richards, *Journal of Low Temperature Physics* **72**, 71 (1988).
2. V. Lefevre, dissertation, Université Pierre et Marie Curie-Paris VI (1984).
3. R.C. Wayne, R.M. Cotts, *Physical Review* **151**, 264 (1966).
4. A. Abragam, *The principles of nuclear magnetism* (Oxford university press), 32 (1961).
5. A.V. Klochkov, M.S. Tagirov, *Low Temperature Physics* **41**, 50 (2015).
6. M.S. Tagirov, *JETP Letters* **61**, 652 (1995).
7. H.E. Moller, X.J. Chen, M.S. Chawla, et al., *J. Magn. Res.* **135**, 133 (1998).
8. P.J. Nacher, *Poincaré Seminar* 159 (2007).
9. E.M. Alakshin, B.M. Gabidullin, A.T. Gubaidullin, et al., arXiv preprint arXiv:1104.0208. (2011).
10. G.A. Dolgorukov, V.V. Kuzmin, A.V. Bogaychuk, et al., *Magn. Reson. Solids* **20**, 18206 (2018).

O11

Magnetic properties of Fe, Ni-doped TiO_2 layers formed on titanium by plasma electrolytic oxidation: experiment and theoretical modeling

P.V. Kharitonskii[1], M.V. Adigamova[2], I.V. Lukiyanchuk[2], A.Yu. Ustinov[2], E.S. Sergienko[3,4], A.Yu. Ralin[5], K.G. Gareev[1,4], E.A. Setrov[1]

[1]*Saint Petersburg Electrotechnical University "LETI", 197022 Saint Petersburg, Russia*

[2]*Institute of Chemistry, Far Eastern Branch, Russian Academy of Sciences, 690022 Vladivostok, Russia*

[3]*Saint Petersburg University, 199034 Saint Petersburg, Russia*
e.sergienko@spbu.ru

[4]*Ioffe Institute, 194021 Saint Petersburg, Russia*

[5]*Far Eastern Federal University, 690922 Vladivostok, Russia*

Plasma electrolytic oxidation (PEO) of titanium in an electrolyte with solid particles of iron and nickel hydroxides allows obtaining magnetically active titania coatings with iron and nickel compounds. Previously, PEO coatings doped only with Fe [1] and Fe+Ni in a ratio of 1:1 [2] were studied. The present work is aimed at a comprehensive experimental study of the magnetic properties of PEO coatings on titanium formed in electrolytes with different $Fe(OH)_3$: $Ni(OH)_2$ ratios (1:0; 3:1; 1:1; 1:3; 0:1) and theoretical modeling of the causes of magnetism in correlation with composition, morphology and phase state.

PEO-coated samples were obtained similarly to Ref. [2]. The structure and composition of the coatings were investigated using scanning and transmission electron microscopy (SEM, TEM), X-ray photoelectron spectroscopy (XPS), energy dispersive analysis (EDS), X-ray phase analysis (XRD) and magnetic force microscopy (MFM). The hysteresis characteristics were determined by ultra-sensitive magnetometry using a SQUID magnetometer at 300 K.

All formed coatings exhibit ferromagnetic properties at room temperature (example in Fig. 1a). According to complex studies, including XRD analysis, XPS, and the Lowry test (Fig. 2), the causes of ferromagnetism are the presence of maghemite, hematite, nickel ferrite, and other oxides in the coatings. Magnetic characteristics depend on the Fe:Ni ratio and are related to the morphology of coatings (Fig. 1b, c), localization of Ni- and Fe-enriched nanocrystallites in the pores (Fig 1в) and their chemical heterogeneity.

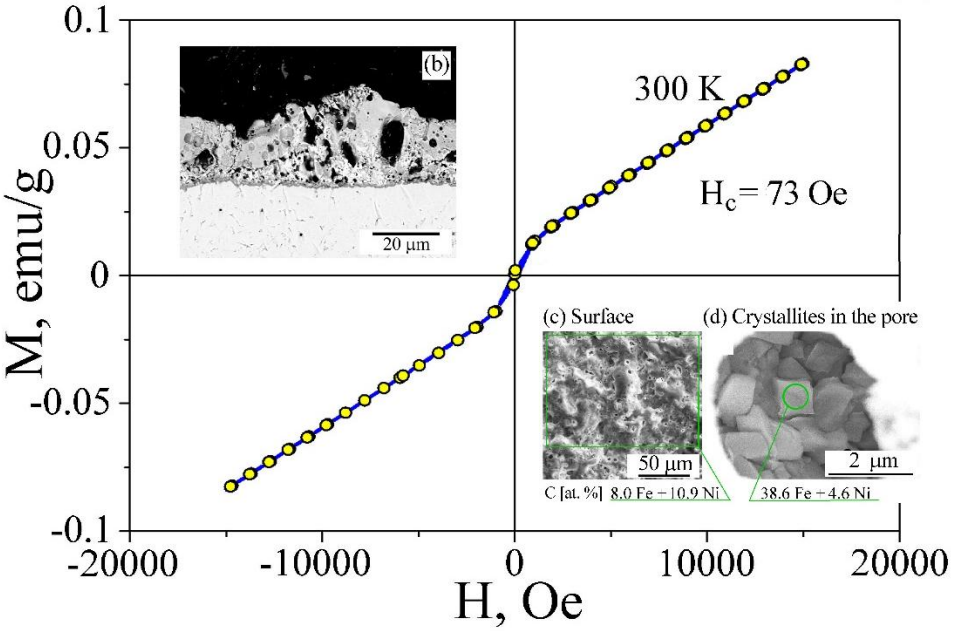

Figure 1. Field dependences of magnetization *M(H)* (a), cross-section (b), surface morphology (c) and crystallites in the pore (d) for PEO-coated sample (Fe:Ni=1:1).

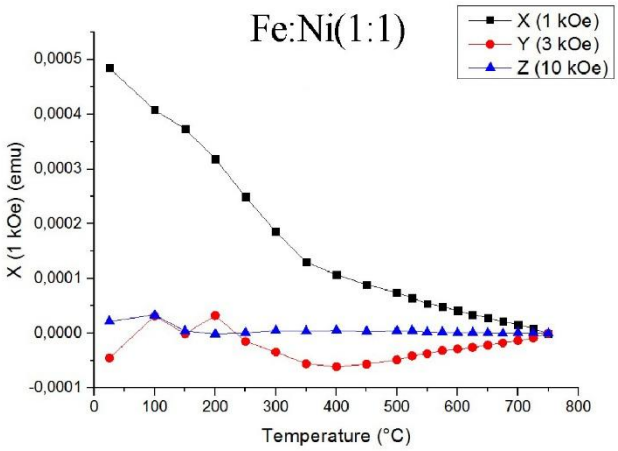

Figure 2. Example of Lowry test for PEO-coated sample Fe:Ni(1:1).

Theoretical modeling of the hysteresis characteristics (Table) was performed using two micromagnetic models: two-phase chemically inhomogeneous particles (TPh) and an ensemble of particles with effective spontaneous magnetization (SDEM), taking into account the magnetostatic interaction and chemical inhomogeneity of the ferromagnetic fraction of the coating [3]. A good agreement was obtained between the calculated and experimental hysteresis characteristics, showing the contribution of both the strongly magnetic and weakly magnetic fractions. In all coatings, the strongly magnetic fraction is represented mainly by two-phase chemically inhomogeneous particles. With the predominance of Fe, the bulk concentration of the weakly magnetic fraction reaches 50%. With increasing Ni content, its fraction sharply decreases several times.

Table 1. Experimental values of hysteresis parameters of PEO-coated samples: saturation magnetization M_s, residual saturation magnetization, coercive force H_c (Oe) and coercive force by residual magnetization H_{cr}.

Sample	M_s [A/m]	M_{rs} [A/m]	H_c [kA/m]	H_{cr} [kA/m]
Fe	82.1	6.12	2.8	18.1
Fe:Ni(3:1)	345.0	36.9	6.0	33.4
Fe:Ni(1:1)	672.0	122.0	10.6	31.3
Fe:Ni(1:3)	247.0	40.8	12.4	30.4
Ni	275.0	67.3	11.7	29.0

Formation of coatings by PEO technique, their study by XPS, SEM, and EDX methods was carried out within the framework of the Institute of Chemistry FEB RAS State Order (project no. FWFN(0205)-2025-0001).

Scientific studies were performed at the Research park of SPbU: Center for Diagnostics of Functional Materials for Medicine, Pharmacology and Nanoelectronics; Center for Nanotechnology; Center for Geo-Environmental Research and Modeling (GEOMODEL); Center for Microscopy and Microanalysis. Some of the research was carried out in the Center for Collective Use on the basis of the Institute of Chemistry of FEB RAS.

1. V.S. Rudnev, P.V. Kharitonskii, et al., *J. Alloys Compd.* **816**, 152579 (2020).
2. M.V. Adigamova, I.V. Lukiyanchuk, et al., *Mat. Chem. Phys.* **275**, 125231 (2022).
3. P.V. Kharitonskii, E.A. Setrov, et al., *Bull. Russ. Acad. Sci.: Phys.* **89**(4), 487 (2025).

O12

Charge compensation model for the lateral expansion of ferroelectric domains during polarization reversal by force-microscope tips

B. Sturman, E. Podivilov

Institute of Automation and Electrometry of RAS, 630090 Novosibirsk, Russia
sturman@iae.nsk.su

Nanoscale polarization reversal by applying voltage pulses to conductive tips of scanning force microscope (SFM) is an exciting and important area of domain engineering in ferroelectrics. Numerous experiments show, see, e.g., [1-4], that the transversal size of the generated counter-domains can strongly exceed the tip size and significantly depend on the pulse amplitude U and duration τ. Often the inverted domain diameter $2r_0$ lies on the μm scale. Schematic of the lateral expansion phenomenon is shown in Figure 1. In contrast to capacitor-like configurations, the necessary compensation of typically huge polarization charges (and depolarizing fields) cannot be ensured by free electrode charges. The nature and characteristics of the necessary charge compensation, as well as the regularities of the lateral expansion, represent thus a challenging problem.

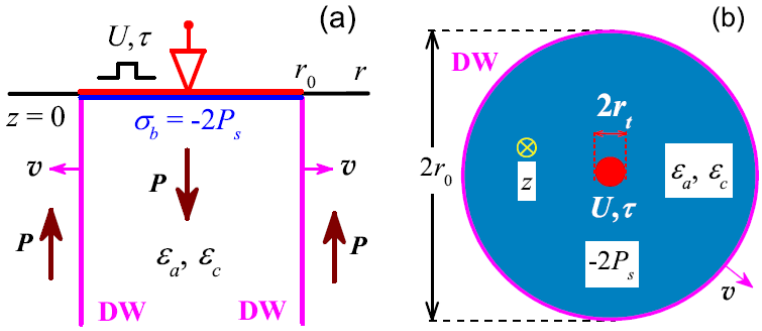

Figure 1. An illustration of the lateral domain expansion at application of a U,τ voltage pulse to a SFM tip, side view (a) and top view (b). The blue color indicates the bound polarization charge $2P_s$ to be overcompensated. The compensating charges come (injected) from the tip. The after-pulse domain radius is r_0, the lateral expansion velocity is $v(r_0)$, the effective tip radius is r_t and the transversal and longitudinal dielectric constants are ε_a and ε_a. The sample thickness can be larger and smaller than r_0.

We propose a relatively simple self-consistent model capable of quantitative explanation of a large body of experimental data on the tip-induced lateral domain expansion relevant to lithium niobite (LN) crystals. Our theory is based on the idea of conductive domain walls (DWs), which has a strong experimental and theoretical backgrounds [5,6] and is found to be relevant to the description of the fundamental ferroelectric properties [7,8]. Just conduction of the top surface and DW is responsible for the charge compensation. Also, we employ the well known experimentally based Merz law for the velocity of the lateral expansion v. Our model provides an expression for the after-pulse domain radius r_0 as a function of U and τ. It includes only two fit parameters – the Merz velocity pre-exponent v_* and the ratio of DW and top-surface conductivities σ_w/σ_t – and sufficient for the explanation of two existing substantially different sets of experimental data [2,3] relevant to stoichiometric LN crystals.

In addition to explanations of details of the charge compensation model and of comparison with experiments, we also consider the differences with the existing alternative models of the lateral expansion.

1. M. Molotskii, A. Agronin, et al., *Phys. Rev. Lett.* **90**, 107601 (2003).
2. B.J. Rodriguez, R.J. Nemanich, et al., *Appl. Phys. Lett.* **86**, 012906 (2005).
3. M. Lilienblum, E. Soergel, *J. Appl. Phys.* **110**, 052012 (2011).
4. E.V. Shishkina, E.V. Pelegova et al., *ACS Appl. Electron. Mater.* **3**, 260 (2021).
5. R.K. Vasudevan, W. Wu, et al., *Adv. Funct. Mater.* **23**, 2592 (2013).
6. P. Bednyakov, B. Sturman, et al., *NPJ Comput. Mater.* **4**, 65 (2018).
7. B. Sturman, E. Podivilov, *JETP Letters* **116**, 246 (2022).
8. E. Podivilov, N. Masnev, B. Sturman, *JETP Letters* **119**, 793 (2024).

O13

Regular domain structures with the symmetrically twisted walls in 5% MgO:$LiNbO_3$

S.M. Shandarov[1], D.E. Belskaya[1], E.N. Savchenkov[1], A.V. Dubikov[1], N.I. Burimov[1], M.A. Chuvakova[2], A.R. Akhmatkhanov[2], V.Ya. Shur[2]

[1]*Tomsk State University of Control Systems and Radioelectronics, 634050 Tomsk, Russia*
stanislavshandarov@gmail.com

[2]*Ural Federal University, 620002 Ekaterinburg, Russia*

The specific features of the Bragg diffraction for Gaussian probe beam with a wavelength $\lambda = 632.8$ nm and an elliptical cross section on regular domain structures (RDS) in a 5% MgO:$LiNbO_3$ crystal was observed experimentally in [1]. The efficiency for that kind of diffraction has a strong dependence on the position of the center of the probe laser beam with a waist size $2\Delta z \approx 25$ μm along the polar *Z* axis of the crystal. The observed in [1] experimental results are presented by dots in Figure 1.

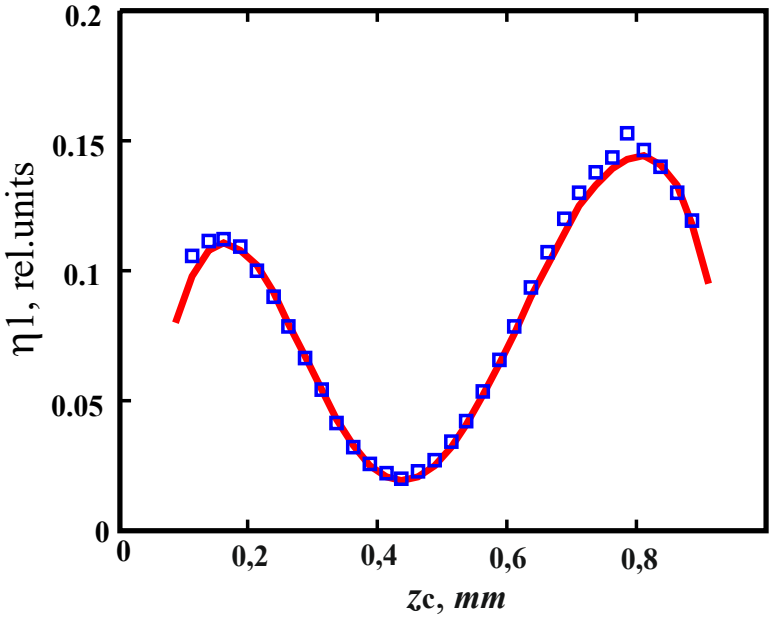

Figure 1. Dependence of the efficiency of Bragg diffraction on RDS with twisted walls in a 5% MgO:$LiNbO_3$ crystal versus the position of the probing beam along the polar Z axis. The points are the results of the experiment [1]; the solid curve is the calculated dependence.

To elaborate the theoretical model of Bragg diffraction of elliptical Gaussian probe beam on RDS with inclined walls [1] we apply the approach described in this paper to the case of RDS with symmetrically twisted walls. By using the representation of the form for twisting domain walls through a power series as well as the least-squares method we fit the calculated dependence of diffraction efficiency versus the position of the probing beam along the polar Z axis, which is shown in Fig. 1 by solid curve, to the experimental data. As can be seen, the behavior of the theoretical curve corresponding to the Bragg diffraction of elliptical Gaussian probe beam on RDS under consideration with the twisting domain walls formed by polarization switching in a congruent 5% MgO:$LiNbO_3$ crystal is in a satisfactory quantitative agreement with the experimental results.

This study was funded by the Ministry of Science and Higher Education of the Russian Federation within the framework of the state order for 2023-2025 (job-order FEWM-2023-0012).

1. E.N. Savchenkov, A.V. Dubikov, D.E. Belskaya, S.M. Shandarov, M.A. Chuvakova, A.R. Akhmatkhanov, V.Ya. Shur, *Bull. Rus. Acad. Sci.: Phys*. **88**, S413 (2024).

O14

Kinetics of domain structure in layered bismuth titanate $Bi_4Ti_3O_{12}$ single crystals

A.P. Turygin, A.D. Ushakov, E.D. Savelyev, M.S. Kosobokov, S.A. Melnikov, V.Ya. Shur

School of Natural Sciences and Mathematics, 620000 Ural Federal University, Ekaterinburg, Russia
anton.turygin@urfu.ru

Ferroelectric materials are widely used to create various nonlinear optical devices [1], microelectromechanical systems [2], data storage devices [3,4]. One of the important tasks is the creation of high-temperature piezoelectric materials that can operate at temperatures of 400°C and higher [5]. It was reported that bismuth-containing ferroelectrics with a layered structure (Aurivillius phase) have high T_C (> 500°C), high temperature stability of functional properties, low aging rate, which makes them promise for high-temperature applications [6]. Also, one of the potential applications of such ferroelectrics is the creation of non-volatile memory [7]. One of such materials is bismuth titanate ($Bi_4Ti_3O_{12}$, BiT), which has a relatively high ferroelectric phase transition temperature (~675°C) and high spontaneous polarization (Ps = 50 μC/cm^2). The polar axis in BiT lies at angle of 5° to the cleavage plane.

The as-grown domain structure and growth of isolated domains during local switching by a biased SPM tip on (100) cut of bismuth titanate $Bi_4Ti_3O_{12}$ single crystal. The as-grown domain structure consists of lamellar domains with submicron period. It was found that polarization reversal on (100) cut of BiT leads to formation of out-of-plane oriented domain with 90° and in-plane wedge-like domain with 180° domain walls (Fig. 1). The typical for ferroelectric crystals dependences of the domain sizes on parameters of the switching pulses were obtained: linear on amplitude (voltage) and logarithmic on duration. The domain wall motion during local switching was considered in terms of kinetic approach. The domain growth has been attributed to stochastic mechanism of nucleation. The activation and bias fields of domain wall motion were extracted by fitting of the field dependence for domain wall motion in *a* and *c* crystallographic directions.

The obtained results provide insights into domain kinetics in ferroelectrics with C_2 symmetry and can aid in the development of domain engineering techniques.

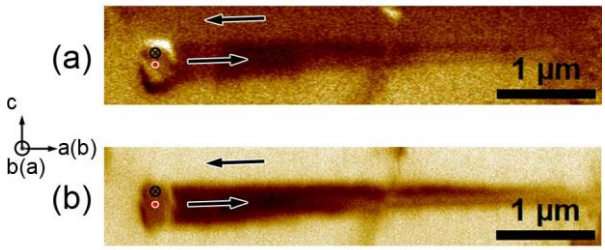

Figure 1. Local switching on the *a*-cut of BiT. PFM images of the domain structure: (a) vertical and (b) lateral signal. U_{sw} = 100 V, t_{sw} = 1 s.

The research was made possible by the Russian Science Foundation (Project No. 24-72-00170). The equipment of the Ural Center for Shared Use “Modern nanotechnology” Ural Federal University (Reg. No. 2968) was used.

1. V.Ya. Shur, A.R. Akhmatkhanov, I.S. Baturin, *Appl. Phys. Rev.* **2**, 040604 (2015).
2. J.F. Scott, C.A. Paz de Araujo, *Science* **246**, 1400 (1989).
3. X. Liu, Y. Liu, W. Chen, J. Li, L. Liao, *Nanoscale Res. Lett.* **7**, 285 (2012).
4. N. Setter, D. Damjanovic, L. Eng, et al., *J. Appl. Phys.* **100**, 051606 (2006).
5. S.E. Cummins, L.E. Cross, *J. Appl. Phys.* **39**, 2268 (1968).
6. H. Chen, B. Shen, J. Xu, J. Zhai, *J. Alloys Compd.* **551**, 92 (2013).
7. H. Watanabe, T. Mihara, H. Yoshimori, C.A.P. de Araujo, *Jpn. J. Appl. Phys.* **34**, 5240 (1995).

O15

Shungite as a strengthening component of the thin polarizing polymer films

L.O. Fedorova[1,2], P.V. Kuzhakov[2,3], N.V. Kamanina[1,2,3]

[1]*Saint-Petersburg Electrotechnical University "LETI", 197376 St. Petersburg, Russia*
loresafyoct@gmail.com

[2]*Petersburg Institute of Nuclear Physics named after B.P. Konstantinov of National Research Center "Kurchatov Institute", 188300 Gatchina, Leningrad Region, Russia*

[3]*Vavilov State Optical Institute, 192171 St. Petersburg, Russia*

Thin polymer polarizing films have been in the spotlight of the scientific community for the past decades due to their key role in modern display panels and optoelectronics. In LC and OLED displays, the polarizer is a mandatory component, which can account for more than 10% of the cost of the display itself. At the same time, the most popular due to their high efficiency are *H*-type polarizers, which are made on the basis of the iodine-dyed polyvinyl alcohol (PVA). The polyvinyl alcohol as a polymer provides important advantages for polarizers: flexibility and low weight allow such films to be used in curved or portable devices, and roll technologies allow them to be produced in large volumes. Optimization of the structure and properties of polarizing films in the form of selection of technological methods and parameters makes it possible to maintain the relevance of this material in mass production

One of the disadvantages of thin polymer films is their low mechanical strength. For the greater preservation and prevention of mechanical damage, films are laminated, but additional laminating layers can increase optical losses due to multiple reflections at the interfaces. This problem can be eliminated by nanostructuring the polymer matrix, for example, with the shungite, which is known for its strengthening properties.

Previously, colleagues from our research group developed the flexible polymer polarizers 0.1 mm thick with the addition of the graphene oxide, which turned out to be twice as strong as a pure polymer matrix and are already ready for use in displays. In this work, we studied the effect of the shungite nanoparticles embedded in the volume of the PVA matrix on the mechanical properties of the polarizing films based on it. The experimental research method was testing the film surfaces for microhardness using the PMT-3M device. It was found that an increase in the microhardness of PVA polarizers by 14.3 MPa under a load of 5 g occurs with the addition of 0.05 wt.% shungite. In addition, the greater stretching of the films contributes to their greater mechanical strength. Thus, for the polarizers with a shungite concentration of 0.05 wt.%, an increase in stretching from 1.8 to 3.3 times contributes to an increase in microhardness by 18 MPa under a load of 5 g. The experimental data were compared with the theoretical calculations obtained using the GaussView5.0 and Gaussian 09W programs.

To assess the adequacy of the structuring polarization films with shungite, other studies of their properties were conducted. First of all, using the SF-26 spectrophotometer, the transmission spectra were measured and the values of the degrees of polarization were calculated, since these parameters are of primary importance when creating polarizers. It was found that sensitization of PVA films with the shungite nanoparticles allows obtaining a degree of polarization of more than 97% in the entire visible spectral range, which makes it possible to improve the quality of the optical devices. In addition, the film surfaces were tested for wettability with water drops using the OSA 14EC device.

The study was partially supported by a grant from the Russian Science Foundation № 24-23-00021, https://rscf.ru/prjcard_int?24-23-00021.

1. R. Wu, K. Jiang, X. Jiang, *Optics Letters* **3**, 774 (2024).
2. Y. Zhou, Z. Guo, H. Gu, *Nat. Photon*. **18**, 922 (2024).
3. N. Kamanina, L. Fedorova, *Nanomaterials* **14**, 11 (2024).
4. E.F. Sheka, N.N. Rozhkova, *RENSIT* **1**, 3 (2016).

O16

Polarization loss in partially switched thin ferroelectric films

E.B. Kalika, I.G. Margolin, A.A. Chouprik

Moscow Institute of Physics and Technology, Dolgoprudny, Moscow Region, 141700 Russia
kalika.eb@phystech.edu

Ever since the discovery of ferroelectric properties of hafnium oxide [1], it has been recognized as a successful candidate for application of non-volatile memory devices, particularly, ferroelectric random-access memory (FRAM). Hafnia films demonstrate ferroelectric properties even in nanometer-thick films solving the device scalability problem [2]. Furthermore, research indicates that non-volatile memory devices utilising hafnium oxide films exhibit low power consumption and nanosecond processing speeds, thus positioning them as competitive alternatives to flash memory, their prevailing market competitor. The endurance of FRAM memory devices has already been shown to be one to two orders of magnitude greater than that of flash memory at this current stage of development [3] and, given the electronic nature of information storage, the endurance of HfO_2-based FRAM is potentially unlimited.

The operating voltage is the key parameter that determines the switching endurance of a memory device. Application of high operating voltage gives rise to phenomena such as accelerated migration of charged defects that can, in turn, result in electrical breakdown of the device [4]. In contrast, low operating voltage causes incomplete domain switching, thereby maintaining the film in a partially switched polarization state. Müller et. al. have demonstrated that the rate of polarization loss is higher in partially switched films [5] and, therefore, there is a negative correlation between the endurance and the retention of a FRAM device. Thus, the main issue now is to determine the optimal operating voltage in order to maximize both endurance and retention time of the device. The limiting factor to this research is that the standard retention time stated by the electronics market is 10 years and there is yet no universal method for the estimation of polarization loss.

In the present study, we initially conduct a series of experimental retention tests to investigate the aging of $Hf_{0.5}Zr_{0.5}O_2$ (HZO) films in both fully and partially switched polarization states and provide a comparative analysis. This data provides insight into the phenomenon of polarization loss in partially switched ferroelectric films, as well as the physical mechanisms that facilitate it. Then, a theoretical model is proposed for the prediction of retention time and polarization loss in FRAM devices when recording information in partially switched polarization state. The model is based on the physical phenomenon of imprint, which is characterized by the emergence of a built-in electric field due to the redistribution of charges under the field of spontaneous polarization [6]. Based on the initial experimental data, the proposed model allows one to predict the switching *I-V* curve at time point of interest. Furthermore, it has the capacity to predict polarization loss in HZO-based capacitors in both fully and partially switched polarization states and, consequently, can be applied to identify the optimal balance between the retention and endurance of the FRAM device.

The work is financially supported by the Russian Science Foundation (Project No. 25-19-00493).

1. T.S. Böscke, J. Müller, D. Bräuhaus, U. Schröder, U. Böttger, *Appl. Phys. Lett.* **99**(10), 102903 (2011).
2. M.H. Park, H.J. Kim, Y.J. Kim, W. Lee, T. Moon, C.S. Hwang, *Appl. Phys. Lett.* **102**(24), 242905 (2013).
3. V.V. Mikheev, E.V. Kondratyuk, A.A Chouprik, *Physical Review Applied* **18**, 064084 (2022).
4. A.A. Chouprik, E.V. Kondratyuk, V.V. Mikheev, et al., *Acta Materialia* **204**, 116515 (2021).
5. J. Müller, T.S. Böscke, S. Müller, et al., *2013 IEEE International Electron Devices Meeting*, 10.8.1 (2013).
6. G. Arlt, H. Neumann, *Ferroelectrics* **87**, 109 (1988).

O17

Transparent $MgAl_2O_4$ nanoceramics with carbon quantum dots

A.N. Kiryakov[1,2], T.V. Dyachkova[2], A.P. Tutunnik[2] I.V. Baklanova[2], O.G. Reznitskikh[2], A.N. Enyashin[2]

[1]*Ural Federal University, 620002 Ekaterinburg, Russia*
arseny.kiriakov@urfu.ru

[2]*Institute of Solid State Chemistry UD of RAS,* 620108 *Ekaterinburg, Russia*

The development of functional optical materials is an important task of modern photonics and optoelectronics. Recent advances in obtaining highly efficient carbon quantum dots have shown the promise of their use as new light-emitting devices without expensive rare earth elements and toxic production [1-3]. Due to the high temperature stability of low-dimensional carbon, such a material can be considered as a functional additive in the synthesis of optical nanoceramics. This allows modifying the optical and electronic properties of ceramics and using it as a tunable phosphor [4]. The aim of this work is to develop a new approach to modifying $MgAl_2O_4$ optical ceramics with carbon nanoparticles.

Ceramics were obtained by thermobaric pressing of a mixture of $MgAl_2O_4$ and ultrasound-dispersed graphene. The synthesis parameters: pressure 6 GPa, time 10 minutes, temperatures from 573 to 973 K using a toroid-type high-pressure cell. During the synthesis, the required pressure was first built up, after which the graphite heater was heated. In the work, a comprehensive analysis of the structural parameters was performed based on X-ray diffraction, FTIR, and Raman spectroscopy data. The photoluminescent characteristics were analyzed, as well as the kinetic dependences of PL in the temperature ranges from 4 to 300 K. Computer simulation was performed based on the developed model.

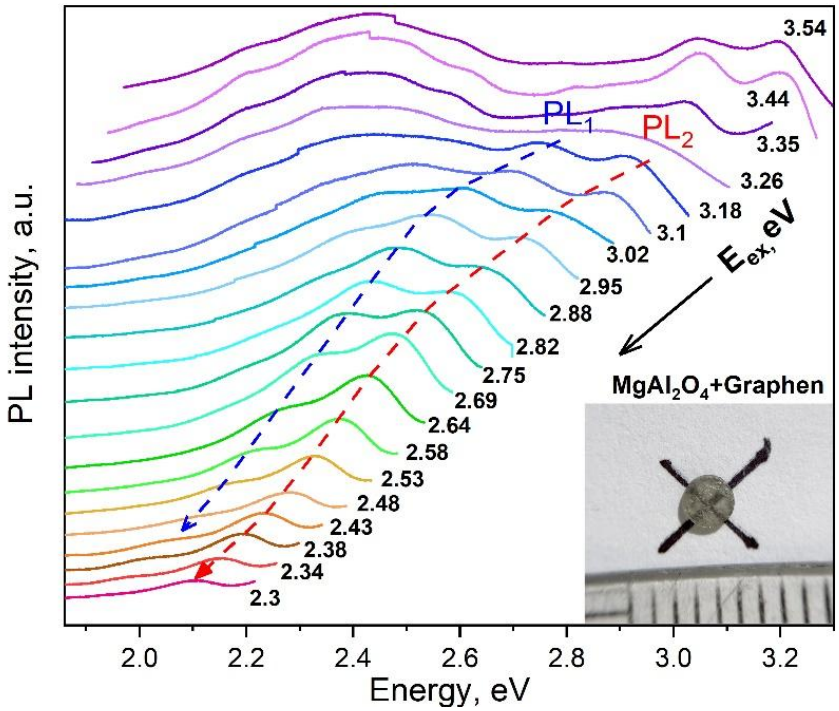

Figure 1. Photoluminescence spectra of transparent nanoceramics with the addition of dispersed graphene.

Under synthesis conditions of 6 GPa and a temperature range from 573 K to 673 K, the graphene additive weakly desorbed impurity molecules. It was found that under such synthesis conditions, the nanocomposite replicates the optical characteristics of the original dispersed graphene in isopropyl alcohol. Carbon particles have a set of sorbed bases on the surface, which form local energy levels in carbon nanoparticles and exhibit photoluminescence bands with energies of 2.3 eV and 3.0 eV. An increase in the composite synthesis temperature leads to the desorption of surface chemically bonded compounds, such as CH and CO. As a result of this process, the energy states of carbon nanoparticles change. It is shown that synthesis in the temperature range from 773 K to 873 K allows the formation of optically transparent ceramics and at the same time provides partial desorption of impurity molecules.

The graphene regions cleared of impurity molecules function as graphene quantum dots, with a characteristic shift in the PL signal maximum in the range of 2.9 eV–2.2 eV due to the quantum-size effect (Fig. 1). Computer modeling has shown the validity of the interpretation of experimental data. The combination of temperature and baric conditions used allows obtaining a unique functional composite material based on a mixture of oxide and carbon with a tunable luminescence spectrum.

The study was supported by the grant of the Russian Science Foundation No. 23-72-01024, https://rscf.ru/project/23-72-01024/.

1. X. Ye, M. Qi, M. Chen, L. Zhang, J. Zhang, *Adv. Mater. Interfaces* **10**, 2201941 (2023).

2. S.K. Tiwari, *et al.*, Magical Allotropes of Carbon: Prospects and Applications, *Critical Reviews in Solid State and Materials Sciences* **41**, 257 (2016).

3. P.S. Karthik, A.L. Himaja, S. Prakash Singh, A. Info, *Carbon Letters* **15**, 219 (2014).

4. A. Kiryakov, *et al.*, *Appl. Mater. Today* **36**, 102067 (2024).

O18

Excellent dielectric energy storage properties of Pb-free BNT-based ceramic achieved via phase structure modification

Xing Zhao, Gang Liu

School of Materials and Energy, Southwest University, 400715 Chongqing, China
liugang13@swu.edu.cn

The applications of (Bi, Na)TiO_3-based ceramics in capacitive energy storage are limited by the incommensurate recoverable energy storage density with the energy storage efficiency [1, 2].

In this work, we selected BNT as the model system and proposed a straightforward strategy, namely "high entropy & grain engineering", to achieve both high η and W_{rec} in BNT-based ceramics. The detailed design rationale is illustrated in Figure 1. In this work, $Sr_{0.85}Nd_{0.1}TiO_3$ (SNT) and Nb^{5+} are employed as dual entropy modulators. On one hand, the ΔS_{conf} of the BNT-based ceramics increases with the increase in SNT and Nb^{5+}contents, resulting in high-entropy ceramics when $\Delta S_{conf} > 1.5$ R. The high-entropy state allows a more complex domain configuration having different lattice structures below Tm, facilitating a high ΔP. Meanwhile, the introduction of Nd^{3+} [3, 4] may move R+T co-existence state to the vicinity of room temperature. On the other hand, the ionic radius of Sr^{2+} is larger than that of the A-site cations of BNT, suggesting an enhanced ΔG_{strain} that can further increase BDS of the resultant BNT-based ceramics. In addition, Nb^{5+} will play a critical role in broadening the dielectric peak to improve dielectric temperature stability [5]. Consequently, an ultrahigh recoverable storage density of 7.22 J/cm^3 and energy storage efficiency near 90.0% are attained under the electric field of 510 kV/cm. In addition, the energy storage performance also exhibits good stability against temperature and frequency.

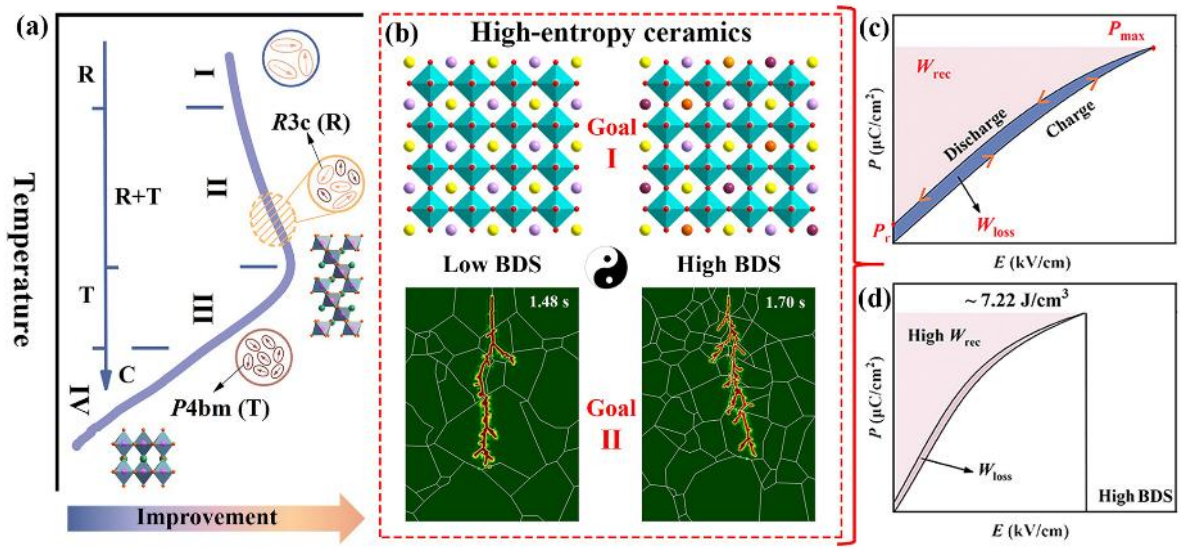

Figure 1. The strategy diagram to achieve a good balance between W_{rec} and η adopting the high-entropy strategy and grain engineering together.

1. Y.B. Adediji, A.M. Adeyinka, D.I. Yahya, O.V. Mbelu, *Energy Ecol. Environ.* **8**, 401 (2023).
2. F. Yan, J. Qian, S. Wang, J. Zhai, *Nano Energy* **123**, 109394 (2024).
3. A. Jain, Y.G. Wang, H. Guo, *Ceram. Int.* **47**, 10590 (2021).
4. C. Wang, Y. Huan, L. Hou, Y. Liu, X. Wang, R. Zhu, T. Wei, *Journal of Mat. Science*, **59** 1486 (2024).
5. W. Zhu, H. Guo, Z.Y. Shen, F. Song, W. Luo, Z. Wang, Y. Li, *J Am Ceram Soc* **106**, 3633 (2023).

O19

Control of mesoporous structure of PZT films prepared via self-assembly techniques

V.A. Yakushev[1], A.S. Vishnevskiy[1], D.S. Seregin[1], D.A. Abdullaev[2], K.A. Vorotilov[1]

[1]*MIREA - Russian Technological University, 119454 Moscow, Russia*
yakushev@mirea.ru

[2]*Institute of Nanotechnology of Microelectronics of the Russian Academy of Sciences, 119334 Moscow, Russia*

Lead zirconate titanate (PZT) thin films are widely used in semiconductor technologies due to their ferroelectric, piezoelectric and pyroelectric properties [1]. Porous PZT films demonstrate better merit for some applications due to large perovskite grains, lower mechanical stress, decreased dielectric constant, increased surface area and the possibility of using them as a template for creating composite heterostructures with new properties [2].

One promising method of obtaining such structures is molecular self-assembly, which involves adding surfactants to a sol-gel alkoxide solution. At a critical micelle concentration, polar organic molecules spontaneously form mesostructures within an inorganic body. Porous inorganic materials are formed by removing this organic phase. The molecular self-assembly process involves the interaction between micelle shells and alkoxide molecules. For this reason, the chemical composition and molecular weight of the surfactant strongly influence the porous structure of the obtained films. This study aims to investigate the formation of mesoporous PZT films using various cationic and non-ionic surfactants, including Pluronic® L61, Pluronic® L121, Brij® 98, and cetyltrimethylammonium bromide (CTAB).

Zirconium(IV) isopropoxide, an isopropanol complex of titanium (IV) isopropoxide, and anhydrous lead acetate were dissolved in 2-methoxyethanol at a zirconium-to-titanium molar ratio of 0.48:0.52, with the lead content exceeding the stoichiometric amount by 15%. Various amounts of surfactants were then added to obtain sols with a surfactant content of 0–40 wt.%. After stirring, the solution was spin-coated onto substrates. The substrates were silicon wafers with a structure of Si/SiO_2 (300 nm)/TiO_2 (10 nm)/Pt (150 nm) and highly doped p-type silicon with a resistivity of 0.005 Ω·cm. The effects of various surfactants with different relative molecular weights on the refractive index, thickness, open porosity and pore radius values were analysed using spectral and adsorption ellipsometric porometry (Sentech SE850). The dependencies of capacitance and polarization versus electric field at different frequencies were measured using an MDC complex equipped with an Agilent 4284A LCR meter and an AixACCT TF Analyser 2000. The microstructure of the films was analysed using scanning electron microscopy (FEI Nova NanoSEM 230).

The highest open meso-sized porosity value (V_{open}) was obtained when Pluronic® L61 was used as a surfactant. Increasing the content of this surfactant in the film-forming solution was found to increase the pore radius. However, V_{open} and R_{ads} decreased when the concentration reached 30 wt.%, due to a limited number of reaction groups. The minimum refractive index among the samples was obtained using CTAB at a concentration of 30 wt.%, attributed to the formation of macropores. Electrical measurements indicate the presence of ferroelectric hysteresis and a decreased dielectric constant in the obtained porous PZT thin films. Thus, it has been found that the microstructural and electrical properties of porous PZT films can be tuned by selecting the proper surfactant.

This work was supported by the Russian Science Foundation (RSF), grant No. 23-79-30016.

1. N. Izyumskaya, Y.-I. Alivov, S.-J. Cho, H. Morkoç, *Crit. Rev. Solid State Mater. Sci.* **32**, 111 (2007).
2. D.S. Seregin, L.A. Delimova, V.A. Yakuschev, et al., *Mater. Chem. Phys.* **332**, 130224 (2025).

O20

Scanning Probe Microscopy today – from micro and nanoelectronics to molecular biology and medicine

V.A. Bykov, T.G. Matyushin

XILLECT LLC, TECHNOSTACK HOLDING LLC, Moscow, Russia
vbykov@mac.com

To date, the development of SPM allows for active and effective research in many areas of science and industry – from fundamental and applied research of materials and processes to practical medicine.

The devices allow recording:

Profile of surface structures and its dependence on the contact pressure;

Non-uniformity of the friction force in the probe-surface system;

Non-uniformity of adhesive forces;

Distribution of surface potential (Kelvin mode);

Distribution of electrical capacitance in the cantilever-surface system;

Distribution of thermal conductivity;

Distribution of Young's modulus;

Diagnostics of elastic deformation limits;

Distribution of magnetic forces;

Distribution of piezoelectric characteristics of surface structures;

Possibility of surface modification with creation and study of the properties of the obtained nanostructures.

In combination with visible and IR spectroscopy, Raman spectroscopy it is possible to study the optical properties of surfaces with a spatial resolution of up to 10 nm, and with the use of tunable lasers in the IR range it is possible to obtain information on the distribution of functional groups on the surface.

By now, our group of companies has created atomic force microscopes for studying plates up to 200 mm in diameter with a resolution down to atomic, which is especially interesting for applied and fundamental research in the field of nanoelectronics. Figure 1 shows a photo of the N-LEKTA device, currently installed in the Zelenograd Nanotechnology Center.

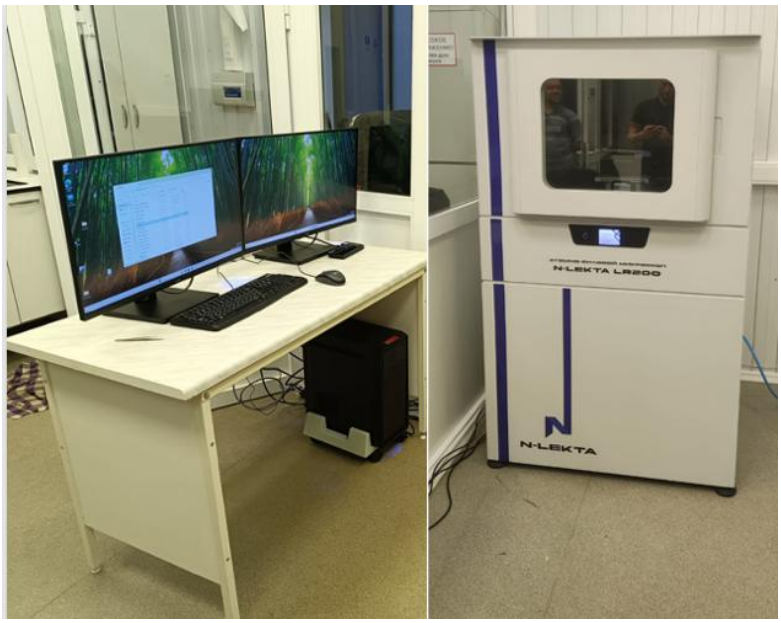

Figure 1. AFM N-LEKTA LR200 developed and manufactured by KSILLECT LLC, TECHNOSTEK Group of Companies, currently in operation at ZNT Center, Zelenograd.

Using the N-LEKTA LR200 AFM, it is possible to comprehensively study samples up to 200×200×20 mm in size with the ability to obtain atomic resolution in a conventional laboratory. The device is equipped with an internal thermal stabilization system. The operating temperature inside the device is set at 5–7 degrees above room temperature. The device is equipped with a powerful active vibration protection system, ensuring the ability to achieve atomic resolution when working in a laboratory without additional vibration and acoustic protection systems.

The device is equipped with a tubular piezo scanner with 3-coordinate capacitive sensors, providing a scan size of up to 100×100×10 μm^3 – 2×2×0.2 μm in high-resolution mode at a noise level of no more than 300 pm in X, Y and 30 pm in Z. The noise of the control electronics is no more than 5 $\mu V/Hz^{1/2}$. The device allows studying and monitoring many technological processes of both modern nanoelectronics and working in most other applications, including current modes, magnetic force microscopy modes, atomic force microscopy with automatic determination of scanning parameters.

For testing and studying biological objects, especially biological cells, the so-called capillary microscopy is very interesting and productive. The technique itself was proposed in the late 80s of the last centuries by Paul Hansma and was developed and turned into an informative one thanks to the work of Yuri Korchev and his group.

The measurements are carried out on a solid surface in an aqueous electrolyte solution. A glass capillary with an outlet from 100 to 20 nm is used as a probe in the system, into which a metal, most often silver chloride, electrode is inserted. The second electrode is placed in the electrolyte solution. The studies are carried out in the so-called hopping mode (suggested by Korchev).

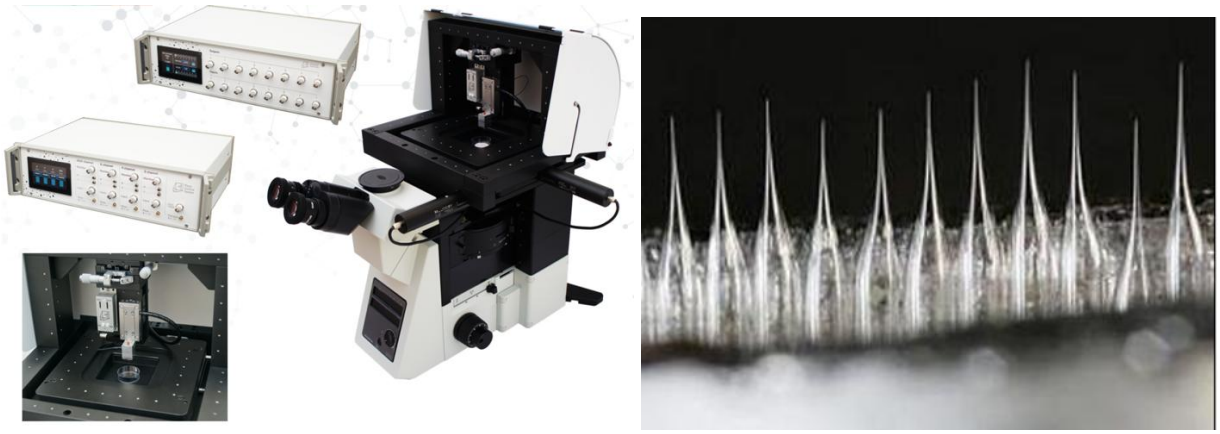

Figure 2. Capillary microscope of the research laboratory of A.S. Erofeev at the University of MISiS (Moscow) and the appearance of capillaries.

To study the optical properties of surfaces in the visible (Raman spectroscopy with a spatial resolution of up to 10 nm) and IR spectral regions with a resolution significantly exceeding diffraction limitations (near-field apertureless optical microscopy), specialized devices are being developed by joint efforts of Russian and Belarusian specialists and are currently being used in a number of research organizations, further improvement of which will allow their use to shift to industry. It is also possible to develop apertureless infrared and terahertz spectroscopes with a spatial resolution of up to 10 nm for high-quality surface analysis, which requires tunable infrared lasers.

O21

Novel half-metallic ferromagnet Gd_4Sb_3 with anomalous properties

S.T. Baidak[1], A.V. Lukoyanov[1,2]

[1]*M.N. Mikheev Institute of Metal Physics, Ural Branch RAS, 620108 Ekaterinburg, Russia*
baidak@imp.uran.ru

[2]*Institute of Physics and Technology, Ural Federal University, 620002 Ekaterinburg, Russia*

Research on half-metallic ferromagnets is of great interest to spintronics due to its unusual transport and electronic properties. In these compounds, it is possible to observe 100% spin polarization for electrons with energy close to Fermi energy and in such a case only electrons with a certain spin projection have non-zero conductivity, also in contrast with semimetals half-metallic materials have high current carrier concentration and density of states near the Fermi level. For example, these materials, especially the ones containing rare earth elements, are suggested for the use in magnetic random access memory (MRAM) and different magnetic devices [1]. In our research for the first time it was shown that the electronic structure of the Sb-based compound Gd_4Sb_3 exhibit half-metallic properties [2,3]. The calculations of the electronic structure were performed using the GGA+U method, which takes into account strong electronic correlations in the 4f shell of gadolinium. The calculations revealed a ferromagnetic type of magnetic ordering, and the calculated magnetic moment turned out to be 31 μ_B/f.u., which is mainly due to the half-filled 4f shell of Gd. Interesting features of the band structure of the Gd_4Sb_3 compound were revealed in the spin-polarized type of calculation. We found that the majority spin projection has completely metallic properties with many bands crossing the Fermi level and a high density of states in this region. It was also found that the band structure of the minority spin projection has an energy gap of 0.67 eV with a complete absence of states at the Fermi level and its vicinity. Later, the results were confirmed by another group, but only the anomalous Nernst and Hall effects were experimentally detected, no other studies were conducted [4]. The results obtained make the Gd_4Sb_3 compound a new interesting half-metal candidate with additional experimental studies needed to confirm this result. More detailed information on the study can be found in the published works [2,3].

This research was carried out with the support of the Russian Science project No. 22-42-02021.

1. S. Gupta, *Handbook on the Physics and Chemistry of Rare Earths* **63**, 99, (2023).
2. S.T. Baidak, A.V. Lukoyanov, *International Journal of Molecular Sciences* **24**, 8778 (2023).
3. S.T. Baidak, A.V. Lukoyanov, *Journal of Physics: Conference Series* **2701**, 12091 (2024).
4. Y. Han, C. Qiu, W. Ren, Y. Wu, L. Jiang, X. Luo, C. Chen, C. Fang, S. Ma, *Physical Review B* **110**, 144405 (2024).

O22

Topological spin semimetal band structure of $Co_{1.5}Mn_{1.5}Al$ compound

E.D. Chernov, A.V. Lukoyanov

M.N. Mikheev Institute of Metal Physics of Ural Branch of RAS, 620108 Ekaterinburg, Russia
chernov_ed@imp.uran.ru

The cobalt-based Heusler alloys are of special interest of scientific community because they can be attributed to half-metallic ferromagnets (HMF) [1], spin gapless semiconductors (SGS), topological semimetals (TSM), or recently proposed so-called topological spin semimetals combining half-metallicity and semimetallic properties in different spin channels [2]. These features result in large/giant magnetoresistance, high spin polarization, and a variety of crystal structure types [3] other properties productive for spintronic, magnetooptical or memory applications [4]. In particular, Co_2MnAl was found to exhibit the Weyl semimetal properties [5] manifested by exotic properties such as the Fermi arc surface states, the chiral anomaly effect, and the anomalous Hall effect. In this study, we performed first-principles calculations for $Co_{1.5}Mn_{1.5}Al$ which is the intermediate case of equal Mn and Co concentrations. Experimentally $Co_{1.5}Mn_{1.5}Al$ is crystallized in $L2_1$-phase (space group No. 225) with the lattice parameter of 5.76 Å. The calculations were performed within the framework of density functional theory (DFT) using the generalized gradient approximation with PBEsol potentials. To account for and investigate the influence of electronic correlations on the electronic and magnetic properties of the alloys, the DFT+U method was employed with the Coulomb interaction parameter U = 3 eV and the exchange interaction parameter J = 0.86 eV [6]. Additionally, our calculations incorporating spin-orbit coupling for the 3d orbitals of cobalt and manganese were carried out. For $Co_{1.5}Mn_{1.5}Al$, a series of calculations were performed to determine the energetically favorable substitution of cobalt positions by manganese. The calculations revealed that the most energetically favorable configuration involves placing manganese ions on the equivalent Co1 and Co2 sites. $Co_{1.5}Mn_{1.5}Al$ exhibits topological spin semimetal properties with the 100% spin polarization in our DFT calculations. The magnetic moments of manganese ions occupying the cobalt sites reversed their spin orientation, acquiring the magnetic moment of 1.78 μ_B. The total magnetic moment of the compound decreased notably to 1.5 μ_B. Including spin-orbit coupling in the doped $Co_{1.5}Mn_{1.5}Al$ compound did not lead to substantial modifications. Thus, the Heusler $Co_{1.5}Mn_{1.5}Al$ alloy exhibits intriguing electronic and magnetic properties, including full spin polarization and topological spin semimetal band structure.

This study was supported by the Russian Science Foundation, project no. 24-72-00152.

1. E.I. Shreder, A.A. Makhnev, K.G. Suresh, M.G. Kostenko, E.D. Chernov, V.G. Ivanov, A.V. Lukoyanov, *Mod. Phys. Lett. B* **36**, 2150573 (2022).

2. J. Nag, R. Venkatesh, A. Jha, P. Stamenov, P.D. Babu, A, Alam, S.G. Warrie, *ACS Appl. Electron. Mater.* **5**, 5944 (2023).

3. E.D. Chernov, A.N. Filanovich, E.I. Shreder, V.V. Marchenkov, L.A. Stashkova, A.V. Lukoyanov, *Appl. Phys. A: Mater. Sci. Process.* **130**, 783 (2024).

4. K. Elphick, W. Frost, M. Samiepour, T. Kubota, K. Takanashi, H. Sukegawa, S. Mitani, A. Hirohata, *STAM* **22**, 235 (2021).

5. P. Li, J. Koo, W. Ning, J. Li, L. Miao, L. Min, Y. Zhu, Y. Wang, N. Alem, C.-X. Liu, Z. Mao, B. Yan, *Nat. Commun.* **11**, 3476 (2020).

6. E.D. Chernov, A.V. Lukoyanov, *Magnetochemistry* **9**, 185 (2023).

O23

Hysteresis characteristics and frequency-field dependencies of magnetic susceptibility for $Fe_{75}Ga_{25}$ alloy

P.V. Kharitonskii[1,2], V.I. Nikolaev[1], S.A. Pul'nev[1], K.G. Gareev[2], A.Yu. Ralin[3], E.S. Sergienko[1,4]

[1]*Ioffe Institute, 194021 Saint Petersburg, Russia*

[2]*Saint Petersburg Electrotechnical University "LETI", 197022 Saint Petersburg, Russia*
kggareev@yandex.ru

[3]*Far Eastern Federal University, 690922 Vladivostok, Russia*

[4]*Saint Petersburg University, 199034 Saint Petersburg, Russia*

Fe-Ga (Galfenol) alloy system has great promise as a new magnetostrictive smart material for actuator, sensor, and energy harvesting applications [1,2], magnetostrictive devices operating at frequencies of up to 100 kHz [3,4]. In this work, we studied the $Fe_{75}Ga_{25}$ alloy obtained in the Laboratory of Shaped Crystals Physics at Ioffe Institute by vacuum melting method from high-purity materials: carbonyl Fe with 99.999% purity and Ga with 99.999% purity.

The results of the study of the $Fe_{75}Ga_{25}$ alloy's magnetic characteristics are shown in Figure 1.

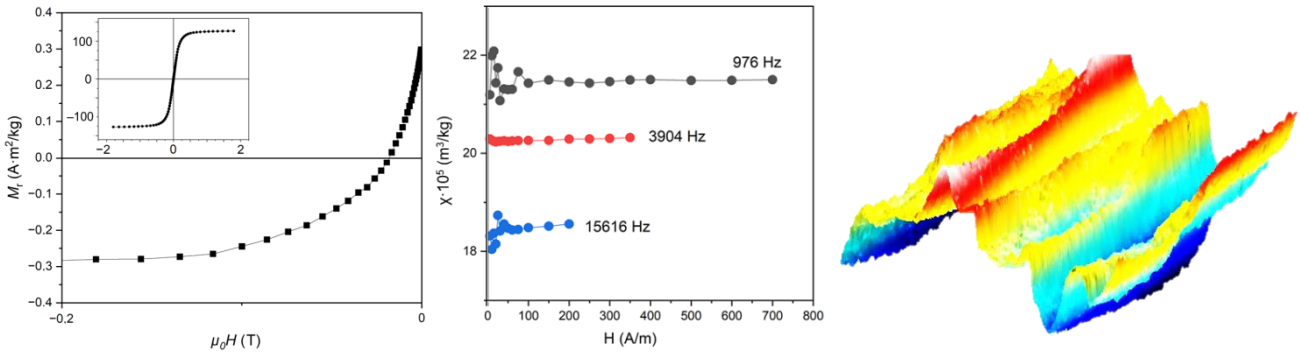

(a) (b) (c)

Figure 1. Magnetic characteristics of $Fe_{75}Ga_{25}$ alloy at 295 K: (a) hysteresis loop with DCD curve, (b) frequency-field dependencies of mass-normalized magnetic susceptibility, (c) 3D reconstruction of magnetic force microscopy (MFM); scanning area size 16×18 μm².

The obtained hysteresis characteristics for the alloy were: H_c = 0.5 mT, H_{cr} = 18.1 mT, M_s = 126.6 A·m²/kg, M_{rs} = 0.3 A·m²/kg. The values of M_s and H_s are in good agreement with the results given in the works [4, 5]. The review article [3] presents the results of MFM of $Fe_{81}Ga_{19}$ and $Fe_{72.2}Ga_{27.8}$ alloys. The domain structure has a dendritic shape with branches of ~10 μm long and ~0.5–1.5 μm wide. Figure 1c shows the MFM results for $Fe_{75}Ga_{25}$, which show branches of a dendritic structure with a width of ~2 μm.

In the studied $Fe_{75}Ga_{25}$ alloy, the presence of a similar magnetic structure, which is dendritic formations with magnetically inhomogeneous regions localized in them ("single-vortex" [6]), allows us to assume that the frequency-field dependence χ (Fig. 1c) is due to the inertia of the motion of these regions. The decrease in χ with an increase in frequency from 976 Hz to 3904 Hz is ~6%, and with an increase in frequency to 15616 Hz ~9%.

The research was carried out using the equipment of the resource centers of the SPbSU Research Park: Centre for Geo-Environmental Research and Modelling (GEOMODEL), Centre of Microscopy and Microanalysis, Centre for Innovative Technologies of Composite Nanomaterials.

1. E.M. Sammers, T.A. Lograsso, M. Wun-Fogle, *J. Mater. Sci.* **42**, 9582 (2007).
2. J. Atulasimha, A.B. Flatau, *Smart Mater. Struct.* **20**, 043001 (2011).
3. I.S. Golovin, V.V. Palacheva, A.K. Mohamed, A.M. Balagurov, *Phys. Met. Metallogr.***121**, 851 (2020).
4. V. Milyutin, R. Bureš, M. Fáberová, *Condens. Matter* **8**, 80 **(**2023).
5. M. Palit, H. Basumatary, S. Pandian, *J. Mater. Sci.* **60**, 1647 (2025).
6. P.V. Kharitonskii, V.I. Nikolaev, R.B. Timashov et al., *Phys. Solid State* (2025). Article is in press.

O24

Oscillations and drift of domain walls in iron garnet plates in harmonic magnetic field

S.E. Pamyatnykh, D.S. Mekhonoshin, L.A. Pamyatnykh

[1]*Ural Federal University, 620083 Ekaterinburg, Russia*
Pamyatnykh.Sergey@urfu.ru

The results of experimental study and numerical simulations of oscillations and drift of domain walls (DWs) in iron garnet plates in harmonic magnetic field in the temperature range of 300-250 K are presented.

The results are presented for a (111) plate of $(TbErGd)_3(FeAl)_5O_{12}$ iron garnet, plate thickness L = 50 μm, saturation magnetization Ms = 38 Gs, cubic and uniaxial magnetic anisotropy constants are equal to $K_1 = -3.8 \cdot 10^3$ erg/cm^3 and $K_u = 1 \cdot 10^3$ erg/cm^3, respectively.

Dynamic domain structure was studied using stroboscopic setup based on the magneto-optical Faraday effect (laser wavelength λ = 532 nm). The temperature was maintained constant using LINKAM THMS600 heating and freezing stage.

The dependences of coordinates and velocities of DWs in harmonic magnetic field with frequency f = 120.5 Hz at field amplitudes up to H_{dr} – the amplitude of external magnetic field, at which the drift of DWs starts in the sample [1], are obtained (Fig. 1a,b). The dependences of the DW drift velocity on the amplitude of external harmonic field in the specified temperature range are given in Figure 1c.

It is established that the motion of the DWs in harmonic magnetic field has asymmetric character (Fig. 1a,b), and the character of the asymmetry can change with changes in temperature and amplitude of the external field. The obtained dependences of the DW drift velocities on the external field amplitude at different temperatures show that in the sample under study there is a change in the direction of the drift to the opposite as the temperature decreases (Fig.1c). A possible reason for the change of the drift direction is a change of the gradient of internal fields in the sample with the change of temperature [2].

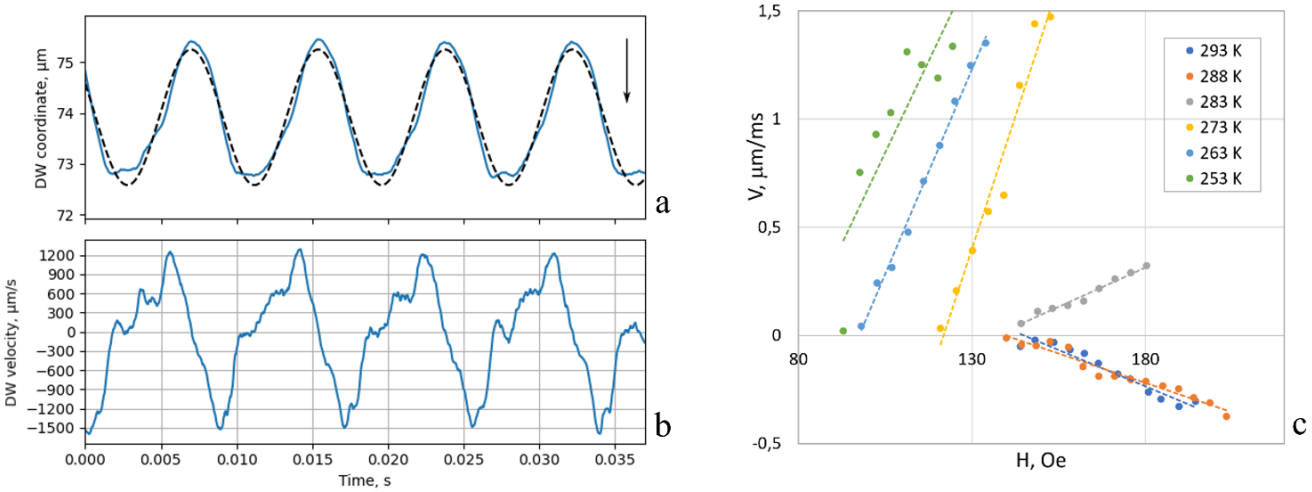

Figure 1. Dependence of a) coordinate of DW on time; b) velocity of DW on time in harmonic magnetic field (frequency f = 120.5 Hz, amplitude H_0 = 38 Oe) at temperature T = 283 K. The arrow indicates the direction of subsequent DW drift. c) Dependences of DW drift velocities on amplitude of external harmonic magnetic field with frequency f = 120.5 Hz at different temperatures.

The research was carried out with the financial support of the Ministry of Science and Higher Education of the Russian Federation within the framework of the state assignment (topic FEUZ-2023-0020).

1. L.A. Pamyatnykh, D.S. Mekhonoshin, S.E. Pamyatnykh, L.Yu. Agafonov, M.S. Lysov, G.A. Shmatov, *Physics of the Solid State* **61**(3), 483 (2019).

2. L. Pamyatnykh, M. Lysov, S. Pamyatnykh, G. Shmatov, *Journal of Magnetism and Magnetic Materials* **542**, 168561 (2022).

O25

Optical properties of the tetraborate family crystals: DFT simulations

S.N. Krylova, A.S. Alexandrovsky

Kirensky Institute of Physics Federal Research Center KSC SB RAS, 660036 Krasnoyarsk, Russia
slanky@iph.krasn.ru

The tetraborate crystals are the most promising optical materials in the UV range, as nonlinear optical (NLO) materials or host phases for luminophores. The wide practical applications of these materials are due to the unique physical properties of borates. In particular, they have wide transparency range, outstanding NLO, luminescence, piezoelectricity, relatively high resistance against laser-induced damage. [1] Of greatest interest are the crystals MeB_4O_7 (Me=Sr, Pb, Sn), which belong to the space group $Pmn2_1$. In this symmetry, significant nonlinear properties can be observed in crystals. The structure of the PbB_4O_7 crystal is presented in Figure 1.

The purpose of the present study is to perform the computer simulation of absorption spectra, electronic band structures and nonlinear coefficients of SrB_4O_7, PbB_4O_7, and SnB_4O_7 and to compare the results of the simulation with experimental in order to reveal the formation of transparency window and the origin of large nonlinear coefficients.

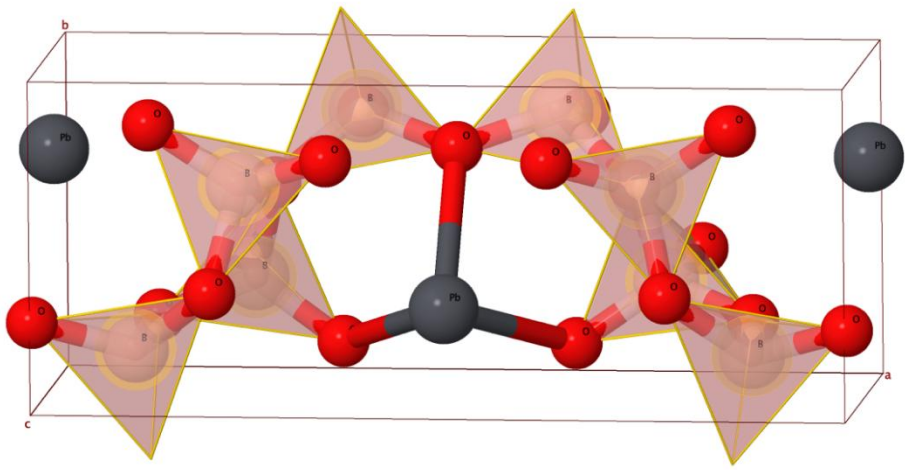

Figure 1. PbB_4O_7 crystal structure: Pb atoms - in black, oxygen atoms in red, boron atoms in light brown colors.

The theoretical simulation was performed within the framework of density functional theory in the CASTEP software package. The cell geometry was optimized by minimizing the total energy. To minimize energy, we used the Broyden-Fletcher-Goldfarb-Shanno (BFGS) algorithm. The Ecut energy was chosen to be 1030 eV. The 2x4x4 k-point Monkhrost-Pack grid was applied. The total energy convergence was 1.0×10^{-9} eV/atom. We used norm-conserving potentials for all atoms. The following valence electrons for B were considered: 2s2; for Sr: 4s2, 4p6, 5s2; for O: 2s2, 2p4; for Pb: 5s2, 5p6, 5d10, 6s2, 6p2. The PBEsol (GGA) and HSE03 correlation functional functionals were used to calculate the optimized geometry and optical properties. The comparison of computer-simulated absorption/transmission spectra in addition to determination of the band gap from the band diagram is applied to strontium and lead tetraborates. Excellent agreement is obtained for the simulation of the fundamental absorption edges of both PbB_4O_7 and SrB_4O_7. For SrB_4O_7, a spectral region is determined where the difference between the experimental and calculated spectra is due to indirect interband transitions.

S. Krylova and A. Alexandrovsky acknowledge the support by the state assignment of the Kirensky Institute of Physics FRC KSC SB RAS.

1. M. Mutailipu, K.R. Poeppelmeier, S. Pan. Borates, *Chemical Reviews*, **121**(3), 1130 (2020).

2. S.J. Clark, M.D. Segall, C.J. Pickard, P.J. Hasnip, M.I. Probert, K. Refson, M. C. Payne, *Zeitschrift fur kristallographie-crystalline materials* **220**, 567 (2005).

O26

On the nature of transport phenomena during proton exchange technological process

V.A. Demin, M.I. Petukhov, A.V. Sosunov, A.B. Volyntsev

Perm State National Research University, 614990 Perm, Russia
demin@psu.ru

Extremely complex transfer processes characterize the technology of waveguides production by proton exchange method in a lithium niobate single crystal. The working fluid, which acts as a source of protons, is a melt of benzoic acid C_6H_5COOH. This is the simplest organic acid of the aromatic series. Proton exchange occurs because of dissociative absorption of protons into the crystal, accompanied by the extrusion of lithium ions back into the working fluid. Electrokinetic transport phenomena in the melt of benzoic acid are fundamentally different from diffusion processes in the crystal, however, these processes are interrelated.

The dynamics of crystal protonation is of greatest interest to technologists, which is why historically the first calculations were made of crystal hydrogen saturation, as a result of which optical waveguides are formed in it [1]. Numerical modeling of the electrokinetic processes occurring in benzoic acid began much later [2]. These studies have shown that the different mobility of lithium ions and benzoate ions leads to the formation of a double electric layer near the surface of the crystal, which can significantly affect the rate of protonation.

Experimental data reliably show that the concentration front of protons in the volume of the crystal moves in dependence on time according to the root law and has a sharp, practically stepped profile. It is even more surprising that the so-called nonlinear diffusion equation [3] is the most efficient for describing the penetration of protons deep into the crystal. It is obtained from a more general quasi-linear second order diffusion equation in the consequence of assumption about a power dependence of the diffusion coefficient on the concentration. The difference from classical diffusion is expressed by the stepped nature of the profile and means the finite speed of disturbance propagation in the system. Even more unexpected is the fact that in the case when the exponent in the diffusion coefficient is equal two, the equation transforms into the Leibenson equation, known in filtration theory. It is used to describe the regular motion of the filtration front of an adiabatic gas in a porous medium.

This work was funded by Ministry of Education and Science of the Perm Region № С-26/37.

1. S.T. Vohra, A.R. Mickelson, S.E. Asher, *J. Appl. Phys.* **66**(11), 5161 (1989).
2. V.A. Demin, M.I. Petukhov, R.S. Ponomarev, M. Kuneva, *Langmuir* **39**, 10855 (2023).
3. V.V. Pukhnachev, *J. Appl. Mech. and Tech. Phys.* **36**(2), 169 (1995).

O27

Reflection of the stripe domains during polarization reversal process in lithium niobate crystal modified by soft proton exchange

E.D. Savelyev[1], A.P. Turygin[1], A.R. Akhmatkhanov[1], A.V. Sosunov[2], A.R. Kornilicyn[2], V.Ya. Shur[1]

[1]*Institute of Natural Sciences and Mathematics, Ural Federal University, 620002 Ekaterinburg, Russia*
evgeny.savelyev@urfu.ru

[2]*Perm State University, 614990 Perm, Russia*

We present an experimental study of domain-domain interactions during polarization reversal in congruent lithium niobate (LN) crystals modified by soft proton exchange (SPE) [1]. *In situ* optical imaging of domain kinetics during application of uniform electric field revealed the formation and growth of stripe domains oriented along three equivalent Y crystallographic directions on both polar surfaces (Z+ and Z–). When approaching an existing domain, the growing domain undergoes "reflection" – a 120° change in growth direction. A pronounced difference in the reflection process was observed at opposite polar surfaces: (1) at Z+ surface it occurs at distances 13–21 μm via two successive 60° rotations ($Y^+ \rightarrow Y^- \rightarrow Y^+$) (Fig. 1a–c), (2) at Z– surface it occurs at distances 30–50 μm via four 30° rotations ($Y^- \rightarrow X \rightarrow Y^+ \rightarrow X \rightarrow Y^-$) (Fig. 1d–f).

The reflection distance (d_{stop}) was inverse proportional to the external field E_{ex}. The effect was attributed to the action of residual depolarization field (E_{rd}) near the existing domain. Fitting of the experimental dependence by Eq. 1 yielded a residual bound charge density of 16 μC/cm^2, indicating 78% screening efficiency of the depolarization field. The lower values of d_{stop} on Z+ are related to higher conductivity of head-to-head domain walls and more effective screening of depolarization field [2].

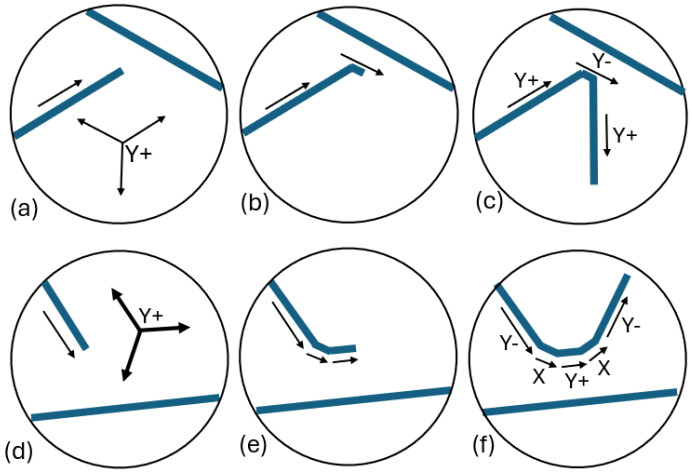

Figure 1. The schemes of domain reflection at (a-c) Z+ and (d-e) Z- polar surfaces.

$$d_{stop}(E_{ex}) = \frac{\sigma_{rd} w}{2\pi\varepsilon_0 (E_{ex} - E_{rd.z}^{gr} - E_{th})} \cos(\alpha) \qquad (1)$$

where σ_{rd} is the surface density of residual bound charge of the standing stripe domain, w is its width, ε_0 is the vacuum dielectric constant, α is the angle between the $\boldsymbol{E_{rd.z}^{st}}$ vector and the polar axis, $E_{ex.z}$ the polar component of the applied field, $E_{rd.z}^{gr}$ is the polar component of the residual depolarization field produced by the bound and external screening charges of the stripe domain, E_{th} is the threshold field.

These findings provide critical insights for domain engineering in SPE waveguides, enabling precise control of periodic poling for nonlinear photonic applications.

The equipment of the Ural Center for Shared Use “Modern nanotechnology” Ural Federal University (Reg.№ 2968) was used. The research funding from the Ministry of Science and Higher Education of the Russian Federation (Ural Federal University Program of Development within the Priority-2030 Program) is gratefully acknowledged.

1. E. Savelyev, A. Akhmatkhanov, et al., *Phys. Stat. Sol. Rapid Res. Lett.* **18**, 2300420 (2023).
2. X. Chai, J. Lian, C. Wang, et al., *J. Alloys Comp.*, **873**, 159837 (2021).

O28

Raman scattering study of phase transformations in $PbCo_{1/3}Nb_{2/3}O_3$ relaxor ferroelectrics

N.K. Derets[1], A.I. Fedoseev[1], J.-H. Ko[2], S.G. Lushnikov[1]

[1]*Ioffe Institute,* 194064 *St. Petersburg, Russia*
deretsnk@mail.ioffe.ru

[2]*Hallym University, 24252 Chuncheon, Republic of Korea*

A comprehensive Raman scattering study was performed on single crystals of $PbCo_{1/3}Nb_{2/3}O_3$ (PCN), a relaxor ferroelectric with perovskite structure containing 3d magnetic ions, over a wide temperature range from 650 K down to 80 K. PCN belongs to a broader family of complex perovskites with formula AB'B"O_3, known for frequency-dependent dielectric anomalies, and the presence of polar nanoregions (PNR). While these features are shared across relaxors, PCN exhibits additional complexity due to the presence of Co^{2+} and Co^{3+} ions, whose variable valence leads to charge fluctuations and phase separation phenomena. This study was motivated by the need to clarify how such electronic and structural heterogeneities influence lattice dynamics and relaxor behavior.

Polarized Raman spectra were recorded in both VV and VH geometries to investigate phonon behavior and quasielastic light scattering (QELS) across different temperature regions. The spectra revealed several characteristic features, including broad, well-polarized modes and anisotropic QELS, similar to those observed in PMN relaxor [1,2]. However, unlike in PMN, no distinct anomalies were observed near the dielectric permittivity maximum at $T_m \approx 250$ K, indicating an absence of connection between dielectric response and lattice dynamics in PCN [2].

The low-frequency phonon modes demonstrated nontrivial temperature dependencies in both frequency and linewidth. In VH polarization, the mode with the lowest frequency softened continuously down to the lowest measured temperature, while the mode above it exhibited a clear anomaly near both $T_1 \approx 283$ K and $T_2 \approx 230$ K, with T_2 possibly corresponding to the beginning of charge separation in the lattice. Low frequency mode, detected in VV polarization, showed a frequency minimum around $T_3 \approx$ 170 K, which was identified as the endpoint of phase separation, and linewidth maximum around T_1. These temperature points, T_2 and T_3, appear to mark key steps in the transformation of local charge states, driven by tunneling between Co^{2+} and Co^{3+} ions, and formation of regions with distinct electronic order.

The high-frequency mode showed a more conventional temperature dependence dominated by anharmonic effects. Its behavior followed the three-phonon model at high temperatures, but a clear deviation from this trend was observed below T_1, likely indicating a structural or electronic transformation not associated with a macroscopic phase transition [3].

QELS components in both VV and VH configurations displayed strong temperature dependence. In VH polarization, the QELS intensity increased upon cooling, reaching a maximum around T_2 and a secondary peak near T_3, before rapidly decreasing at lower temperatures. In VV polarization, a similar trend was found, though with only one distinct temperature maximum at T_3. These results suggest that QELS in PCN arises from at least two types of dynamic fluctuations: one linked to polar nanoregions, and another to emerging charge-ordered domains. This behavior contrasts with PMN, where QELS intensity peaks near T_m and gradually vanishes at lower temperatures [4].

Overall, the findings reveal that in PCN, the relaxor state is not governed solely by polar nanoregions but is strongly affected by dynamic charge ordering and local structural distortions introduced by 3d magnetic ions. The absence of phonon and QELS anomalies at T_m further supports the idea that the dielectric peak in PCN is not associated with any specific phase transition but instead reflects complex and overlapping relaxation processes. These insights advance the understanding of how variable-valence magnetic ions change relaxor behavior and may help to develop new materials, where both dielectric and magnetic functionalities are required.

1. R.A. Cowley, S.N. Gvasaliya, S.G. Lushnikov, B. Roessli, G.M. Rotaru, *Adv. Phys.* **60**, 229 (2011).
2. A.A. Bokov, Z.-G. Ye, *Journal of Advanced Dielectrics* **2**, 1241010 (2012).
3. M. Balkanski, R.F. Wallis, E. Haro, *Phys. Rev. B* **28**, 1928 (1983).
4. O. Svitelskiy, J. Toulouse, G. Yong, Z.-G. Ye, *Phys. Rev. B* **68**, 104107 (2003).

O29

Are oxygen vacancies driving ferroelectric domain repeatability?

E. Hemaprabha[1], A. Hershkovitz[2,3], D. Khorshid[2,3], L. Ma[4], S. Liu[4,5], S. Cohen[6], Ya. Ivry[2,3]

[1]*Department of Metallurgical and Materials Engineering, Indian Institute of Technology Madras, 600036 Chennai, India*
hemaprabha@iitm.ac.in

[2]*Department of Materials Science and Engineering, Technion – Israel Institute of Technology, 3200003 Haifa, Israel*

[3]*Solid State Institute, Technion – Israel Institute of Technology, 3200003 Haifa, Israel*

[4]*Key Laboratory for Quantum Materials of Zhejiang Province, School of Science, Westlake University, 310024 Hangzhou, China*

[5]*Institute of Natural Sciences, Westlake Institute for Advanced Study, 310024 Hangzhou, China*

[6]*Nuclear Research Center – Negev, 84190 Beer Sheva, Israel*

When ferroelectric materials are cooled below the Curie temperature (T_C), they undergo a symmetry reduction that leads to the formation of polarization domains. While these domains are expected to form randomly during repeated thermal cycles, literatures suggest that factors such as ferroelastic domain constraints and domain-pinning effects may introduce a degree of memory in their distribution.[1,2] This work explores the randomness and reproducibility of domain structures during sequential ferroelectric-ferroelectric and ferroelectric-paraelectric thermotropic phase transitions, focusing on the role of oxygen vacancies as potential pinning centers.

Variable temperature atomic-force microscopy (AFM), piezoresponse force microscopy (PFM) were used to capture domain patterns during the thermal cycling in barium titanate. Transmission electron microscopy tools with *in-situ* heating capabilities were used to validate the presence and immobility of oxygen vacancies at domain walls, as predicted by ab-initio models. The study reveals a high correlation (0.81 ± 0.05) between domain structures over repeated ferroelectric-paraelectric cycles (AFM and PFM). Domain walls exhibit significant pinning effects due to oxygen vacancies, which remain immobile even upon heating (above T_C) and cooling below T_C (Fig. 1A). Further, to domain repeatability was also captured during ferroelectric-ferroelectric phase transition (Fig. 1B). These findings highlight the critical role of oxygen vacancies in preserving the domain repeatability in ferroelectric materials.

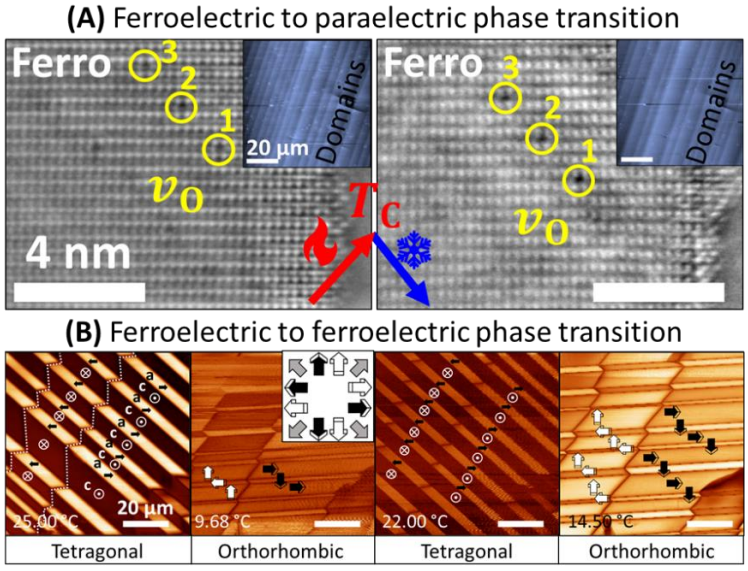

Figure 1. Domain wall pinning and thermal repeatability. (A) Oxygen vacancies cause strong domain wall pinning that remains unchanged across heating and cooling through ferroelectric-paraelectric transition. (B) Domain configurations are reproducibly retained during ferroelectric-ferroelectric phase transitions, indicating robust thermal memory effects.

1. C.T. Nelson *et al.*, *Science* **334**, 968 (2011).
2. X. Ren, *Nat. Mater.* **3**, 91 (2004).

O30

Modeling of cation disorder and distribution of anion vacancies in non-stoichiometric solid solutions based on lead magnoniobate

A.R. Lebedinskaya, A.G. Rudskaya

Southern Federal University, 344090 Rostov-on-Don, Russia
lebed1989@rambler.ru

Disordered ferroelectrics are the basis of most modern ferro- and piezoelectric materials, an active search for new methods and approaches to the creation of new materials with improved characteristics on their basis is underway. A special place among the most promising disordered ferroelectrics is occupied by relaxor ferroelectrics, which significantly surpass the currently widely used materials in a number of parameters. In the A- and B-sublattices of relaxors, described by the formula ABO3, disorder in the distribution of atoms is initially observed, which was the original basis for explaining the unique set of observed physical properties [1]. In the case of lead magnoniobate (PMN), it is impossible to increase the degree of ordering using technological processing. The presence of defects and structural disorder can not only radically change the properties of the ferroelectric material.

According to the model of compositional disordering [2], structural inhomogeneities arising due to differences in the ionic radii of the original and substituting atoms in the cation sublattices affect the distortion of oxygen octahedra, which is accompanied by a change in the position of the ferroelectric ion. The aim of this work is to model the disordering of the cation sublattice and the associated distribution of anion vacancies in the structure of ferroelectric ceramics of non-stoichiometric compositions based on lead magnoniobate in the absence of an electric field. Lead magnoniobate (PMN) is a model object, the properties and structure of which have been most thoroughly studied at present. Numerous structural studies of PMN show that the crystal has cubic symmetry up to the temperature of liquid helium [3]. At the same time, despite the abundance of experimental studies, theoretical ideas about the nature of the processes occurring in these compounds have not been finally formed, which complicates a targeted search for new compounds with promising properties. The modeling process was carried out on the data obtained on ferroelectric ceramics of the following compositions: $(1\text{-}x)PbMg_{1/3}Nb_{2/3}O_3 - x\ PbMg_{1/2}Nb_{1/2}O_{2.75}$ with x=0, 0.1, …1 [3].

Since ceramic materials are polycrystals, their properties differ in many respects from those of single crystals. This difference is due to the occurrence of structural defects that are absent or present in small quantities in single crystals, but also lead, for example, to the occurrence of a relaxor state. In the case of macroscopically homogeneous materials, it is point defects that have a great influence on the smearing of the phase transition. However, the main reason for observing relaxor properties in materials, which is not directly related to the technology of obtaining the material, is the disordered distribution of different ions over crystallographically equivalent positions. Fluctuations of Nb^{5+} and Mg^{2+} ions in the B-sublattice are sources of random electric fields, which leads to freezing of ferroelectric domains of the nanometer scale [4].

In the framework of our model, randomly distributed dipoles in the system, arising due to the disordered displacement of ions in the cation sublattices and the resulting distortion of oxygen octahedra, were considered as the main source of random fields. At this stage of modeling ionic systems, we tried to take into account surface effects by introducing special boundary conditions, since it is the surface that is an important source of defects.

1. G.A. Smolensky, et al., *Physics of the Solid State* **11**, 2906 (1960).
2. A.A. Bokov, et al., *Z. Kristallogr*. **226**, 99 (2011).
3. A.R. Lebedinskaya, et al., *Advanced Materials. Springer Proceedings in Physics* **224**, 267 (2019).
4. M.D. Glinchuk, et al., *Physical Review B* **98**, 094102 (2018).

O31

Features of synthetic hydroxyapatite with substitution of calcium cations by magnetic manganese and iron ions

V.S. Bystrov[1], E.V. Paramonova[1], N.V. Bulina[2], S.V. Makarova[2], N.V. Eremina[2], S.V. Semenov[3], L.A. Avakyan[4]

[1]*Institute of Mathematical Problems of Biology, RAS, 142290 Pushchino, Russia*
vsbys@mail.ru

[2]*Institute of Solid State Chemistry and Mechanochemistry, Siberian Branch, RAS, 630090 Novosibirsk, Russia*

[3]*FRC Kirensky Institute of Physics, Siberian Branch, RAS, 660036 Krasnoyarsk, Russia*

[4]*Physics Faculty, Southern Federal University, 344090 Rostov-on-Don, Russia*

Hydroxyapatite (HAP) is a widely used biocompatible material in many biomedical applications, often used for regeneration and replacement of bone tissue, since it is its mineral component [1]. The cationic substitutions in the HAP structure greatly affect its physical properties, biocompatibility and implants survival based on HAP introduced into the body [2,3]. The properties of HAP structure, with Calcium cations replaced by Iron and Manganese magnetic ions, were studied using density functional theory (DFT) methods in combination with the experimental studies on mechanochemical synthesis.

It has been previously shown that HAP structure has piezoelectric and ferroelectric properties [4]. These features affect the electrical properties of HAP surface layers, changing the work function of electrons, which is important for the adhesion and survival of bone cells and bone tissue growth. The introduction of the magnetic ions creates additional magnetic properties of HAP structure. Magnetic biomaterials are of great interest for regenerative medicine, since they allow the use of magnetic therapy, which promotes better bone tissue restoration, with surgical and drug treatment [5]. In addition, magnetic materials can be used to detect tumors using magnetic resonance imaging [5]. Moreover, such HAP materials, besides biocompatibility and bioactivity, have superparamagnetic properties, which can be used for local heat treatment (hyperthermia) and targeted drugs delivery [6].

Basic data on the configuration of the cation-substituted HAP [$Ca_{10-x}M_x(PO_4)_6(OH)_2$, where M = Fe, Mn], at the different concentrations x of the introduced Fe and Mn cations and the high-precision DFT calculations method using the PBE(GGA) and HSE hybrid functional, are presented in [7,8]. Results showing good data agreement with experiments: the parameters and volume of Fe-HAP and Mn-HAP unit cell decrease with an increase of Fe and Mn substitutions, that is similar to the case for Mg/Ca substitutions in Mg-HAP. However, there are significant differences in the changes in their properties for these substituents. For the Mn-HAP case the additional electronic energy levels Ei were detected inside the band gap Eg of Mn-HAP. Depending on the concentration of Mn, the photoexcitation energy changes, and its effective value Eg* becomes less than the band gap Eg in the unsubstituted HAP. The arisen magnetic properties of Mn-HAP are proportional to the amount of Mn introduced and energy levels Ei, filled by spin-up electrons. While the spin-down electrons is absent for Mn-HAP. In Fe-HAP case, the features are more complex; both electrons with spin up and spin down are here. This also changes the band gap and creates effective values of photoexcitation Eg*. In addition, here there are more electrons with spin up relative to electrons with spin down, but their number is still proportional to the growth of substitutions. As a result, the total magnetic moment of Fe-HAP differs from Mn-HAP and the total magnetization value for Fe-HAP is less than that of Mn-HAP. Experimental measurement of magnetization was also performed on both types of Fe-HAP and Mn-HAP samples, prepared at a concentration of x = 1, which showed characteristic dependences on the applied magnetic field. These measurements were performed at room temperature. At low temperatures it will be done in near future.

1. S.V. Dorozhkin, *Mater. Sci. Eng. C Mater. Biol. Appl.* **55**, 272 (2015).
2. M. Šupova, M. *Ceram. Int.* **41**, 9203 (2015).
3. V. Bystrov, E. Paramonova, L. Avakyan, J. Coutinho, N. Bulina, *Nanomaterials* **11**, 2752 (2021).
4. V. Bystrov, E. Paramonova, L. Avakyan, S. Makarova, N. Bulina, *Ferroelectrics* **618**, 1173 (2024).
5. H. Inam, et al., *Int. J. Mol. Sci.* ***25***, 2809 (2024).
6. S. Mondal, et al., *Int. J. Nanomedicine* **12**, 8389 (2017).
7. V.S. Bystrov, E.V. Paramonova, L.A. Avakyan, et al., *Materials* **16**, 5945 (2023).
8. V. Bystrov, E. Paramonova, L. Avakyan, S. Makarova, N. Bulina, *Next Materials* **8**, 10058 (2025).

POSTER

PRESENTATIONS

P1

Pseudo-transitions in one-dimensional anisotropic spin models

Y.D. Panov[1], D.N. Yasinskaya

Ural Federal University, 620062 Ekaterinburg, Russia
yuri.panov@urfu.ru

One-dimensional spin models provide a convenient framework for testing fundamental concepts in statistical physics and are widely used to describe the properties of real materials, including molecular-based heterometallic compounds and coordination polymers. Decorated Ising chains often admit exact solutions, exhibit rich ground-state phase diagrams with multiple frustrated phases, and may display pseudo-transitions previously observed in spin ice models. Unlike conventional phase transitions, which are associated with the emergence of an order parameter, a pseudo-transition involves a rapid replacement of a frustrated state (quasi-phase) by a low-entropy state at a finite temperature. Crucially, pseudo-transitions preserve the analyticity of all thermodynamic functions.

The occurrence of pseudo-transitions can be attributed [1] to the residual entropy properties of the system: a pseudo-transition emerges near the boundary between ground-state phases if the residual entropy remains continuous across the boundary from at least one phase. The frustrated one-dimensional Potts model [2] demonstrates that this criterion is directly linked to the microscopic incompatibility of ground-state phases at the phase boundary. In this model, as in many others, pseudo-transitions manifest through a step-like temperature dependence of entropy (resembling first-order transitions), and a sharp peak in heat capacity (analogous to second-order transitions). Similar behavior is observed for magnetization and magnetic susceptibility, prompting the introduction of pseudo-critical exponents [3] by analogy with conventional phase transitions. It can be shown [2] that the universal values of these exponents are determined by the algebraic structure of the largest and subleading eigenvalues of the model's transfer matrix, along with the corresponding approximations of thermodynamic quantities near the pseudo-transition.

By mapping the spin chain to a Markov process, we conducted a detailed study of the frustrated ground-state phases in a generalized diluted one-dimensional Ising model with two types of non-magnetic charged impurities [4]. This model reveals, for the first time, a new type of pseudo-transition [5]. We show that its origin lies in phase separation: within a charge-ordered quasi-phase formed by charged non-magnetic impurities, nuclei of an (anti)ferromagnetic quasi-phase emerge. The system's thermodynamic properties can be accurately described using Maxwell's phenomenological construction for the free energy of the two quasi-phases. This approach yields analytical expressions for the concentration dependence of the pseudo-transition temperature, and the temperature-dependent fraction of the (anti)ferromagnetic phase below the pseudo-transition, which fully govern the behavior of other thermodynamic functions. Comparison with exact solutions clarifies the limitations and validity of the phenomenological description.

This study was supported by the Ministry of Science and Higher Education of the Russian Federation, project FEUZ-2023-0017.

1. O. Rojas, *Brazilian J. Phys.* **50**, 675 (2020).
2. Y. Panov, O. Rojas, *Phys. Rev. E* **103**, 062107 (2021).
3. O. Rojas, J. Strecka, M.L. Lyra, S.M. de Souza, *Phys. Rev. E* **99**, 042117 (2019).
4. D.N. Yasinskaya, Y.D. Panov, *Phys. Solid State* **66**, 1068 (2024).
5. D. Yasinskaya, Y. Panov, *Phys. Rev. E* **110**, 044118 (2024).

P2

First-principles study of magnetic and half-metallic properties of $Mn_2Co_{1-x}Ni_xSn$ alloys with spin polarization

N.S. Solovyev[1], A.V. Lukoyanov[1,2]

[1]*Ural Federal University named after the first President of Russia, B.N. Yeltsin, 620002 Ekaterinburg, Russia n.s.solovyev@urfu.me*

[2]*M.N. Mikheev Institute of Metal Physics, Ural Branch of RAS, 620108 Ekaterinburg, Russia*

Half-metallic Heusler alloys have the potential to be used in spintronics [1] due to the existence of a band gap for one of the spin projections providing a possibility for 100% spin-polarized current. These alloys also display useful thermoelectric, optical [2] and transport properties [3]. In this work, we present the results of first-principles calculation of the electronic structure and magnetic properties of inverse $Mn_2Co_{1-x}Ni_xSn$ Heusler alloys for x = 0 – 1. The alloys crystallize in the XA-type Heusler structure with space group F–43m. For x=0, the alloy Mn_2CoSn is found to be a semiconductor in the majority spin projection and a metal in the minority spin one, i.e., being a half-metal. In this composition, there is a band gap of less than 1 eV in the majority spin direction, thus the spin-polarization of current is almost full. The other compositions for x = 0.25, 0.5, 0.75, 1 are metallic in both majority and minority spin directions with spin polarization approaching 0.3. When replacing Co ions with Ni, the electronic states which formed the band gap in Mn_2CoSn move lower than the Fermi energy. A peak of states in the majority spin direction located above the Fermi level without nickel, moves to the Fermi energy with the increased Ni concentration. Total magnetization of Mn_2CoSn is –3 μ_B, which satisfies the Slater-Pauling rule, increasing the nickel ion concentration causes the magnetization to drop to –0.75 μ_B. Magnetic moments of the Ni, Co and Sn ions stays almost constant, –0.1, –1 and –0.01 μ_B respectively. The manganese ions labeled as Mn1 and Mn2 are ordered antiferromagnetically and magnetic moment of Mn2 is approximately equal to –3 μ_B for all x. In Mn_2CoSn, the Mn1 ions have the magnetic moment of 0.66 μ_B. In the intermediate concentration alloy $Mn_2Co_{0.75}Ni_{0.25}Sn$, the magnetic moment of Mn1 is 1.9 μ_B. In the alloys with the higher Ni concentrations, the magnetic moment of Mn1 is 2.3-2.6 μ_B. Thus, in this work, we demonstrated the effect of the ratio of nickel and cobalt on the electronic structure and magnetic properties of $Mn_2Co_{1-x}Ni_xSn$ Heusler alloys for x = 0 – 1. It was found that in Mn_2CoSn there is a band gap in the majority spin direction, making it half-metal, while other alloys are metallic and have a decreasing magnetization with the decreasing cobalt concentration. The work was carried out within the framework of the state assignment of the Ministry of Science and Higher Education of the Russian Federation for IMP UrB RAS.

1. J. Ma, J. He, D. Mazumdar, K. Munira, S. Keshavarz, T. Lovorn, C. Wolverton, A.W. Ghosh, W.H. Butler, *Phys. Rev. B* **98**, 094410 (2018).

2. S. Sharma, D.C. Gupta, *Mater. Sci. Eng. B* **314**, 118070 (2025).

3. S. Chatterjee, S. Chatterjee, S. Giri, S. Majumdar, *J. Phys.: Condens. Matter* **34**, 013001 (2021).

P3

Features of the conduct of near-electrode processes in lithium niobate crystals $LiNbO_3$ with different domain structures

V.E. Umylin, N.S. Kozlova, E.V. Zabelina, A.A. Mololkin, A.V. Korchagin, D.A. Kiselev, T.S. Ilina

National University of Science and Technology MISIS, 119049 Moscow, Russia
v.umylin@mail.ru

Lithium niobate crystal $LiNbO_3$ is a well-known uniaxial ferroelectric crystal with a high Curie temperature (1142 °C) and is widely used in quantum optics, acousto- and optoelectronics to create electro-optics products, nonlinear optics, devices on surface and bulk acoustic waves, piezoelectric and magnetoelectric sensors, devices on charged domain walls.

To create devices based on $LiNbO_3$ elements, various cuts with applied conductive coatings are used. As it is known [1] that in samples of polar cuts of crystals without preliminary polarization and other external influences the electromotive force occurs, and under short-circuiting conductive coatings the short-circuit currents (SCC) are observed. As it is shown [2] that under heating the SCC can exchange the flow direction and magnitude by orders. These processes can affect the electrophysical and dielectric properties significantly, and even the phase stability of the material. And to the functional characteristics of the devices and instruments of which they are the working elements as a consequence. Such effects lead to the degradation and aging of the surfaces of crystalline elements and thereby change the properties of these elements.

The aim of this work was to study the features of the conduct of near-electrode processes in lithium niobate crystals $LiNbO_3$ with different domain structures.

For the measurements, samples of Z-cuts of congruent $LiNbO_3$ crystals in the form of rectangular plates, with different domain structures and different materials of conductive coatings (In, Ag) were prepared. Previously the samples have not exposed to any stimulating external effects: no temperature, no electric field, no radiation.

The samples with symmetrical (identical) conductive coatings relative to the polarity of the sample side were studied. The polarity of the samples was determined using a piezotester. The SCC and their temperature dependences were measured in the temperature range from room temperature to 300 °C without applying an external electric field. The SCC on the samples were recorded using the hardware complex with the special software developed in our laboratory (certificate of state registration of the computer software No. 2025615960).

The first results of the study of temperature dependences of the short-circuit current in $LiNbO_3$ crystals with single-domain and polydomain structures have been obtained. In single-domain crystals with an increase in temperature, the short-circuit current changes by orders of magnitude, while in polydomain samples, the short-circuit current increases several times. When conductive coatings are applied, the current flows in negative direction, while when Ag is used, the SCC flows in positive direction.

Studies of the features of the conduct of near-electrode processes in $LiNbO_3$ crystals were carried out in the accredited laboratory of semiconductor materials and dielectrics «Single crystals and stock on their base» NUST MISIS with financial support from the Ministry of Education and Science of Russia within the framework of the state assignment to universities FSME-2023-0003.

1. N.S. Kozlova, E.V. Zabelina, M.B. Bykova, et al., *Russian Microelectronics* **48**, 146 (2019).
2. N.S. Kozlova, E.V. Zabelina, O.A. Buzanov, et al., *IEEE ISAF*, 1 (2019).

P4

Phenomenological theory of a single domain wall in lithium niobate and lithium tantalate

E.L. Rumyantsev

School of Natural Sciences and Mathematics, Ural Federal University, 620000 Ekaterinburg, Russia
evgeny.rumiantsev@urfu.ru

The phenomenological treatment of the structure of antiparallel 180^0 domain walls in lithium niobate and lithium tantalate is carried out within Ginzburg-Landau-Devonshire theory. It is shown that these walls are not of pure Ising type but are of mixed Bloch-Neel-Ising character. Previously this fact has been pointed out and confirmed by density-functional calculations and corresponding thermodynamic treatment in number of papers [1-3]. Contrary to the results presented in [2], where an effect of the perturbation of the polarization confined to the plane orthogonal to the wall plane is induced by the strain, we show that the desirable result can be obtained by considering the polarization subsystem only. Moreover, we do not analyze as usual the corresponding Euler-Lagrange equations but used variational method used in quantum mechanical problems. Such approach allows us to obtain physically clear analytical expressions easy for interpretation. As in the cited papers it is shown that the difference in contribution of induced by the wall orthogonal polarization leads to the drastic difference in the domain wall energy as the function of orientation. Especial attention is paid to the energetics of so-called X and Y walls confined to XZ and YZ planes correspondently. The crucial role in the presented treatment is due to the forth order parameter $\gamma P_z\left(P_x^2 P_y - P_y^3\right)$ which has been omitted in free energy expansion in [2] while the term of the same symmetry structure has been taken into account in elastic energy expression.

We show that the sign of γ determines if the movement of the given wall type is thermodynamically preferable. For $\gamma > 0$ the Y walls oriented in x^+ direction is energetically favored as regards X walls in y^+ direction. The important property of Y walls is that in this case the walls oriented in x^+ and x^- possess equal surface energy. Thus, they are candidates for initiating of arising of hexagonal domains. The presented treatment predicts that Y walls have Bloch –type rotation behavior in full correspondence with the results of atomistic simulations [3]. The X walls under the same condition demonstrate different behavior for the walls oriented in y^+ and y^- directions. Under condition that $\gamma > 0$, the surface energy of the wall in y^- orientation is less as compared with one pointing in y^+ direction. The arising and movement of X walls thus can explain the observation of triangular domains in lithium tantalite. Within our approach it is shown that X walls if arisen must possess mixed Ising-Neel-type character which is also in accord with density-functional calculations [3].

In summary we argue that proposed treatment allows to reveal the dependence of observed polarization behavior on the parameters in Ginzburg-Landau-Devonshire free energy expansion. Such simple and time-conserving treatment can be also useful for prediction and analyzation of the temperature dependence of observed polarization reversal patterns.

The author is grateful for financial support of the Ministry of Science and Higher Education of the Russian Federation (state task FEUZ-2023-0017).

1. D. Lee, R.K. Behera, P. Wu, et al., *Phys. Rev. B* **80**, 060102 (2009).
2. D.A. Scrymgeour, V. Gopalan, A. Itagi, et al., *Phys. Rev. B* **71**, 184110 (2005).
3. D. Lee, H. Xu, V. Dierolf, et al., *Phys. Rev. B* **82**, 014104 (2010).

P5

Raman identification of rare earth oxide phases in high-entropy ceramics: DFT approach

E.A. Buntov[1], M.I. Melnikova[1], Yu.V. Schapova[2], A.N. Kiryakov[1,3], T.V. Dyachkova[3], A.P. Tutunnik[3]

[1]*Ural Federal University, 620002 Ekaterinburg, Russia*
e.a.buntov@urfu.ru

[2]*Zavaritsky Institute of Geology and Geochemistry, 620110 Ekaterinburg, Russia*

[3]*Institute of Solid State Chemistry, 620108 Ekaterinburg, Russia*

Rare earth oxides are crucial for advancing optoelectronic technologies and developing high-performance optical devices such as lasers, LEDs, display elements, photodetectors, and UV/IR radiation converters. Despite their technological significance, the multipart high entropy compounds are hardly characterized by standard XRD methods due to a complex composition [1]. In this case the optical methods are useful to reveal the lattice type of each component. This study aims to perform an in-depth investigation of the structural and surface characteristics of rare earth oxides exhibiting different crystal lattice types.

The high entropy oxide (HEO) [2] of the composition $(Y_{0.2}Eu_{0.2}Gd_{0.2}La_{0.2}Er_{0.2})_2O_3$ was obtained as a result of chemical precipitation of a mixture of hydroxides with subsequent heat treatment of the obtained precipitate. The average size of the coherent scattering region for obtained nanopowder was determined to be 20-30 nm in accordance with the X-ray diffraction full-profile analysis. The HEO nanopowder was degassed for 3 hours at 680°C.

Experimental Raman spectra were obtained using a LabRAM HR Evolution Raman spectrometer. The modeling was carried out using the Materials Studio software package with the CASTEP module, which employs density functional theory (DFT) to calculate the phonon modes under GGA approximation.

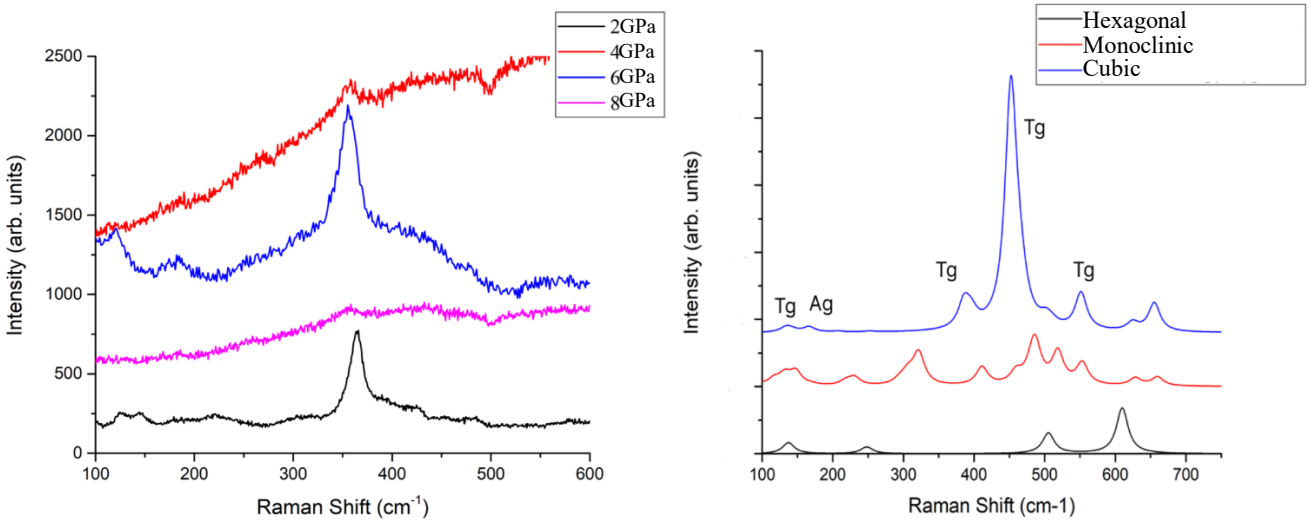

Figure 1. Left: $(Y_{0.2}Eu_{0.2}Gd_{0.2}La_{0.2}Er_{0.2})_2O$ ceramics Raman spectra under different synthesis pressures. Right: Calculated scattering curves for Y_2O_3 crystal with known lattice types.

Figure 1 shows the spectra obtained using an excitation source with a wavelength of 633 nm for the compound $(Y_{0.2}Eu_{0.2}Gd_{0.2}La_{0.2}Er_{0.2})_2O$ synthesized at 2, 4, 6 and 8 GPa. For the samples synthesized at 2 and 6 GPa, identical Raman spectra are observed with the fundamental vibrational mode located at 365 cm^{-1} and 355 cm^{-1}, respectively. Comparing figures 1 and 2, we can say that the experiment observes the Tg vibrational mode, i.e. the vibrations of the atoms are symmetrical. The calculated positions of the spectrum lines are shifted to the right along the x-axis by 13 cm^{-1}.

The calculated results of Raman scattering show satisfactory agreement with both theoretical predictions and experimental data, within the expected margin of measurement error. This confirms the applicability of the DFT-based approach for investigating the optical properties of chemically complex compounds.

The study was supported by the grant of the Russian Science Foundation No. 24-22-00268.

1. S.V. Ushakov, S. Hayun, W. Gong, A. Navrotsky, *Materials* **13**(14), 3141 (2020).

2. A.N. Kiryakov, Yu.A. Kuznetsova, E.A. Buntov, T.V. Dyachkova, J. Murugan, A.Yu. Chufarov, A.P. Tyutyunnik, *Journal of the European Ceramic Society* **45**(9), 117316 (2025).

P6

Magnetic properties of $Ca_{0.3}Sr_{0.3}La_{0.3}Mn_{0.5}Ti_{0.5}O_3$

I.V. Yatsyk[1], R.F. Likerov[1], R.M. Eremina[1], R.G. Batulin[2]

[1]*Zavoisky Physical-Technical Institute, FRC Kazan Scientific Center of RAS, 420029 Kazan, Russia*
I.Yatzyk@gmail.com

[2]*Institute of Physics, Kazan Federal University, 420008 Kazan, Russia*

In recent years, scientists have shown great interest in high-entropy perovskite-type compounds, in which solid solutions are formed from five or more elements in relatively equal concentrations, since they can be stabilized by the high entropy of mixing. The properties of such materials strongly depend on the crystal structure. High-entropy compounds have a wide range of applications [1, 2], including sensors [3], catalysts [4], and some of them are potentially attractive for high-temperature applications in industries such as aerospace, energy production, automotive, turbine technology, etc., where the materials must withstand extremely high temperatures [5].

The first high-entropy materials to attract the attention of scientists were high-entropy alloys. Since 2015, high-entropy oxides have been produced [6], followed by high-entropy metallic diborides [7], carbides [8], fluorides [9], and sulfides [10].

The aim of this work is to study the magnetic properties of the high-entropy compound $Ca_{0.3}Sr_{0.3}La_{0.3}Mn_{0.5}Ti_{0.5}O_3$ using electron spin resonance (ESR) and magnetometry methods, determine the phase transition temperatures, and construct phase diagrams.

The ESR method allows one to study the dynamics of magnetic properties of the studied compounds both in an ordered state and in the paramagnetic region.

The synthesis of polycrystalline powder of $Ca_{0.3}Sr_{0.3}La_{0.3}Mn_{0.5}Ti_{0.5}O_3$ has been carried out via the solid-state route using precursor materials including $CaCO_3$ (≥99%), $SrCO_3$ (≥99%), $CaCO_3$ (≥99%), La_2O_3 (≥99%), TiO_2 (≥99%), and Mn_2O_3 (≥99%). Initially, the precursor powders have been mixed in a ball mill with zirconia balls in an ethanol medium. The resulting mixture is then dried overnight in a hot air oven. Subsequently, the dried powder underwent calcination at 1323 K for 10 hours under air atmosphere. The calcined powder is then pressed into pellets using a hydraulic press and sintered at 1373 K for 6 hours under an air atmosphere. Detailed conditions for growing samples are given in [11].

EPR measurements were performed using a Bruker EMXplus (Xband) spectrometer, equipped with continuous-flow N2 cryostats. In these measurements we used the X-band with a frequency of 9.4 GHz, a temperature range of 117-339 K, and a magnetic-field range of 0–1.4 T. The ESR spectra are shown in Figure 1.

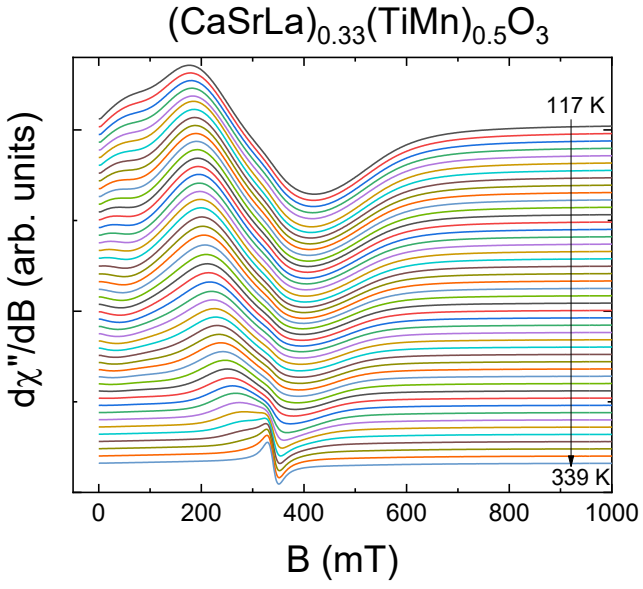

Figure 1. Evolution of the electron spin resonance spectrum with temperature in the range from 117 to 339 K for $Ca_{0.3}Sr_{0.3}La_{0.3}Mn_{0.5}Ti_{0.5}O_3$.

It can be seen that the shape of the magnetic resonance line from 117 K to 339 K changes greatly, which indicates a change in the magnetic phase. The phase transition temperature is near room temperature.

The work was carried out at the expense of a grant from the Academy of Sciences of the Republic of Tatarstan, provided to young candidates of science (postdoctoral students) for the purpose of defending a doctoral dissertation, carrying out research work, and also performing work functions in scientific and educational organizations of the Republic of Tatarstan within the framework of the State Program of the Republic of Tatarstan "Scientific and Technological Development of the Republic of Tatarstan.

1. S. Albedwawi, A. AlJaberi, G. Haidemenopoulos, K. Polychronopoulou, *Materials & Design.* **202**, 109534 (2021).
2. B. Musicó, D. Gilbert, T. Ward, K. Page, et al., *APL Materials* **8**, 040912 (2020).
3. Y. Zhang, D. Wang, S. Wang, *Small* **18**, 2104339 (2021).
4. K. Li, W. Chen, *Materials Today Energy* **20**, 100638 (2021).
5. P. Sathiyamoorthi, H. Kim. *Advanced Engineering Materials* **20**, 1700645 (2017).
6. A. Sarkar, Q. Wang, A. Schiele, M. Chellali, et al. *Adv. Mater.* **31**, 1806236 (2019).
7. J. Gild, Y. Zhang, T. Harrington, S. Jiang, et al. *Scientific Reports* **6**, 37946 (2016).
8. S. Alvi, H. Zhang, F. Akhtar, *High-Entropy Materials* (IntechOpen) (2019) ISBN 978-1-78985-947-8.
9. X. Chen, Y. Wu, *Journal of the American Ceramic Society* **103**, 750 (2019).
10. J. Kuang, P. Zhang, Q. Wang, Z. Hu, et. al. *Corrosion Science.* **198**, 110134 (2022).
11. T. Bhattacharya, R. Banerjee, T. Maiti, *Phys. Chem. Chem. Phys.* **26**, 28874 (2024).

P7

Investigation of phase transitions in PMN-PT using birefringence microscopy

E. Pelegova[1], I. Biran[1], V. Shur[2], S. Gorfman[1]

[1]*Department of Materials Science and Engineering, Tel Aviv University, 6997801 Tel Aviv, Israel*
pelegova@tauex.tau.ac.il

[2]*Ural Federal University, 620000 Ekaterinburg, Russia*

(1-x)$PbMg_{1/3}Nb_{2/3}O_3$-x$PbTiO_3$ (PMN-PT) crystals have attracted significant attention due to their exceptional electromechanical properties, which remain among the highest reported to date. As other perovskite-based materials, PMN-PT exhibits a series of structural phase transitions characteristic of the perovskite framework. However, despite extensive research, key aspects of these transitions – such as transition temperatures, the nature (order) of the transitions, the presence or absence of hysteresis, and the associated microstructural changes - remain incompletely understood.

This study aims to contribute new insights into these phenomena by employing innovative and previously underutilized experimental technique based on optical birefringence [1]. Additionally, we have developed and refined a birefringence imaging microscopy (BIM) system, which can be utilized for study of structural phase transitions in a broad range of materials [2].

We investigated polished PMN-50PT single crystals using the BIM ROTOPOL system [3], built on the base of an Olympus BX-53 microscope. The setup includes a rotatable polarizer, a Linkam THMSG600 optical heating stage, a circular analyzer, and a CCD camera. By measuring the intensity of transmitted light at various polarizer angles, the system generates images of optical retardation (|sin δ|) and optical orientation (principal axes of the optical indicatrix cross-section). These optical parameters are correlated with the crystallographic axes, determined independently via single-crystal X-ray diffraction.

Our results provide valuable information on the temperature-dependent symmetry and domain structure of the crystals. Figure 1 contains false-color images of |sin δ| and φ during phase transition, illustrating the spatial distribution of optical anisotropy and orientation. Additional examples and findings will be presented in the poster.

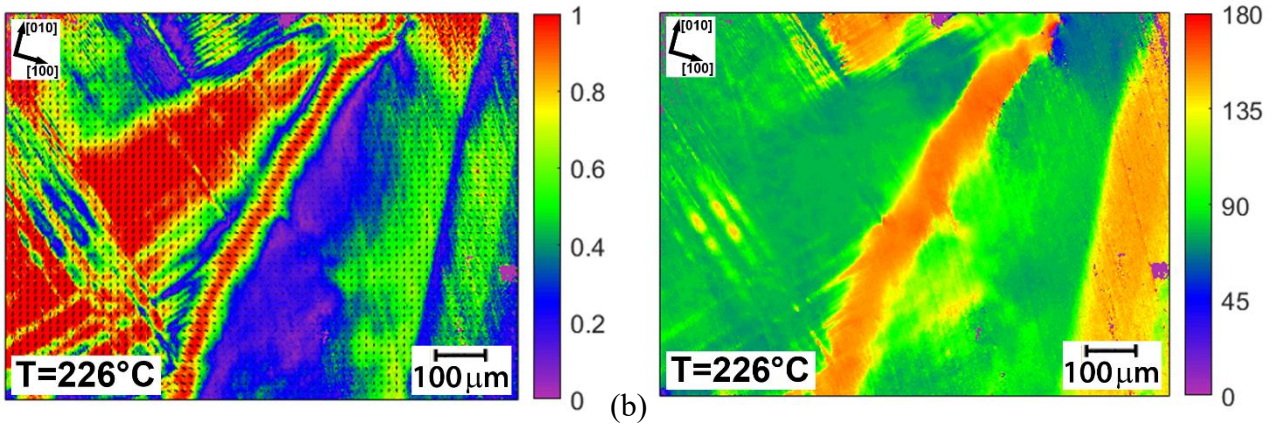

Figure 1. False-color images of (a) |sin δ| and (b) φ obtained by birefringence optical microscopy in PMN-PT single crystal during phase transition. Temperature 226°C. Crystallographic directions are marked.

1. J.-W. Sun, Z. Xu, S.-G. Lee, et al., *IEEE Trans. Ultrason. Ferroel. Freq. Contr.* **72**, 2 (2025).
2. A.M. Glazer, J.G. Lewis, W. Kaminsky, *Proc. R. Soc. Lond. A* **452**, 2751 (1996).
3. http://cad4.cpac.washington.edu/ROTOPOLhome/ROTOPOL.htm

P8

Features of pyroelectric and dielectric properties of PVDF-based composites obtained by crystallization in a corona discharge field

G.I. Shnaidshtein[1], E.V. Alexandrov[1], E.V. Barabanova[1], A.N. Belov[2], A.V. Solnyshkin[1]

[1]*Tver State University, 170100 Tver, Russia*
g.shnaidshtein@mail.ru

[2]*National Research University of Electronic Technology, 124498 Zelenograd, Moscow, Russia*

Films based on polyvinylidene fluoride (PVDF) are widely used as functional elements in sensors and transducers. Their effectiveness is determined by relatively high pyroelectric and piezoelectric activity, which is due to the presence of spontaneous polarization in the polar β-phase of the polymer and the pyroelectric coefficient value [1].

It is known [2] these characteristics of PVDF films depend on an amount of the ferroelectric crystalline β-phase. At the same time, the amount of the polar β-phase depends both on the manufacturing conditions of the film structures and on external influences during crystallization and/or post-processing.

The purpose of this work was fabrication of PVDF-based composites comprised polar inclusions of deuterated triglycine sulfate (DTGS) and lead zirconate titanate (PZT) oriented during the crystallization to enhance pyroelectric activity, as well as study their pyroelectric and dielectric properties.

PVDF-based composites were obtained by the solvent cast method under a constant electric field induced by a corona discharge. For electrical measurements, aluminum electrodes were deposited on the surface of the composites using thermal sputtering. Pyroelectric properties were studied by a dynamic method using laser irradiation modulated with rectangular shape pulses. Dielectric characteristics (dielectric permittivity and loss tangent) were determined using the LCR-meter E7-30. Two series of film samples composite and pure PVDF were characterized in terms of their dielectric and pyroelectric properties. The composite films were prepared using the method described above, while the PVDF films were obtained via solvent casting in the absence of an electric field and subsequently subjected to corona poling after curing. A comparative analysis of the properties of both series was performed.

It was shown that the samples exhibit noticeable pyroelectric activity. In particular, the calculated pyroelectric coefficient (γ) yields values ranging from $0.01 \cdot 10^{-4}$ to $0.2 \cdot 10^{-4}$ C/(m^2·K), depending on the type of filler and its concentration. This value coincides with the γ value for PVDF films manufactured by the standard method.

It was found that the electric field applied during crystallization does not have a noticeable effect on the dielectric characteristics. The dielectric permittivity (ε) is approximately 12 in the low-frequency region ($f < 10$ kHz). The tangent of dielectric loss (tan δ) for this frequency range does not exceed 0.02. In the high-frequency region, significant dispersion of dielectric properties is observed, characterized by a decrease in ε to approximately 8 at $f = 1$ MHz, while the δ value increases to 0.2.

The dispersion of dielectric properties of PVDF-based composite samples does not depend on the film manufacturing method noticeably. However, the dielectric permittivity of films obtained by the standard method is approximately 10-15% lower.

1. A.J. Lovinger, *Science* **220**, 1115 (1983).
2. T. Tansel, *Journal of Polymer Research* **27**, 95 (2020).

P9

Obtaining of hyperdoped Si surface layer via pulsed laser melting

D.E. Tkachuk, P.A. Paletskikh, A.R. Akhmatkhanov, V.I. Pryakhina

Institute of Natural Sciences and Mathematics, Ural Federal University, 620002, Ekaterinburg, Russia
daria.tkachuk@urfu.ru

Silicon plays a pivotal role in modern technology, demanding advanced optical and physical characteristics, which leads to modifications achieved through doping processes. High concentrations of specific deep or shallow impurities in hyperdoped silicon induce a unique electronic structure within the bandgap, thereby enhancing its spectral properties by enabling broadened light absorption capabilities – including near- and mid-infrared regions – which are essential for optoelectronics applications [1,2].

To exceed equilibrium solubility limitations, nonequilibrium techniques must be employed. Among these, pulsed laser melting excels compared to traditional ion implantation and thermal annealing because it minimizes structural damage while maintains high dopant concentrations, ensures fast processing, allows precise parameter control, and facilitates doping localization [1-4] – all crucial for advancing functional materials development. Our study focused on investigating variations in impurity introduction under diverse laser irradiation conditions.

We used single crystalline <100> silicon wafers coated with thin metallic layers ranging from 5 to 100 nm thicknesses. Ti, xCr, Zn, Ag, or Au served as doping materials. These substrates underwent treatment using 100-ns-pulse laser beams at a 1064-nm-wavelength (MiniMarker 2-M20 laser system, LTC, featuring Yb-fiber). Different experimental configurations examined various combinations of average radiation power (P_{ave}), pulse frequency (f), and scanning speed, resulting in varied fluences calculated as $E = P_{ave}/f/S$, where S is a beam area. The parameters selections aimed to ensure efficient impurity diffusion while minimizing ablation effects.

The dopant element incorporated into the surface layer was verified by X-ray photoelectron spectroscopy (XPS, K-Alpha+, ThermoFisher Scientific) and energy dispersive X-ray spectroscopy (EDS) measurements. Moreover, non-destructive nanosecond laser pulses simultaneously treated and annealed the silicon, restoring its crystallinity as evidenced by Raman microspectroscopy analysis (Alpha 300AR, Witec).

Spectral data obtained using a spectrophotometer (Cary 5000, Agilent) showed enhanced near-infrared absorption rates in laser hyperdoped samples relative to untreated silicon. This enhancement correlates directly with both the initial metal film thickness and cumulative laser pulse energy input. Increased light absorption arises from energy levels formed within the silicon bandgap caused by impurity incorporation facilitated by nanosecond laser irradiation.

The work was supported by Russian Science Foundation (project 25-22-00326). The equipment of the Ural Center for Shared Use “Modern Nanotechnologies” Ural Federal University (Reg. № 2968) was used.

1. J. Fu, D. Yang, X. Yu, *Phys. Status Solidi A* **219**, 2100772 (2022).
2. S.Q. Lim, J.S. Williams, *Micro* **2**, 1 (2022).
3. M. Kovalev, A. Nastulyavichus, I. Podlesnykh, et al, *Materials* **16**, 4439 (2023).
4. V. Pryakhina, S. Kudryashov, M. Kovalev, et al, *Opt. Laser Technol*. **188**, 112945 (2025).

P10

Visible-blind near-infrared photodiode based on hyperdoped silicon

P.A. Paletskikh, D.E. Tkachuk, V.I. Pryakhina, A.R. Akhmatkhanov

Institute of Natural Sciences and Mathematics, Ural Federal University, 620002, Ekaterinburg, Russia
polina.paletskikh@urfu.ru

Hyperdoping allows for impurity concentrations beyond equilibrium solubility limits, introducing deep-level defects into the silicon's bandgap. An increased impurity concentration widens the intermediate band, facilitating efficient sub-bandgap optical absorption of infrared radiation [1,2]. Additionally, it enhances semiconductor conductivity and supports the fabrication of silicon-based photodetectors and photodiodes. In this study, we explored the changes in resistivity and current induced by exposing hyperdoped silicon to infrared light irradiation.

We investigated silicon wafers with a surface layer hyperdoped with select transition metals (gold, chromium). Previous studies have demonstrated increased optical absorption in the near-infrared spectrum for such materials [1-4]. Substrates of pure silicon as well as those doped with either n- or p-type conductivity were utilized. Hyperdoping was achieved through nanosecond laser pulse irradiation of substrates coated with metal films of varying initial thicknesses.

We measured the photoresponse dependence on incident radiation power for silicon with the hyperdoped layer under 1550 nm wavelength irradiation (a continuous fiber laser). Indium ohmic contacts were applied to the silicon surfaces to ensure complete irradiation of hyperdoped area. The current-voltage characteristics were measured using configurations with electrodes placed either on the same side or on opposite sides.

The measured dependencies showed a decrease in resistance with increasing laser irradiation power, which was attributed to the absorption of infrared light by hyperdoped silicon. Higher doping levels resulted in more pronounced changes. Current characteristics also varied depending on the type of initial substrate. Donor/acceptor impurities in the substrates and the doping parameters influence the extent of photoresponse change, correlating with increased optical absorption in the respective samples.

Possible mechanisms underlying the influence of film thickness and laser parameters on hyperdoped silicon are discussed. The findings lay the groundwork for reproducibly creating hyperdoped silicon detectors suitable for the near-infrared range.

The research funding from the Ministry of Science and Higher Education of the Russian Federation (Ural Federal University Program of Development within the Priority-2030 Program) is gratefully acknowledged. The equipment of the Ural Center for Shared Use «Modern Nanotechnologies» Ural Federal University (Reg. № 2968) was used.

1. J. Fu, D. Yang, X. Yu, *Phys. Status Solidi A* **219**, 2100772 (2022).
2. S.Q. Lim, J.S. Williams, *Micro* **2**, 1 (2022).
3. M. Kovalev, A. Nastulyavichus, I. Podlesnykh, et al, *Materials* **16**, 4439 (2023).
4. V. Pryakhina, S. Kudryashov, M. Kovalev, et al, *Opt. Laser Technol*. **188**, 112945 (2025).

P11

Investigation of capillary rise on the aluminum substrates structured by nanosecond laser irradiation

D.A. Shivarova, A.S. Bayankina, D.K. Kuznetsov, V.Ya. Shur

Institute of Natural Sciences and Mathematics, Ural Federal University, 620002 Ekaterinburg, Russia
daria.shivarova@urfu.ru

Functionalization of material surfaces, especially in terms of wettability control, is a topical issue in various fields of technology. The creation of hierarchical micro- and nanostructures using laser structuring provides unique opportunities for precise control of surface morphology and chemical composition, significantly affecting fluid dynamics. Capillary rise, as one of the fundamental mechanisms of spontaneous fluid motion, plays a key role in such systems, which is of crucial importance for the development of micro- and nanofluidics, cooling of electronic devices, as well as biological and chemical sensors [1].

In this study, 0.5 mm thick aluminum plates were processed using a MiniMarker 2 - M20 precision fiber laser marking system (OOO Laser Center, Russia) with a wavelength of 1064 nm and a pulse duration of 110 ns. The resulting surface structures were imaged using an Auriga Crossbeam Workstation (Carl Zeiss).

The dynamics of capillary rise was studied by immersing the samples in a liquid bath while simultaneously recording the liquid front motion. Laser treatment in scanning mode with a line density of 0.5 to 25 mm^{-1} resulted in the formation of periodic microchannels. The inner walls and outer edges of the microchannels are decorated with particles ranging in size from a few nanometers to several micrometers, thereby forming a hierarchical micro- and nanostructure on the surface of the aluminum plate. The thickness of the nanoparticle layer reaches 1.5 μm.

Capillary rise in a microchannel system goes through several stages, each of which is described by a power dependence of the form $h \sim t^n$, where h is the traveled distance, t is time, and n is an exponent varying from 0.1 to 2. The best-known regime is the classical flow described by the Lucas-Washburn equation with $h \sim t^{1/2}$, which is a stable capillary flow in which capillary forces are balanced by viscous resistance.

It was shown that the dynamics of capillary rise for all samples corresponded to the $h \sim t^{1/2}$ regime, which is explained by the homogeneous geometry of the microchannels and the predominance of viscous and surface forces over inertial ones, which ensures the stability of the liquid flow [2-5]. The maximum velocity of the waterfront is achieved at a channel density of 5 mm^{-1}. It was shown that an increase in the surface roughness between the channels leads to a monotonic increase in the capillary rise velocity at a fixed channel density.

Long-term storage of samples in air leads to gradual degradation of superhydrophilic properties with subsequent transition to a superhydrophobic state. The transition of structured surfaces from a hydrophilic state to a hydrophobic state can be caused by a few factors: partial destruction of oxide layers and formation of hydrophobic functional groups on the surface, as well as adsorption of hydrophobic hydrocarbons from the environment in which the samples are stored.

The equipment of the Ural Center for Shared Use “Modern nanotechnology” Ural Federal University (reg. no. 2968) was used. The authors are grateful for financial support of the Ministry of Science and Higher Education of the Russian Federation (state task FEUZ-2023-0017).

1. G.B. Abadi., M. Bahrami, *Scientific Reports* **12**, 14867 (2022).
2. E.W. Washburn, *Physical Review* **17**, 273 (1921).
3. S. Das, et al, *Phys. Rev. E* **86**, 067301 (2012).
4. T. Andrukh, et al, *Soft Matter* **10**, 609 (2014).
5. D.X. Deng, et al, *International Journal of Heat and Mass Transfer* **77**, 311 (2014).

P12

Formation of self-organized domain pattern in polydomain near-stoichiometric lithium tantalate crystals by electron beam irradiation

E.A. Abramova, A.R. Akhmatkhanov, A.S. Slautina, M.A. Chuvakova, D.S. Chezganov, V.Ya. Shur

School of Natural Sciences and Mathematics, Ural Federal University, 620026 Ekaterinburg, Russia
e.pashnina@urfu.ru

A study of domain structure formation under irradiation with a focused electron beam (e-beam) was carried out in near-stoichiometric lithium tantalate (NSLT). Comparison of domain formation in the samples with monodomain and pre-poled polydomain states was done. The key geometric parameters of domain structures formed by dot irradiation were measured. These findings highlight the potential of e-beam irradiation for precise domain engineering in NSLT crystals for nonlinear optical applications.

Single crystal of lithium tantalate ($LiTaO_3$) is one of the key ferroelectric materials for nonlinear optics due to its broad transparency range, high damage threshold, and strong nonlinear coefficients [1]. NSLT offers a unique balance between low coercive fields and stability, making it ideal for domain engineering [1]. Traditional electric-field poling methods allow us to create periodic domain structures for applications like second-harmonic generation, but e-beam irradiation provides superior precision and flexibility for nanoscale patterning. This study explores e-beam-induced domain formation in NSLT, focusing on the role of pre-poled polydomain states in stabilizing nanoscale structures for advanced photonic devices.

NSLT crystals were grown by the Czochralski method (Fomos Materials, Russia) and cut perpendicular to the Z–axis. The studied samples had the single domain and pre-poled polydomain states. The polydomain state with micro- and nanoscale domain structure was created by partial polarization reversal of the sample covered by photoresist layer [2]. For e-beam irradiation of the samples the irradiated Z- polar surface was covered by photoresist layer and a solid Cu electrode was deposited on the Z+ polar surface. The domain structure was imaged by confocal Raman microscopy (CRM), Cherenkov-type second harmonic generation microscopy (SHGM) and scanning electron microscopy (SEM).

Irradiation of initial monodomain samples resulted in the formation of irregularly shaped domains. A linear dose (D) dependence of the switched area was observed for accelerating voltages (U) 14 kV and 16 kV, whereas at 12 kV, the dependence is significantly nonlinear and saturated for doses above 300 pC. In the bulk, the domain splits into isolated segments of arbitrary shape. The maximum domain depth reached 730 μm for U = 16 kV and D = 900 pC.

Dot irradiation of the polydomain sample resulted in the formation of rounded domains. The formation of multiple backswitched domains of reverse polarity inside the switched domain was observed. Two types of these domains have been distinguished: (1) irregularly shaped randomly distributed domains, (2) quasi-regular arrays of nanodomains. Four concentric regions within a structure of quasi-regular nanodomains were analyzed: (1) central region with homogeneously distributed nanodomains, (2) nanodomain arrays arranged in spiral chains, (3) nanodomain arrays arranged in randomly oriented chains, (4) external part without nanodomains.

The model based on the action of the field produced by the charge injected into the near-surface layer of the crystal is proposed for explanation of the formation of quasi-regular nanodomain arrays.

The authors are grateful for the financial support of the Ministry of Science and Higher Education of the Russian Federation (state task No. FEUZ-2023-0017). Equipment of the Ural Center for Shared Use “Modern Nanotechnologies” Ural Federal University (Reg. No. 2968) was used.

1. X. Xiao, J. Si, S. Liang et al., *Crystals* **13**, 1031 (2023).
2. M.A. Chuvakova, E.M. Vaskina, A.R. Akhmatkhanov et al., *Ferroelectrics* **496**, 92 (2016).

P13

Hatched domain walls in potassium titanyl phosphate crystals

A.S. Bayankina[1], D.A. Shivarova[1], M.A. Chuvakova[1], A.R. Akhmatkhanov[1], A.P. Turygin[1], V.Ya. Shur[1], K.P. Melnik[2], G.I. Schwartzman[2], A.A. Tik[3], J.V. Kuleshov[3]

[1]*School of Natural Sciences and Mathematics, Ural Federal University, 620026 Ekaterinburg, Russia*
Antonina.Baiankina@urfu.ru

[2]*Tomsk State University of Control Systems and Radioelectronics, 634050 Tomsk, Russia*

[3]*LLC "CrOM", 634050 Tomsk, Russia*

Potassium titanyl phosphate ($KTiOPO_4$, KTP) is a uniaxial ferroelectric crystal with a high phase transition temperature and high nonlinear-optical properties. This material is actively used in various applications, such as nonlinear optics and laser technologies [1,2]. It is known that polarization reversal in some representatives of KTP family is accompanied by formation of micro- and nanoscale striped domains. This phenomenon is called "hatching", and the domains formed during this process are termed as a "hatched domains" [3,4]. This effect attracts considerable attention due to possible creation of self-organized periodical stripe domain structures for nonlinear frequency conversion applications [1,2]. In this work, we report formation of hatched domains during polarization reversal of KTP single crystals.

Studied KTP single crystalline plates were cut perpendicular to the polar axis and polished to optical quality. An experimental system based on an LMA10 optical polarizing microscope (CARL ZEISS, Germany), a Mini UX100 high-speed camera (Photron, USA), an NI-6251 data acquisition board (National Instruments, USA), and a TREK 20/20C high-voltage amplifier (TREK, USA) was used to study polarization reversal. A saturated aqueous LiCl solution was used as an electrode. The imaging of static domain structure after partial polarization reversal was performed by piezoresponse force microscopy (PFM) using NTEGRA Aura (NT-MDT Spectrum Instruments, Russia) and Asylum MFP-3D (Asylum Research, USA) scanning probe microscopes.

In situ optical imaging has shown that reverse polarization reversal leads to formation of residual domains resulting in significant acceleration of subsequent forward polarization reversal. PFM imaging after subsequent partial forward polarization reversal has revealed the formation hatched domains elongated along Y crystallographic direction (Fig. 1). Two types of hatched domains were distinguished: (1) domains formed at the wall of the growing macro-domain with length 1.4 ± 0.3 μm and linear density 7 μm^{-1}, and (2) residual domains formed during previous reverse switching with length 7.4 ± 1.8 μm and much lower linear density (Fig. 1). It was shown that both types of the hatched domains are unstable and shrink with time. Obtained results are important for further development of domain engineering methods in KTP single crystals.

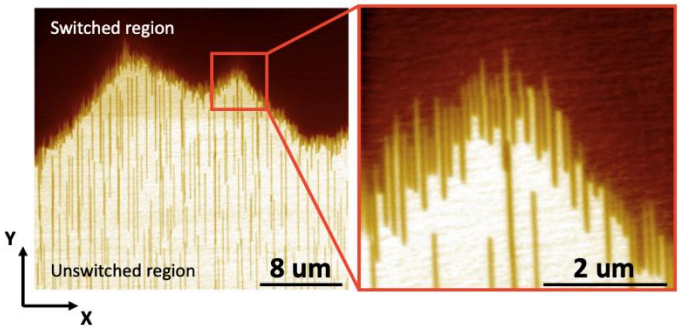

Figure 1. Hatched domain structure obtained after partial forward polarization reversal. PFM image.

The equipment of the Ural Center for Shared Use "Modern nanotechnology" Ural Federal University (reg. no. 2968) was used. The authors are grateful for financial support of the Ministry of Science and Higher Education of the Russian Federation (state task FEUZ-2023-0017).

1. V.Ya. Shur, E.V. Pelegova, A.R. Akhmatkhanov, I.S. Baturin, *Ferroelectrics* **496**, 49 (2016).
2. C. Canalias, V. Pasiskevicius, F. Laurell, *Ferroelectrics* **340**, 27 (2006).
3. V.Ya. Shur, A.A. Esin, M.A. Alam, A.R. Akhmatkhanov, *Appl. Phys. Lett.* **111**, 152907 (2017).
4. A.R. Akhmatkhanov, M.A. Chuvakova, N.A. Dolgushin, et al., *Ferroelectrics* **559**, 1 (2020).

P14

Ferroelectric polarization switching by a strong THz field in $BaTiO_3$ crystal

K.A. Brekhov[1], E.I. Zhemerov[1], A.V. Ovchinnikov[2], E.D. Mishina[1]

[1]*MIREA – Russian Technological University, 119454 Moscow, Russia*
brekhov_ka@mail.ru

[2]*Joint Institute* for *High Temperatures of Russian Academy of Sciences (JIHT), 125412 Moscow, Russia*

The spontaneous polarization is a key order parameter that already serves as the basis for numerous electronic, optical, and electromechanical devices, demonstrating significant potential for creating innovative functionalities. These range from high-density non-volatile memory systems and ultra-sensitive nanoscale devices to neuromorphic computing architectures and energy-harvesting technologies. The basic principle underlying all these applications is the ability of electric fields to switch polarized domains in ferroelectric materials. Moreover, the coupling of ferroelectric polarization with other physical phenomena such as mechanical deformation, magnetic ordering or optical properties provides an exceptional platform for the development of truly multifunctional materials. Therefore, the development of ultrafast and energy-efficient approaches for coherent polarization switching is of critical importance for future developments of ferroelectric technologies.

In recent years, a lot of research has been devoted to developing techniques for rapidly and efficiently switching spontaneous polarization between stable and non-volatile states. The most traditional method involves manipulating polarized domains by applying quasi-static or pulsed electric fields. However, this approach faces challenges in achieving ultrafast (sub-nanosecond) switching speeds and precise spatial control. An alternative approach is all-optical polarization switching, using ultrashort laser pulses capable of driving polarization changes potentially on picosecond time scales.

Several all-optical approaches involving direct excitation of the soft ferroelectric mode or non-linear phononics have been proposed to achieve this goal. However, despite these proposals, the experimental realization of laser-induced polarization switching is still at an early stage. Recently, it was experimentally demonstrated that narrow-band optical pulses tailored to specific spectral lines in the infrared range can permanently switch ferroelectric domains in barium titanate ($BaTiO_3$) [1,2]. Additionally, studies [3,4] have shown the formation and shape evolution of ferroelectric domains in lithium niobate under pulsed infrared laser irradiation, driven by laser-induced pyroelectric fields.

Here we present the study of the domain structure evolution in $BaTiO_3$ crystal under intense THz radiation. Using the PFM technique, we observed that strong THz radiation induces leads not only to depolarization (destruction) of the domain structure but also causes 180° switching of individual domains.

This work was supported by the Russian Science Foundation, grant № 25-19-00575.

1. M. Kwaaitaal, D.G. Lourens, C.S. Davies, A. Kirilyuk, *Scientific Reports* **14**, 24956 (2024).
2. M. Kwaaitaal, D.G. Lourens, C.S. Davies, A. Kirilyuk, *Nature Photonics* **18**, 569 (2024).
3. B. Lisjikh, M. Kosobokov, A. Turygin, A. Efimov, V. Shur, *Photonics* **10**(11), 1211 (2023).
4. V. Shur, E. Pelegova, A. Turygin, M. Kosobokov, Yu. Alikin, *Crystallogr. Rep.* **68**, 756 (2023).

P15

Domain kinetics and periodical poling in single crystals of potassium titanyl-phosphate family for light frequency conversion

M.A. Chuvakova[1], A.R. Akhmatkhanov[1], A.A. Esin[1], I.A. Kipenko[1], V.Ya. Shur[1], A.A. Boyko[2,3], L.I. Isaenko[3], S.A. Zhurkov[3]

[1]*School of Natural Sciences and Mathematics, Ural Federal University, 620000 Ekaterinburg, Russia*
m.a.chuvakova@urfu.ru

[2]*Institute of Laser Physics SB RAS, 630090 Novosibirsk, Russia*

[3]*Novosibirsk State University, 630090 Novosibirsk, Russia*

Single crystals of potassium titanyl-phosphate family with periodical ferroelectric domain structure are one of the promising materials for light frequency conversions [1]. We present the results of measurements of characteristic times and switching fields and *in situ* imaging of domain kinetics in potassium titanyl phosphate Rb:$KTiOPO_4$ (RKTP), potassium titanyl arsenate $KTiOAsO_4$ (KTA) and rubidium titanyl arsenate $RbTiOAsO_4$ (RTA) single crystals.

In situ imaging of domain kinetics in RKTP, KTA and RTA was carried out with the time resolution down to 12.5 μs. The wide range of wall velocities with two orders of magnitude difference was observed for switching in a uniform electric field in RKTP [2]. The kinetic maps allowed analyzing the spatial distribution of wall motion velocities and classifying the domain walls by velocity. The distinguished slow, fast, and superfast domain walls were differed by their orientation. The mobility and threshold fields for all types of domain walls were estimated [3]. The revealed increase in the wall velocity with deviation from low-index crystallographic planes for slow and fast walls was considered in terms of determined step generation and anisotropic kink motion.

Domain kinetics and switching fields in RKTP and KTA were compared. The more pronounced input of slow domain walls in KTA results in creation of narrow stripe domains important for periodical poling [4,5]. Spontaneous backswitching was revealed in RTA single crystals. It was shown that the time interval from the end of switching pulse to the start of spontaneous backswitching process ("domain structure stability time") is proportional to the field applied during polarization reversal.

The periodical domain structure with 40 μm period was created in 3-mm-thick RKTP single crystals for OPO generation at 2.326 μm using the 1.064 μm pulsed pump with 5.6 ns duration at 20 Hz. The single resonance double-pass optical scheme was used. The threshold power energy 630 μJ and generation efficiency 7% were obtained.

We studied the characteristics of a PPKTA OPO with a period of 39.2 μm in the low-temperature-grown KTA sample. Under pumping at 1.053 μm, the signal and idler wavelengths were, 1.54 and 3.31 μm, respectively. The parametric generation threshold turned out to be 130 μJ (for a pump intensity of 14.4 MW cm^{-2}), the quantum efficiency was 27%, and the differential efficiency was 12 % [6].

The obtained knowledge is important for further development of domain engineering in crystals of KTP family required for creation of high power, reliable, and effective coherent light sources.

The authors are grateful for the financial support of the Ministry of Science and Higher Education of the Russian Federation (state task No. FEUZ-2023-0017). Equipment of the Ural Center for Shared Use "Modern Nanotechnologies" Ural Federal University (Reg. No. 2968) was used.

1. V.Ya. Shur, E.V. Pelegova, A.R. Akhmatkhanov, I.S. Baturin, *Ferroelectrics* **496**, 49 (2016).
2. V.Ya. Shur, E.M. Vaskina, E.V. Pelegova, et al., *Appl. Phys. Lett.* **109**, 132901 (2016).
3. V.Ya. Shur, A.A. Esin, M.A. Alam, A.R. Akhmatkhanov, *Appl. Phys. Lett.* **111**, 152907 (2017).
4. A.R. Akhmatkhanov, M.A. Chuvakova, N.A. Dolgushin, et al., *Ferroelectrics* **559**, 1 (2020).
5. A.R. Akhmatkhanov, M.A. Chuvakova, I.A. Kipenko, et al., *Appl. Phys. Lett.,* **115**, 212901 (2019).
6. L.I. Isaenko, A.P. Eliseev, D.B. Kolker, et al., *Quantum Electronics,* **50**, 788 (2020).

P16

Motion of fast and superfast domain walls during polarization reversal in crystals of lithium niobate family

I.A. Kipenko, A.R. Akhmatkhanov, V.Ya. Shur

School of Natural Sciences and Mathematics, Ural Federal University, 620000 Ekaterinburg, Russia
ilya.kipenko@urfu.ru

Single crystals of lithium niobate ($LiNbO_3$, LN) family, including congruent (CLN), near stoichiometric (SLN), MgO-doped congruent (MgOCLN) and stoichiometric (MgOSLN) compositions, are widely used for light frequency conversion due to their high nonlinear optical coefficients [1]. CLN crystals are extensively offered in the market due to low cost and high quality. Doping CLN with MgO (>5 mol.%) lowers photorefractive damage and green-induced infrared absorption (GRIIRA) and it also reduces ferroelectric switching threshold field [2]. SLN requires even lower MgO concentrations for achieving these characteristics [3,4]. Domain engineering via electric field poling with photolithographically patterned electrodes enhances light conversion efficiency reaching the quasi-phase matching conditions but faces challenges due to uncontrolled domain broadening by motion of superfast domain walls [1,5]. Thus, studying domain wall motion across crystals of LN family remains crucial for advancing domain engineering techniques.

The study of superfast domain walls motion during polarization reversal in constant electric field was carried out in single crystals of LN family - congruent, stoichiometric, congruent doped with 5 mol% magnesium oxide (MgOCLN), and stoichiometric doped with 1.3 mol% magnesium oxide (MgOSLN) compositions. The applied voltage pulse was generated by DAQ board PCI 6251 (National Instruments, USA) and amplified by high voltage amplifier TREK 20/20C (Trek Inc., USA). Imaging of domain structure during polarization reversal was carried out using LMA10 optical microscope (CARL ZEISS, Germany) with PLAN 8X /0.1 objective. Recording of instantaneous domain images was performed using high-speed CMOS camera Photron Mini UX100 (Photron, Japan) with a frame rate of up to 5000 FPS.

Analysis of domain kinetics in these crystals included revealing the main domain wall types, extracting their contributions to the switching process, and measuring their velocity dependencies on field and orientation. The observed domain walls were classified into three groups based on orientation and motion velocity: “slow walls”, “fast walls” and “superfast walls”. The dominant role of the fast and superfast walls in the switching process in the whole field range for studied crystals was revealed [6]. Velocity-orientation dependence demonstrated six-fold symmetry for slow domain walls and three-fold for fast and superfast walls. Velocity-field dependence on domain walls in all samples were analyzed using two alternative approaches: linear and exponential fitting [6]. The obtained wall orientations were attributed to the wall structure, characterized by averaged step length [6]. Domain wall mobilities in undoped LN significantly exceed (by 2–3 orders of magnitude) those in MgO-doped compositions, regardless of the wall type. The influence of (i) stoichiometric deviation and (ii) MgO doping on the threshold fields was discussed. Provided studies of kinetics of domain walls of various orientations in LN family main representatives are important for further development of domain engineering methods.

The authors are grateful for the financial support of the Ministry of Science and Higher Education of the Russian Federation (state task No. FEUZ-2023-0017). Equipment of the Ural Center for Shared Use “Modern Nanotechnologies” Ural Federal University (Reg. No. 2968) was used.

1. M.M. Fejer, G.A. Magel, D.H. Jundt, *et al.*, *IEEE Journal of Quantum Electronics* **28**, 2631 (1992).
2. Y. Furukawa, K. Kitamura, A. Alexandrovski, *et al.*, *Applied Physics Letters* **78**, 1970 (2001).
3. Y. Furukawa, K. Kitamura, S. Takekawa, *et al.*, *Optics Letters* **23**, 1892 (1998).
4. V. Gopalan, T.E. Mitchell, Y. Furukawa, *et al.*, *Applied Physics Letters* **72**, 1981 (1998).
5. V. Ya. Shur, A.R. Akhmatkhanov, I.S. Baturin, *Applied Physics Reviews* **2**, 040604 (2015).
6. I.A. Kipenko, A.R. Akhmatkhanov, V.Ya. Shur, *Journal of Advanced Dielectric*s, 2550002 (2025).

P17

Dynamics of the charge injected by SPM tip into ferroelectric

S. Melnikov, M.S. Kosobokov, V.Ya. Shur, D.O. Alikin

School of Natural Sciences and Mathematics, Ural Federal University, 620000 Ekaterinburg, Russia
sem.meln2@gmail.com

Ferroelectrics are currently being actively studied due to the functional properties of domains [1] and domain walls [2]. A scanning force microscopy (SPM) is the most flexible and advanced tool for polarization switching and studying the individual domains. Since the charge injection from biased tip during polarization reversal is the important screening mechanisms [3, 4], a complete understanding of the charge injection dynamics and its effect on the spatial distribution of resulting electric field provides better understanding of the switching kinetics.

Dynamic problem of the charge injection has been simulated using finite element method (FEM) by solving convection-diffusion equation (1) with the boundary condition (2) for charge injection from the probe contact area into the sample volume:

$$\frac{\partial \rho}{\partial t} + div\left(\rho\mu\vec{E} - D\vec{\nabla}\rho\right) = 0 \quad (1)$$

$$\boldsymbol{n}\left(\rho\mu\vec{E} - D\vec{\nabla}\rho\right) = \frac{E_{z\,tip}}{R_{cont}} \quad (2)$$

where $E_{z\,tip}$ is the local value of the vertical z-component of the electric field under the probe, R_{cont} is the specific resistance of the probe-sample contact, ρ is the charge density, μ is the charge mobility, and D is the charge diffusion coefficient.

The study reveals that increased charge mobility in the surface layer relative to the volume of the ferroelectric leads to better charge spreading across the surface and respective decrease in the charge density under the probe. The influence of domain wall conductivity on the charge injection dynamics and spatial distribution has been studied. It has been shown that conductive domain walls significantly affect the distribution of the electric field and, accordingly, final distribution of injected charge.

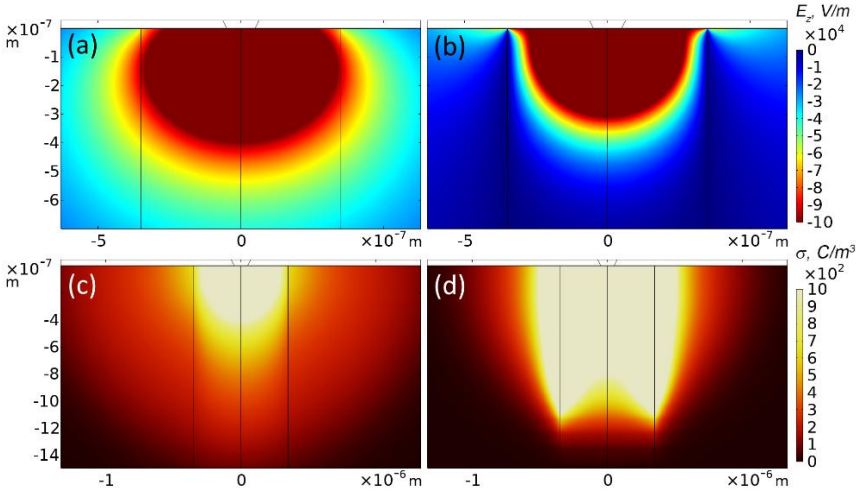

Figure 1. Spatial distributions: (a,b) of the field polar component at the initial moment and (c,d) of the injected charge density 10 ms after injection start for (a,c) non-conductive and (b,d) conductive domain walls.

The research funding from the Ministry of Science and Higher Education of the Russian Federation (Ural Federal University Program of Development within the Priority-2030 Program) is gratefully acknowledged. The equipment of the Ural Center for Shared Use "Modern nanotechnology" Ural Federal University (Reg. no. 2968) was used.

1. J.F. Scott, *Science* **315**, 954 (2007).
2. P. Sharma, et al, *Adv. Funct. Mat.* **32**, 2110263 (2022).
3. Y. Kim, et al, *Appl. Phys. Lett.* **90**, 072910 (2007).
4. A.L. Kholkin, et al, *Nanotechnology* **18**, 095502 (2007).

P18

Creation of the cogged charged domain wall by local switching in lithium niobate

A.P. Turygin, E.D. Greshnyakov, A.R. Akhmatkhanov, V.Ya. Shur

School of Natural Sciences and Mathematics, 620000, Ural Federal University, Ekaterinburg, Russia
anton.turygin@urfu.ru

The intensive study of the domain structure evolution in single crystals of lithium niobate (LN) is stimulated by needs of domain engineering applied for laser frequency conversion based on LN with periodical micro- and nano-domain structures [1,2].

In this work, we have studied experimentally the shape evolution of the interacting initial head-to-head (h2h) and tail-to-tail (t2t) charged domain walls (CDW) and growing isolated domain in the Y-cut $LiNbO_3$ plates. The wedge-like domains were created and grew by electric field application using biased tip of scanning probe microscope. Two h2h and one t2t initial CDWs have been produced during phase transition in the crystal with composition gradients created by in-diffusion and out-diffusion of Li [3].

We have revealed that the domain structure evolution during the interaction of the wedge-like domain with h2h CDW consists of (i) growth of isolated domain at low voltage, (ii) domain merging with initial CDW at moderate voltage, (iii) widening of the rectangular-shaped bump at the initial CDW at high voltage (Fig. 1a). In contrast, the wedge-like domain interaction with t2t CDW for moderate voltages doesn't lead to merging. This fact results in drastic change of the scenario of the domain shape evolution with decreasing the distance between the point application and the initial macroscopic CDW. For low distances the domain elongation is terminated and formation of comb-like domain with zig-zag CDW is observed (Fig. 1b). The formation and growth of cogged CDW has been revealed under application of the series of rectangular switching pulses with increasing amplitude (Fig. 1c,d). Near the t2t CDW domain elongation is slowed down, while the widening of the domain part with neutral walls continues. The growth anisotropy leads to formation of the region with increased local tilt and formation of cogged CDW by generation of additional spikes (Fig.1d). The obtained effects were considered in terms of kinetic approach to domain wall motion taking into account abnormal local field distribution in the vicinity of initial macroscopic CDW with depolarization field effectively screened during its creation.

The discovered effect can be considered for domain wall engineering thus paving the way for manufacturing of the nanoelectronics devices based on the CDWs.

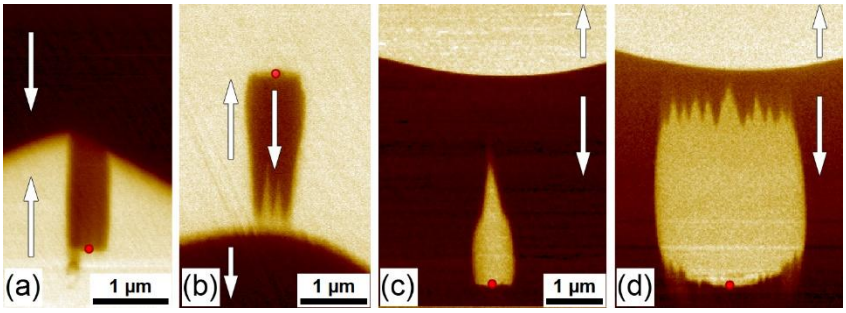

Figure 1. PFM image of domains created near different types of CDW: (a) h2h CDW, - 200 V. Near t2t CDW: (b) 200 V, (c) 100 V, (d) 240 V. Pulse duration 10 s. Red dot indicate position of bias application.

The research was made possible by the Russian Science Foundation (Project No. 24-12-00302). The equipment of the Ural Center for Shared Use "Modern nanotechnology" Ural Federal University (Reg. No. 2968) was used.

1. V.Ya. Shur, *J. Mat. Sci*. **41**, 199 (2006).
2. V.Ya. Shur, A.R. Akhmatkhanov, I.S. Baturin, *Appl. Phys. Rev.* **2**, 040604 (2015).
3. Y. Chen, J. Xu, Y. Kong, et. al., *Appl. Phys. Lett.* **81**, 700 (2002).

P19

Surface charge dynamics at the non-polar cut of lithium niobate

V.A. Vasipullin, A.P. Turygin, M.S. Kosobokov, S.A. Melnikov, V.Ya. Shur, D.O. Alikin

Institute of Natural Sciences and Mathematics, Ural Federal University, 620000 Ekaterinburg, Russia
vova90vasipullin@mail.ru

The creation of domain structures with controlled parameters makes it possible to change the conductivity of ferroelectric crystals due to the accumulation of free charge carriers on the domain walls [1]. The stabilization of domain structures in ferroelectrics is essential for the creation of microelectronic devices such as transistors and memristors [2]. Understanding the dynamics of the screening depolarizing field is important for creation of the stabile domain structure. [3]. During local switching by conductive probe of scanning probe microscope (SPM). One of the key screening mechanisms in this case is the charge injection from SPM tip [4].

In this work, the surface transport of injected charge on Y-cut of lithium niobate single crystals, doping with 5% MgO was studied. Surface potential created by injected charge was measured using Kelvin probe force microscopy (KPFM).

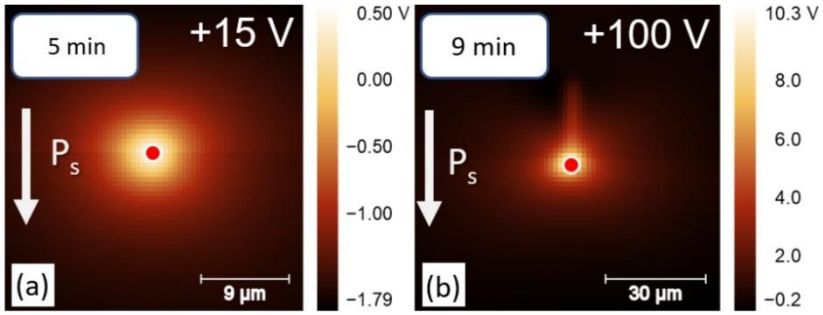

Figure 1. Isotropic distribution of the surface potential after charge injection when a 15 V voltage pulse is applied (a) and anisotropic distribution of the surface potential due to the formation of a wedge-shaped region with charged domain walls (b).

It was shown that for switching pulse amplitude below threshold for the formation of a stable domain (20 V) spatial distribution of surface potential is almost isotropic (Fig. 1a). However, in the process of injected charge relaxation, anisotropy of surface potential distribution relative to the polar axis was observed. This effect has been attributed to the anisotropy of the surface conductivity [5]. The application of switching pulse with amplitude above the threshold leads to formation of wedge-shaped domain with charged domain walls (CDW), which leads to anisotropic distribution of the surface potential due to CDW conductivity (Fig. 1b). Relaxation time of the surface potential drastically increased with amplitude of switching pulse but weakly depends on the pulse duration. With increasing humidity, the relaxation time of the surface charge decreased, and the anisotropy during charge spreading increased. At the same time, increased humidity led to stabilization of the domain structure due to increasing surface conductivity and therefore effective screening of the depolarizing field. The obtained results were analyzed under the assumption of surface diffusion from an instantaneous point source, which allows to extract diffusion coefficients for different crystallographic directions.

The research funding from the Ministry of Science and Higher Education of the Russian Federation (Ural Federal University Program of Development within the Priority-2030 Program) is gratefully acknowledged. The equipment of the Ural Center for Shared Use “Modern nanotechnology” Ural Federal University (Reg. no. 2968) was used.

1. C.S. Werner, et al., *Sci. Rep.* **7**(1), 9862 (2017).
2. A.Q. Jiang, et al., *Nature Materials* **19**(11), 1188 (2020).
3. S.V. Kalinin, et al., *Reports on Progress in Physics* **81**(3), 036502 (2018).
4. S.V. Kalinin, et al., *Nano Letters* **4**(4), 555 (2004).
5. A.A. Esin, et al., *Ferroelectrics* **496**, 102 (2016).

P20

Evolution of as-grown domain structure in calcium orthovanadate crystals

V.V. Yuzhakov[1], E.V. Shishkina[1], M.A. Chuvakova[1], A.R. Akhmatkhanov[1], A.P. Turygin[1], M.S. Nebogatikov[1], E.A. Linker[1], L.I. Ivleva[2], V.Ya. Shur[1]

[1]*School of Natural Sciences and Mathematics, Ural Federal University, 620000 Ekaterinburg, Russia*
vladimir.juzhakov@urfu.ru

[2]*Prokhorov General Physics Institute, Russian Academy of Sciences, 119991 Moscow, Russia*

Calcium orthovanadate $Ca_3(VO_4)_2$ (CVO) is a high-temperature ferroelectric with Curie temperature T_C=1110°C and spontaneous polarization value $68*10^{-2}$ C/m^2 [1]. Nominally pure and doped with rare earth elements, CVO single crystals possess the nonlinear optical properties, which make them promising materials for second harmonic generation [2,3]. The creation of a periodic domain structure can significantly improve the efficiency of radiation frequency converters, which makes it important to study the domain evolution during polarization reversal in CVO.

The investigated 0.4–1.0 mm thick plates of initial and annealed in Ca-rich atmosphere (60 mol.% $CaCO_3$ and 40 mol.% V_2O_5) CVO were cut perpendicular to the polar axis. The polarization was switched at elevated temperature. Three switching modes were used: (1) a single rectangular pulse with amplitude up to 6.5 kV/mm and a duration up to 10 s, (2) a series of 3,500 to 60,000 rectangular pulses with amplitude range from 2.5 to 6.3 kV/mm, duration 200 μs and frequency 50 Hz and (3) by application of 11 rectangular field pulses with amplitude 2.5 kV/mm and duration 3 s. Domain structure evolution was *in situ* optically imaged with simultaneous recording of the switching current. Confocal Raman microscopy and Cherenkov-type second harmonic generation microscopy were used for domain imaging in the bulk.

It was previously shown that the initial domain structure in CVO contains irregularly shaped domains with charged domain walls strongly deviated from the polar direction [4,5]. Isolated round domains are extremely rare, indicating that the optical images of round domains on polar surfaces correspond to cross sections of irregularly shaped domains. The formation of the initial domain structure occurs during cooling near the phase transition. A detailed investigation of the initial domain structure at the cross-section of annealed samples allowed to reveal the fragments of the almost flat CDWs oriented mostly perpendicular to the polar axis.

Polarization reversal in CVO with the initial domain structure consisting of isolated domains with charged domain walls (CDWs) located in the bulk proceeded via formation of the ledges on the CDW and their growth in the polar direction. Analysis of the sequence of instantaneous optical images of the domain structure made it possible for the first time to characterize: (1) the process of growth of individual ledges on the CDW (time dependence of the domain diameter), (2) statistics of the emergence of conical domains on the polar surface (time dependence of the optical current). Statistical analysis of the time dependence of optical currents showed that the rate at which domains reach the surface oscillates and the switching process can be divided into several stages. The obtained time dependence indicates that individual areas of the sample are switched with different delay times caused by to different tilt of the CDWs orientation.

After the top of the growing conical domain touches the polar surface, a current arises along the conductive CDW, which leads to local destruction of the ITO electrode and the formation of a hole, which shape coincides with the domain shape. The reverse switching of the conical domain occurs under the action of the residual depolarizing field $E_{rd} = E_{dep} – E_{scr}$, which, after the formation of a hole in the electrode, grows as a result of the local interruption of external screening. The coincidence of the sizes of the holes and the domains emerging on the surface made it possible to study in detail the domain structure evolution. Analysis of the measured switching currents showed that the contact of the conical domain with the polar surface is accompanied by a current pulse with a duration of about 50 μs. The measured switched charge is close to the value $Q = 2P_SA$, where A is the switched area (hole). The backswitching of the conical domain leads to negative current pulse.

Application of the field pulses series leads to oscillation of the wall, decreasing of the screening efficiency and growth of ledges under the action of partially screened depolarization field [6]. In a CVO

with an initial domain structure the polarization reversal under application of the rectangular pulse series happens in three ways: (1) the growth of domains on the surface, as well as (2) the growth of domains completely in the volume and (3) the continuation of their growth after touching the polar surface.

Using statistical analysis of a sequence of instantaneous domains image, an “optical switching charge” was obtained, corresponding to the time dependence of the total area of emerging domains on the surface. An abrupt increase in the switching charge was observed, each step of which corresponded to the appearance of new domains. In this case, the optical switching current, which is the time derivative of the optical switching charge, consisted of isolated pulses, which made it possible to analyze it in terms of Barkhausen pulses. The obtained data on the optical switching current were analyzed by the Korczak method. For the evolution of the field induced domain structure evolution, the values Hurst exponent is about 0.75 was determined, which indicates the persistent nature of the switching process with long-term trend preservation [7].

It was shown that the pulsed laser irradiation of a Mn:CVO sample by far infrared light absorbed in the surface layer led to formation of a twin structure in the irradiation zone induced by fast local surface heating [8]. The influence of twins on the domain structure has been revealed. The interaction of an existing domain wall with a twin led to the formation of a stripe domain of submicron width at the twin boundary. The shift of the domain walls induced by pulsed laser irradiation was also revealed in the irradiated zone. The wall shift dependence on the local curvature has been revealed. The shift was the most significant for the domain wall parts with maximum curvature. The light induced change of the domain structure was attributed to the action of the pyroelectric field appeared as a result of heating by pulsed laser radiation and subsequent cooling.

Volumetric domain generation in CVO was achieved through localized irradiation using near-infrared femtosecond laser pulses focused at a 500 μm depth within the sample. The irradiation was performed with pulse energies ranging from 0.6 to 2.7 μJ, with the irradiated areas arranged in either matrix or linear configurations. This treatment resulted in the formation of microtracks within the bulk material, accompanied by ferroelectric domains that enveloped these microtracks. A clear correlation was observed between the incident pulse energy and domain characteristics, with higher energy pulses producing proportionally longer domains.

In annealed samples, anomalous kinetics of domain structure evolution were visualized upon application of a series of field pulses [9], occurring in 4 stages: (1) Lateral motion of domain walls located in the volume, leading to the formation of a fresh CDW and the appearance of ledges, in the field. (2) Continuation of the appearance of ledges on the CDW and their growth toward the polar surface, in the field. (3) Complete reverse switching of unstable ledges that appeared far from the edge of a fresh CDW, without a field. (4) Lateral growth of stable ledges that reached the polar surface, in the field.

The research was made possible by Russian Science Foundation (Project № 24-12-00302). The equipment of the Ural Center for Shared Use “Modern nanotechnology” Ural Federal University (Reg.№ 2968) was used.

1. A.M. Glass, S.C. Abrahams, A.A. Ballman et al., *Ferroelectrics* **17**, 579 (1978).
2. P.S. Bechthold, J. Liebertz, *Optics Communications* **27**, 393 (1978).
3. I.S. Voronina, V.V. Voronov, E.E. Dunaeva, et al., *J. Crystal Growth* **555**, 125965 (2021).
4. E.V. Shishkina, E.D. Greshnyakov, P.S. Zelenovskiy, et al., *Ferroelectrics* **576**, 85 (2021).
5. E.V. Shishkina, V.V. Yuzhakov, M.S. Nebogatikov, et al., *Crystals* **11**(12), 1508 (2021).
6. E.V. Shishkina, M.A. Chuvakova, V.V. Yuzhakov, et al., *J. Appl. Phys.* **132**, 184101 (2022).
7. V.V. Yuzhakov, M.A. Chuvakova, E.V. Shishkina, et al., *Ferroelectrics* **604**, 99 (2023).
8. E.V. Shishkina, V.V. Yuzhakov, A.R. Akhmatkhanov, et al., *Ferroelectrics* **592**, 83 (2022).
9. V.V. Yuzhakov, M.A. Chuvakova, A.P. Turygin, et al., *Crystals* **15**(4), 315 (2025).

P21

Effect of Gd substitution on the structure, dielectric and magnetic properties of $BiFeO_3$

N.M.R. Alikhanov[1,2], S.A. Sadykov[1], Sh.P. Faradzhev[1], R.R. Gyulakhmedov[1], D.A. Dadagishiev[1]

[1]*Dagestan State University, 367000 Makhachkala, Russia*

[2]*H. Amirkhanov Institute of Physics, Daghestan Federal Research Center, Russian Academy of Sciences, 367000, Makhachkala, Russia*

alihanov.nariman@mail.ru

Bismuth ferrite (BFO) is a well-known multiferroic that simultaneously combines ferroelectricity and magnetism in a single phase at room temperature with extremely high ordering temperatures (Curie temperature T_C ~ 830°C and Neel temperature T_N ~ 370°C) [1-3]. However, there are a number of problems that limit their practical application: weak ferroelectric characteristics and magnetic properties, and therefore low magnetoelectric coupling. In addition, the high leakage current density associated with this material due to the formation of oxygen ion vacancies and the existence of different oxidation states of Fe ions makes it difficult to use in practical device applications, especially in data storage devices. The most effective methods for solving these problems are considered to be cation substitution, which involves replacing Bi with ions of various elements, including rare earth elements. In this work, we selected gadolinium Gd^{3+} ions as dopants in the Bi^{3+} site.

A series of Gd^{3+} doped nanopowders with the composition formula $Bi_{1-x}Gd_xFeO_3$ (x = 0, 0.05, 0.1, 0.15, 0.2) was synthesized using the combustion method [4]. The diffractograms of nanopowders of the $Bi_{1-x}Gd_xFeO_3$ system are presented in Figure 1. The phase analysis results indicated the presence of a minor phase (less than 5%), namely $Bi_2Fe_4O_9$. It was found that the substitution of bismuth with gadolinium led to distortion and shift of diffraction peaks towards higher angle values, which indicates a transformation of the crystal lattice due to the smaller ionic radius of gadolinium (Gd – 1.053 Å, Bi – 1.17 Å).

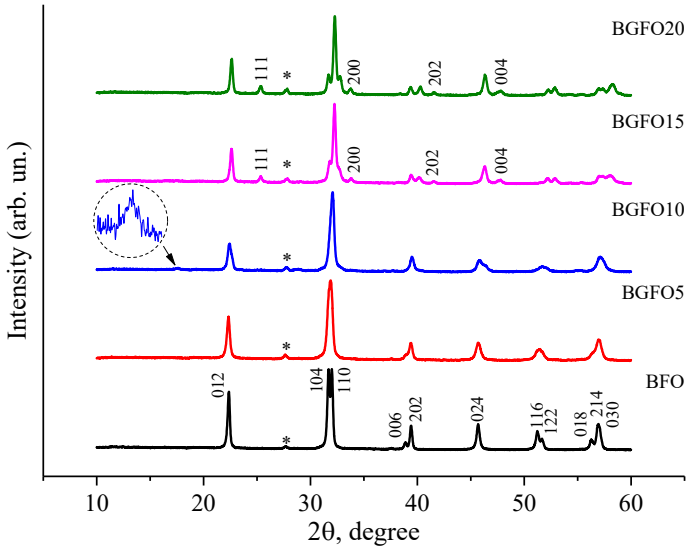

Figure 1. Diffraction patterns of the $Bi_{1-x}Gd_xFeO_3$.

Figure 2 a-b shows the frequency dependences of dielectric constant (ε') and dielectric loss (tanδ) for the original BFO and doped samples measured at room temperature. As figure shows, the Gd^{3+}-modified ceramics do not unambiguously show an increase in dielectric performance with increasing doping degree, although it reflects the active role played by the dopant in modifying the dielectric behavior. A significant dielectric dispersion is observed at low frequencies, whereas in the high frequency region the values of ε' and tanδ remain almost constant, which is a characteristic feature of polar dielectrics. In all compositions (ε') is maximum at low frequencies due to interfacial polarization of Maxwell-Wagner type.

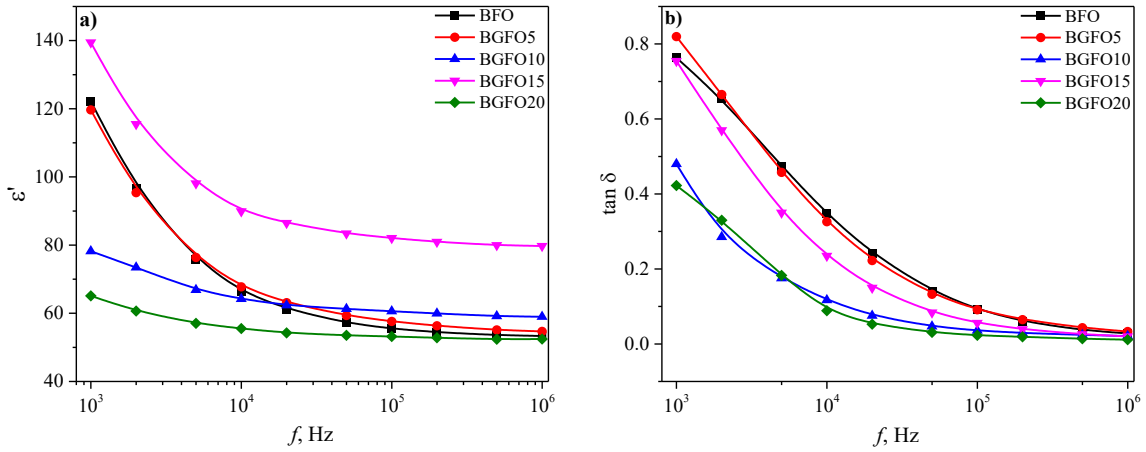

Figure 2. Frequency dependences of ε' (a) and tanδ (b) of $Bi_{1-x}Gd_xFeO_3$.

Among the studied compositions, BGFO15 demonstrates the highest values of ε' at room temperature. The BGFO10 and BGFO20 compositions have lower ε' values than BFO. It is also worth noting that the substituted samples have lower values of tanδ losses relative to the initial composition. The improved dielectric properties of BGFO15 ceramics can be due to the presence of morphotropic phase boundaries between the polar rhombohedral R3c and non-polar orthorhombic Pnma phases. It is noted that BGFO10 and BGFO20 exhibit weak frequency dispersion in the low-frequency region relative to other compositions, i.e. they exhibit frequency stability over the entire frequency range.

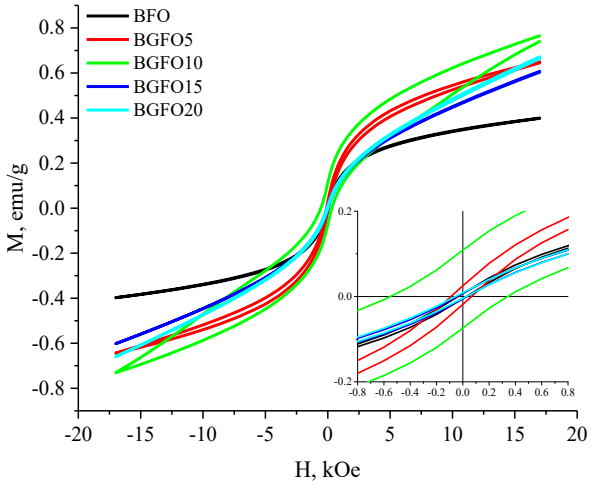

Figure 3. Magnetic hysteresis loops (M-H) of $Bi_{1-x}Gd_xFeO_3$.

Magnetic hysteresis loops for the initial $BiFeO_3$ and gadolinium-doped $BiFeO_3$ at a maximum magnetic field of 17 kOe are shown in Figure 3. All samples exhibit a clear ferromagnetic character. Substitution of gadolinium for bismuth results in an increase in the values of Ms, Mr, and Hc up to x = 0.1, and then a decrease with increasing Gd concentration. The highest observed values are obtained for a sample described by a two-phase system (R3c+Pbam) with a morphotropic phase boundary (MPB) at a Gd content of x = 0.1. Additionally, at this concentration of the dopant, a wasp-waist hysteresis loop is observed.

This study was funded by the Russian Science Foundation (RSF) under project No. 24-22-00416.

1. S. Sharma, J.M. Siqueiros, O.R. Herrera, *J. Alloys Compd.* **853**, 156979 (2021).
2. S. Sharma, C.F. Sánchez Valdés, et al., *J. Mater. Chem. C* **13**, 9138 (2025).
3. J.C. Yang, Q. He, P. Yu, Y.H. Chu, *Annu. Rev. Mater. Res.* **45**, 249 (2015).
4. N.M.R. Alikhanov, M.K. Rabadanov, et al., *J. Mater. Sci. Mater. Electron.* **32**, 13323 (2021).

P22

Comparison of electron transport properties of bulk and rapid melt quenched $(Cu_{(1-x)}Co_x)_2MnAl$ ($0 \le x \le 1$) Heusler alloys

Yu.A. Perevozchikova[1], A.V. Protasov[1], A.A. Semiannikova[1], E.D. Chernov[1], V.Yu. Irkhin[1], A.V. Korolev[1], V.N. Neverov[1], A.V. Lukoyanov[1,2], E.B. Marchenkova[1], V.V. Marchenkov[1,2]

[1]*M.N. Mikheev Institute of Metal Physics UB RAS, 620108 Yekaterinburg, Russia*
yu.perevozchikova@imp.uran.ru

[2]*Ural Federal University, 620062 Yekaterinburg, Russia*

An actual task of modern physics of magnetic phenomena, condensed matter and materials science is the search and comprehensive study of the structural, electronic transport, magnetic and other characteristics of new materials for their use in spintronics, micro- and nanoelectronics. Half-metallic ferromagnets are considered to be one of the most promising materials, since they have a unique electronic structure depending on the spin direction: the presence of a gap (for spin "down") or its absence (for spin "up") is observed at the Fermi energy level [1-2]. This feature can lead to 100% spin polarization of charge carriers. The Heusler alloy Co_2MnAl is half-metallic ferromagnet [3]. Another alloy Cu_2MnAl is prototype for typical Heusler compounds with «ideal» ferromagnetic properties with local moment [4-6]. Both Co_2MnAl and Cu_2MnAl have high Curie temperatures (higher than room temperature), which is important for spintronics devices. It is also known that for practical application a combination of certain electrical and magnetic properties is necessary, which can be achieved by changing the chemical composition of the material and/or its microstructure (for example, with rapid melt quenching). In this work we study electron transport properties of Heusler compounds $(Cu_{(1-x)}Co_x)_2MnAl$ ($0 \le x \le 1$) with a change in their chemical composition and microstructure during the transition from the usual ferromagnetic state of Cu_2MnAl to the state of the half-metallic ferromagnet Co_2MnAl.

Bulk Cu_2MnAl, $Cu_{1.5}Co_{0.5}MnAl$, $CuCoMnAl$, $Co_{1.5}Cu_{0.5}MnAl$, and Co_2MnAl alloys were melted in an induction furnace and then annealed at 1073 K in an argon atmosphere for 72 h, followed by cooling to room temperature. Melt-spun ribbons were fabricated from alloy pieces (weight 3-4 g) in alundum crucibles by induction melting in an argon atmosphere then poured onto the quenching copper drum with the linear velocity of 22 m/s.

The electrical resistivity was measured using the standard four-contact method from 78 K to 350 K. The magnetization and Hall resistivity were investigated at $T = 4.2$ K and magnetic fields up to 50 kOe.

The alloys studied are ferromagnetic. It was revealed that the electrical resistivity of all the alloys has a metallic type and increases when replacing Cu with Co. Dependences of the normal Hall coefficient R_0 and spontaneous magnetization M_s on x correlate to a sufficient degree with each other. The concentration of current carriers is typical for metals. The results obtained are useful in selecting suitable materials for spintronics.

The research was supported by Russian Science Foundation (project No. 25-22-00481, https://rscf.ru/en/project/25-22-00481/, IMP UB RAS, Sverdlovsk region).

1. R.A. de Groot, et al., *Phys. Rev. Lett.* **50**, 2024 (1983).
2. V.Yu. Irkhin, M.I. Katsnel'son, *Phys.-Usp.* **37**, 659 (1994).
3. N.I. Kourov, et al., *Phys. Solid State* **57**, 700 (2015).
4. T. Graf, et al., *Prog. Solid State Chem.* **39**, 1 (2011).
5. X. Liu, et al., *Phys. Rev. B* **108**, 094405 (2023).
6. A. Hamzic, et al., *J. Phys. F: Metal Phys.* **11**, 1441 (1981).

P23

Enhancement of the magnetocaloric effect in the room temperature region in alloys of the GdTSi type

S.P. Platonov[1], A.G. Kuchin[1], R.D. Mukhachev[1], A.V. Lukoyanov[1,2], A.S. Volegov[1,3], V.S. Gaviko[1,3], M.Yu. Yakovleva[1]

[1]*M.N. Mikheev Institute of Metal Physics UB RAS, 620108 Ekaterinburg, Russia*
platonov@imp.uran.ru

[2]*Institute of Physics and Technology, Ural Federal University, 620002 Ekaterinburg, Russia*

[3]*Institute of Natural Sciences and Mathematics, Ural Federal University, 620002 Ekaterinburg, Russia*

Rare earth R intermetallics of the RTSi type, T=Fe [1], Mn [2] are of interest as possible working materials in environmentally friendly and highly economical magnetic refrigerators. In this work, the compounds $GdMn_{1-x}V_xSi$, x=0-0.4 and $GdMn_{1-x}Cr_xSi$, x=0-0.6 were synthesized by the arc melting method.

The Curie temperature T_C (the temperature of magnetic ordering of the 3*d* subsystem) in these compounds changes differently with decreasing manganese content: it decreases from 320 to 305 K for $GdMn_{1-x}Cr_xSi$ and increases from 320 to 365 K for $GdMn_{1-x}V_xSi$. The sublattices of 3*d* and Gd ions are magnetically ordered in the compounds mutually independently, and their ordering temperatures have opposite patterns of change with composition, so they converge in $GdMn_{1-x}Cr_xSi$ and diverge in $GdMn_{1-x}V_xSi$ with a decrease in the manganese content. Due to the change in the temperatures of magnetic ordering of the 3*d* and Gd subsystems towards each other, for compositions x=0.2-0.6 of $GdMn_{1-x}Cr_xSi$ compounds coincide or are close. As a result, the changes in magnetic entropy $-\Delta S_M(T)$ for two magnetic phase transitions in these compositions are summed up and form a single peak, the half-width δT of which decreases exponentially as the Mn content decreases (Figure 1). This single peak value of the MCE is approximately twice as large as the MCE for compositions x=0, 0.1, for which two maxima are observed on the temperature dependence of the MCE(T). Our theoretical DFT+U calculations confirmed the mutually independent magnetic ordering of the 3*d* and Gd subsystems and the magnetic state of the Cr and V ions.

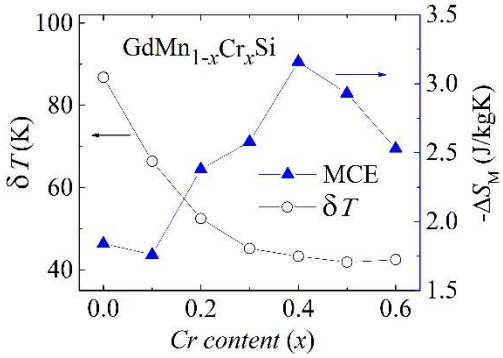

Figure 1. Concentration dependences of the peak change in magnetic entropy $-\Delta S_M$ (T_C) and half-width δT of the peak $-\Delta S_M$ (T) for the $GdMn_{1-x}Cr_xSi$ system, x=0-0.6.

The $GdMn_{0.6}Cr_{0.4}Si$ compound is promising for use in household magnetic refrigerators, since it has a magnetocaloric effect of 3.2 J/kgK and a relative cooling power of 106.8 J/kg with a magnetic field change of 0-17 kOe and a Curie temperature of 310 K, close to room temperature. The MCE at T_C for $GdMn_{1-x}V_xSi$ is almost constant and changes in a narrow range from 1.8 J/kgK to 2 J/kgK for x=0-0.4, although usually doping the alloy and increasing its T_C leads to a drop in the MCE. As a result, the total half-width of all MCE(T) peaks in the $GdMn_{1-x}V_xSi$ system varies over a wide range of 300–380 K.

This study was supported by the grant of Russian Science Foundation No. 24-22-00066, https://rscf.ru/en/project/24-22-00066/.

1. M. Guel-Rodríguez, J. Zamora, et al., *J. Alloys Compd*. **978**, 173452 (2024).
2. S.P. Platonov, A.G. Kuchin, et al., *Physica B: Condensed Matter* **685**, 416060 (2024).

P24

Dielectric and acoustic responses of KNN-based ceramics with $BaTiO_3$ additive

S.R. Al Saedi, A.V. Sopit, L.V. Zhoga

Volgograd State Technical University, 400074 Volgograd, Russia
sandrej74@mail.ru

The low-frequency dielectric and acoustic responses of ferroelectric ceramics $(K_{0.5}Na_{0.5})(Nb_{0.93}Sb_{0.07})O_3$–x$BaTiO_3$+0.5mol.%$MnO_2$ ($KNNS_7$–xBT), where x = 0 – 4 mol.%, were studied in a wide temperature range. The samples were manufactured by solid-phase synthesis [1], had a thickness of 0.50 mm with silver electrodes obtained by burning a silver-containing paste. The dielectric parameters were measured by the bridge method in weak sinusoidal fields. The resonance method was used to measure the acoustic parameters: velocity - υ and absorption coefficient - α of the longitudinal acoustic wave. The aim of the work was to study the effect of $BaTiO_3$ additive on the dielectric and elastic properties of ferroelectric ceramics based on $KNNS_7$.

Figure 1 shows that in the temperature range of 20÷150°C an anomaly is observed in the form of a sudden change in ε′(T) and ε″(T). Studies of acoustic properties (Fig. 2) showed that in the same temperature range, minima are observed on the V(T) dependences, which is a characteristic sign of the restructuring of the ferroelectric material and allows us to conclude that a structural phase transition (SPT) has occurred. It was revealed that the temperature of the SFP between the orthorhombic and tetragonal phases for $KNNS_7$-xBT samples shifts to the room temperature region with an increase in the concentration of $BaTiO_3$ additive.

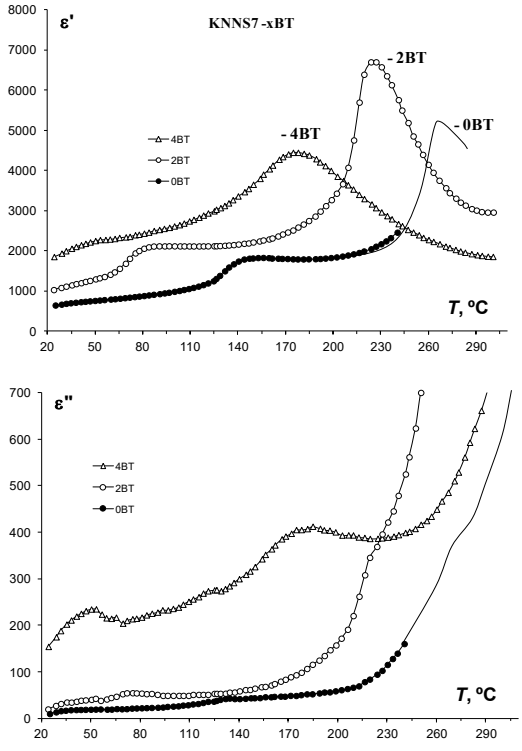

Figure 1. Temperature dependences of the dielectric constant – a) and dielectric losses – b), obtained in the heating and cooling mode in the SFP region at a frequency of 1000 Hz for KNNS7-xBT ceramics.

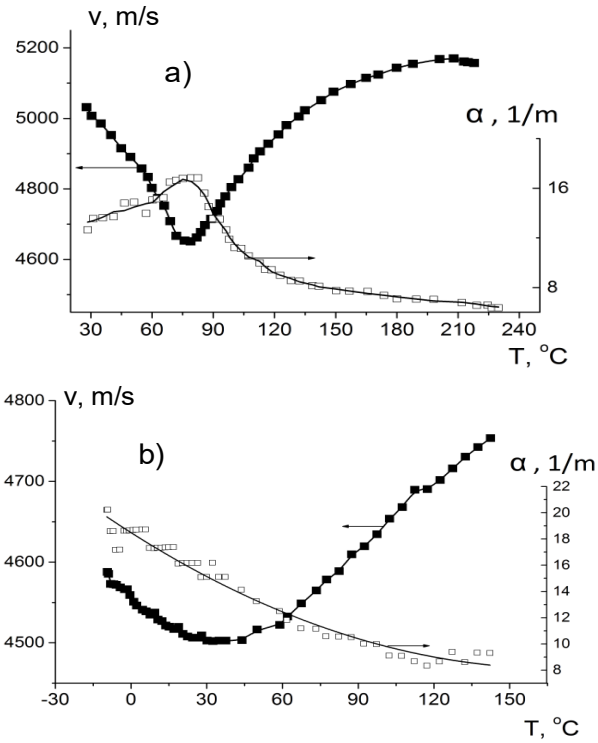

Figure 2. Temperature dependences of the velocity and absorption coefficient of a longitudinal sound wave for the compositions: KNNS7-2BT – a); KNNS7-4BT – b).

1. I. Smeltere, *Summary of the doctoral thesis* (Riga: RTU), 27 (2012).

P25

Effect of barium titanate addition on the photoelectric response of KNN-based ceramics

S.R. Al Saedi, A.V. Sopit, L.V. Zhoga

Volgograd State Technical University, 400074 Volgograd, Russia
sandrej74@mail.ru

Ferroelectric solid solutions based on potassium sodium niobates (KNN) are promising alternatives to lead-containing materials. The investigation of the photosensitive characteristics of lead-free ferroelectric ceramics based on potassium niobate (KNN) is a promising direction in the search for materials that can be used in the development of non-volatile memory devices that using non-destructive readout techniques [1].

The aim of the present work is to study the effect of $BaTiO_3$ additives on the behavior of photoresponse in short-circuited KNN-based ferroceramic samples when illuminated with light at room temperature.

The studies were carried out on polycrystalline ceramic samples of KNN-based with different concentrations of barium titanate $(1-x)(K_{0.5}Na_{0.5})(Nb_{0.93}Sb_{0.07})O_3–xBaTiO_3$+0.5mol.%$MnO_2$ (KNNS7–xBT, where x = 0; 2 and 4 mol%) [2] for the form of plate 0,5 mm thick with silver electrodes obtained by burning a silver-containing paste. The method of measuring the photocurrent is described in [3].

From the behavior of the curves (Fig. 1) it is evident that an increase in relatively small concentrations of barium titanate (BT) leads to a significant increase in the photocurrent, both in the transition region and in the steady-state current region. When the light is turned off, the current drops to zero, which is typical for ferroelectric materials [4].

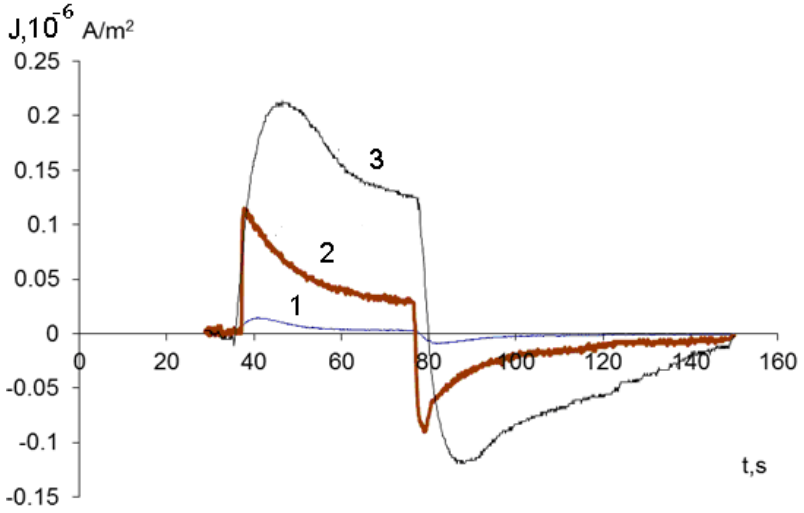

Figure 1. Photocurrent density kinetics of the KNNS7-xBT ferroelectric ceramics at room temperature. Curves: 1 – x = 0, 2 – x = 2 and 3 – x = 4 mol.%.

Analysis of the obtained results indicates that the magnitude of the photocurrent is largely determined by the dielectric properties and, in particular, the remanent polarization, which at room temperature increases with increasing concentration of the $BaTiO_3$ additive.

1. R.M. Magomadov, *Avtoref. dr. f.-m. sciences: 01.04.07.* (Grozny), 25 (2014).
2. I. Smeltere, *Summary of the doctoral thesis* (Riga: RTU), 27 (2012).
3. V.K. Yarmarkin, *Phys. Solid State* **42**(3), 511 (2000).
4. V.M. Fridkin, *Photosegnetoelectrics.* Moscow: Nauka, 264 (1979).

P26

Control of wettability of contacts of sensor elements obtained by deposition of Mo by the SAID method

A.I. Turavets, S.M. Baraishuk

Belarusian State Agrarian Technical University, 220012 Minsk, Belarus
bear_s@rambler.ru

The development and creation of integrated gas sensors is a currently relevant task. This task is especially important in the analysis of gas environments used for storing and transporting products and monitoring the premises where packages are filled with such environments. Such developments are especially relevant in the context of active import substitution. As shown earlier [1], not only thermal stability and sensitivity but also wettability are important for the surface of a gas sensor. In our work, thin films of molybdenum disilicide were obtained by deposition of a metal coating accompanied by irradiation with ions of the same metal [2].

Ion bombardment during the coating process under ion-assisted conditions ensures mutual mixing at the metal/silicon interface. This method of forming a coating on silicon is accompanied by silicide formation. The ratio of the ion flux density to the neutral flux density J_i/J_A was from 0.02 to 0.09 in experiments with Mo, which corresponded to the conditions for coating growth on the substrate. The ion current density varied between 50 and 100 mA/cm^2. The pressure in the vacuum chamber during coating deposition was ~10^{-3} Pa, and the coating deposition rate in different experiments was ~0.16 ÷ 0.45 nm/min. The topography and roughness were studied using AFM. Wettability was estimated from the equilibrium contact angle of water with subsequent modeling of the droplet position [3].

The initial surface had an average roughness of 2.2 nm. The application of Mo coatings led to a change in the topography. At the initial stages (flux of 1.2 10^{16} ion/cm^2), the coating was formed in the form of islands (56.9% of the area). With an increase in the flux to 5.2 10^{16} ion/cm^2, the roughness reached a maximum (2.71 nm), after which it decreased to 2.3 nm. Rare columns 22 nm high, consisting of molybdenum disilicide, were found [1].

In this case, the wettability of the surface changed. The wettability of the initial back contact is 25.1°. When measuring the equilibrium contact angle of wetting the surface of the samples with distilled water, it was found that the application of a Mo-containing coating makes the surface less hydrophilic: the equilibrium contact angle increased to 56.7°–67.4°. In addition, the ECA of the "substrate" is lower than the wetting angle of the "coating". An increase in the wetting angle by 2.45-2.77 times is observed when applying a thin Mo film to glass. The change in the wetting angle has a qualitatively similar dependence with the change in the roughness value. In this case, the dependence of the equilibrium wetting angle on the integral ion flux qualitatively coincided with the change in roughness. Such wettability behavior is in good agreement with the Wenzel model [4], which considers the roughness and heterogeneity of the surface. Modification of the glass surface by applying a coating containing Mo with different integral flows allows controlling the wettability of its surface with water. The real contact angle Θ can be calculated on such a surface as a function of such parameters as the average roughness, the relative difference in heights, the proportional ratio of the free surface energy of the original surface and growing islands (with the observed island mechanism of thin-film coating growth). As well as the contact angle of wetting with water for an ideally smooth surface, established for these contacting solids and liquids.

The paper demonstrates the possibility of controlling the surface properties (wettability) of sensor elements using ion-assisted deposition of Mo coatings. In this case, a thin film of molybdenum disilicide can be formed on the surface, which has both functional and protective properties. The results obtained are important for the development of technologies for the production of thin-film sensor elements on a single silicon chip. The work was supported by the Ministry of Education RB project No. 20211250.

1. S.M. Baraishuk, et al., *SN of the Physics Faculty of MSU* **1**, 2410601 (2024).
2. I.S. Tashlykov, I.M. Belyj, Coating methods: patent BY 2324 (1998).
3. Huang, Hei Lin, *Bulletin of Science and Education* **8**(20), 5 (2016).
4. R.N. Wenzel, *Ind. Eng. Chem.* **28**(8), 988 (1936).

P27

Electromechanical effects in freestanding piezoelectric membranes

A.A. Chouprik, E.A. Guberna, S.V. Ilyev

Moscow Institute of Physics and Technology, 141700 Dolgoprudny, Russia
chouprik.aa@mipt.ru

Ferroelectric HfO_2 thin films have emerged as viable candidates for nonvolatile ferroelectric memories, because of their full compatibility with the modern silicon microelectronics technology [1]. Development of high-performance ferroelectric non-volatile memory devices is the mainstream in the field of ferroelectric HfO_2; however, exploiting the related piezoelectric properties in the piezoelectric devices is another obvious direction. Since high-quality conformal ultra-thin HfO_2 films could be grown by atomic layer deposition technique even on three-dimensional structures, it becomes possible to develop flexible piezoelectric devices with new promising designs exploiting either direct or converse piezoelectric effect, e.g. mechanical energy harvesters, self-contained power supplies as well as transducers, oscillators etc. In general, those expectations have not been met yet. The challenge arose from very small piezoelectric coefficients of hafnium oxide, which are several tens or hundreds of times less than coefficients of classical materials used in modern piezoelectric devices. Improving the relatively small piezoelectric effect in this material and elucidating its potential in complex geometry devices would open new perspectives in the field of piezoelectric devices.

Recently, we demonstrated a giant electromechanical effect in miniature piezoelectric thin-film membrane devices based on 10-nm thick ferroelectric $Hf_{0.5}Zr_{0.5}O_2$ (HZO) film [2]. Compared to the pure piezoelectric effect, the gain of the electromechanical response reaches 25 times, which is related to the asymmetrical shape of membrane. In this work, we exploit the potential of ultra-flexible bridge membranes (Fig. 1) to elucidate two fundamental questions – the effect of substrate flexibility on the piezo- and ferroelectric properties of HZO films and the capability of the atomic force microscope to study flexible three-dimensional piezoelectric devices. On the one hand, comparing the remanent polarization and the domain structure acquired with band-excitation piezoresponse force microscopy (PFM), it was found that the polarization decreases with increasing membrane flexibility and this is accompanied by a prominent increase in domain size. Numerical calculations indicate that this effect is caused by the smaller contribution of mechanical stress during crystallization annealing. The membranes induce a proximity effect on the domain structure of neighboring regions of the HZO film on the rigid substrate. The size of the domains gradually decreases with distance from the membrane. In the case of fully switched polarization, shear electromechanical deformations exceed longitudinal ones two times, which indicates the promising application in devices based on the shear piezoeffect. On the other hand, it has been shown that under certain conditions the domain structure of vertical membrane walls can be studied with the PFM. The PFM results are greatly influenced by the stiffness ratio of the membrane and the cantilever. To measure the electromechanical response, the cantilever must be significantly softer than the membrane, whereas when the stiffness ratio is close, it is possible to measure the spatial distribution of membranes stiffness by analyzing contact resonance frequency maps.

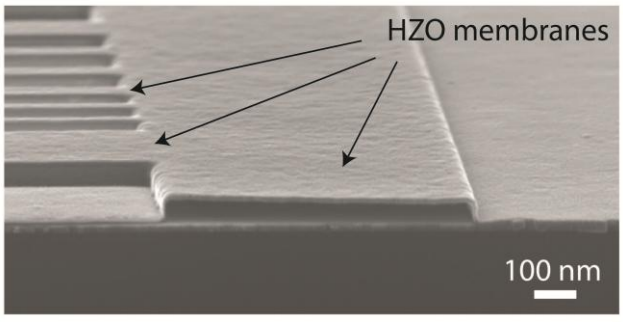

Figure 1. Scanning electron microscopy images of piezoelectric membranes.

The results can be useful for the development of micro-electromechanical systems (MEMS) devices based on conformal piezoelectric films.

The work was supported by the Russian Science Foundation (Project No. 25-19-00493).

1. T.S. Böscke, J. Müller, D. Brauhaus, U. Schröder, U. Böttger, *Appl. Phys. Lett.* **99**, 102903 (2011).

2. E. Guberna, I. Margolin, E. Kalika, S. Zarubin, M. Zhuk, A. Chouprik, *ACS Appl. Mater. Interfaces* **16**, 975 (2024).

P28

Influence of prehistory on the character of reversing dielectric permittivity in cobalt-containing ferroelectric ceramics (1-x)$Ba_{0.95}Pb_{0.05}TiO_3$+xCo_2O_3

S.R. Al Saedi[2], R.V. Dikov[1], L.V. Zhoga[2], A.V. Sopit[2]

[1]*Volgograd State Socio-Pedagogical University, 400001 Volgograd, Russia*
romanodc@yandex.ru

[2]*Volgograd State Tecnical University, 400074 Volgograd, Russia*

In this work, the reversible dielectric constant in cobalt-containing ferroelectric ceramics is studied. Ferroelectric ceramic samples were prepared from high-frequency oxides using traditional two-stage solid-phase synthesis technology. Measurements of the dielectric response on plane-parallel samples of size S = 15 mm^2 (coated with silver electrodes) and thickness d = 0.5 mm were carried out using a bridge method device in a weak alternating field with a frequency of 1 kHz and with a stepwise supply constant bias field $E_=$ with a step 1 kV/cm.

Figure 1 illustrates the reversible dependences for ferroelectric ceramic composition with cobalt oxide concentration x = 0.3 wt%. It was found that during the reverse run of ε'($E_=$) (curve 5, Fig. 1a) at bias fields higher than coercive fields $E_= > E_c$, an anomaly in the form of a kink occurs. It was revealed that during long-term exposure, without external influences, a unipolar state of the sample is formed and the anomaly is transformed into a local minimum (curve 5, Fig. 1b). The causes of the indicated anomalies in the behavior of ε'($E_=$) are discussed from the point of view of the effect on the dielectric response of internal bias fields arising during aging of the material.

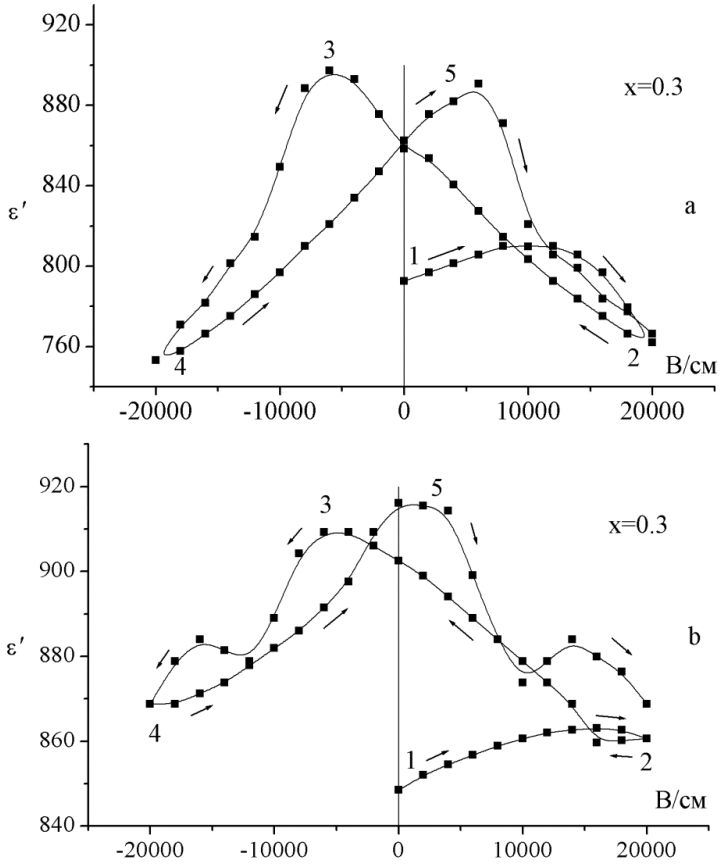

Figure 1. Reversive dependences of $\varepsilon'(E_=)$ in (1−x)$Ba_{0.95}Pb_{0.05}TiO_3$+xCo_2O_3 compounds at T = 25°C.

P29

Effect of top electrode grain size on the remanent polarization of ferroelectric capacitors

S.V. Ilyev, I.A. Mutaev, M.V. Spiridonov, A.A. Chouprik

Moscow Institute of Physics and Technology (National Research University), 141700 Dolgoprudny, Russia
ilev.sv@phystech.edu

Thin ferroelectric films of doped hafnium oxide are considered as a promising material for the development of next-generation non-volatile memory [1]. The advantages of this material include perfect compatibility with modern silicon technology and a high scaling potential down to nanometer thicknesses while retaining remanent polarization. Hafnium oxide is a polymorphic material. Initially, films deposited by atomic layer deposition (ALD) are amorphous, and a subsequent annealing step is required for crystallization. The stable structural phase is the non-polar monoclinic phase. At high temperatures, phase transitions occur into tetragonal and cubic structural phases. These phases are non-polar but serve as parent phases for the polar orthorhombic $Pca2_1$ phase. The orthorhombic phase is metastable, and its stabilization efficiency depends on several factors: film thickness, electrode and substrate materials, annealing temperature and duration, as well as the type and concentration of dopants. To date, there is no comprehensive understanding of the roles all structural and technological parameters play in determining the ferroelectric properties of this material.

This study demonstrates that the macro- and microscopic properties of 10 nm-thick $Hf_{0.5}Zr_{0.5}O_2$ films strongly depend on the grain size of the memory cell electrodes. The relationship between remanent polarization and domain structure has been investigated. Four types of functional Si/W/$Hf_{0.5}Zr_{0.5}O_2$/Pt structures were fabricated, differing only in the sputtering rate of the Pt top electrode deposited by pulsed laser deposition. The technological process was as follows: the bottom W electrode was deposited on a silicon substrate using magnetron sputtering, $Hf_{0.5}Zr_{0.5}O_2$ was grown by ALD, and the top Pt electrode was deposited using pulsed laser deposition. To stabilize the polar orthorhombic phase, rapid thermal annealing was performed for 30 seconds at 550 °C in an Ar atmosphere.

The *P-V* hysteresis curves were measured using the PUND (positive-up negative-down) method with a Keysight B1500A semiconductor device analyzer. The domain structure transformation during polarization switching was studied using in situ band-excitation piezoresponse force microscopy with resonance frequency autotuning, implemented on an NT-MDT Ntegra atomic force microscope [2]. Grain analysis was performed using a JEOL JSM 7001F scanning electron microscope.

At the highest Pt atom energy during deposition of the top electrode film, large grains (~150 nm) and large domains in $Hf_{0.5}Zr_{0.5}O_2$ (200–300 nm) were observed, resulting in a maximum remanent polarization of 22 μC/cm². At the lowest energy, small grains (~10 nm) and small domains (20–50 nm) were observed, with a remanent polarization of 13 μC/cm². At the initial stage of memory cell operation, domain pinning during polarization switching was observed, further reducing remanent polarization. At intermediate energies, intermediate grain sizes, domain sizes, and polarization values were observed. The presumed mechanism of Pt grain size influence is the variation in the length of grain boundaries, which are permeable to oxygen atoms, and consequently, different oxygen vacancy densities in $Hf_{0.5}Zr_{0.5}O_2$. It is well known that a high density of oxygen vacancies promotes the stabilization of the orthorhombic phase in hafnium oxide.

The results indicate the possibility of engineering the functional properties of $Hf_{0.5}Zr_{0.5}O_2$ ferroelectric memory cells by optimizing the technological process of top electrode fabrication.

This work was supported by the Russian Science Foundation (Project No. 25-19-00493).

1. T.S. Böscke, J. Müller, D. Brauhaus, et al., *Applied Physics Letters* **99**(10), 102903 (2011).

2. M. Spiridonov, A. Chouprik, V. Mikheev, A.M Markeev, D. Negrov, *Microscopy and Microanalysis* **27**(2), 326 (2021).

P30

Magnetic inhomogeneities in Fe_3Al epitaxial thin films probed by FMR and time-resolved magnetooptics

A.Kh. Kadikova[1], A.V. Petrov[1], Kh.Sh.A. Taqi [1], B.F. Gabbasov[1], A.I. Gumarov[1], I.V. Yanilkin[1], L.R. Tagirov[1,2], R.V. Yusupov[1]

[1]*Institute of Physics, Kazan Federal University, 420008 Kazan, Russia*
anelyakadikova11@gmail.com

[2]*Zavoisky Physical-Technical Institute, FRC Kazan Scientific Center of RAS, 420029 Kazan, Russia*

Spintronics is currently one of the most promising and rapidly developing fields of microelectronics. All spintronic elements are based on magnetically ordered materials — ferro-, ferri-, and antiferromagnets. One of the most critical requirements for the magnetic materials used is their high magnetic homogeneity and weak magnetization precession damping.

The Fe_3Al system, despite its long history of research [1–5], remains a relevant subject for studying magnetic properties. The significant interest in this compound stems from the variety of crystal structures that form near the stoichiometric ratio Fe:Al = 3:1. This structural diversity leads to a range of magnetic properties. For example, the saturation magnetization of the A2 phase — a disordered solid solution of Al in α-Fe — is higher than that of the B2 phase (an ordered solid solution). This fact is an exception to the general rule for magnetic alloys undergoing ordering. The influence of magnetic homogeneity is discussed in [6], where the authors investigated A2-B2 antiphase boundaries in Fe-Al thin-film systems.

This paper presents the results of magnetic inhomogeneity studies in thin epitaxial Fe_3Al films on MgO (001) substrates using ferromagnetic resonance (FMR) and time-resolved magnetooptical spectroscopy, demonstrating the complementary character of these techniques. It is shown that the magnetic homogeneity of the films strongly depends on their composition and synthesis conditions, which is reflected in the frequency spectrum and magnetization precession damping. We found that Fe_3Al thin-film systems tend to exhibit island-like morphology, regardless of synthesis conditions. No formation of an ordered $D0_3$ phase was observed after short annealing (no more than one hour).

The Gilbert damping constant was estimated to be $\alpha = (2.84 \pm 0.17) \times 10^{-2}$ for a magnetically homogeneous $Fe_{70}Al_{30}$ thin film with a thickness of 20 nm. This value corresponds to the constant typical of Fe_3Al in the disordered A2 phase [4]. Nearly all synthesized thin-film systems exhibit two FMR lines in their spectra, consistent with time-resolved magneto-optical measurements. For example, $Fe_{75}Al_{25}$ and $Fe_{70}Al_{30}$ thin films deposited at room temperature and annealed in vacuum at 450°C are magnetically inhomogeneous, as evidenced by at least two or even three frequency components in the magnetization precession and its rapid damping. $Fe_{75}Al_{25}$ films synthesized at a substrate temperature of 400°C exhibit both low-frequency (3–6 GHz) and high-frequency (18–19 GHz) precession components in a 0.3 T field applied along the normal direction. The latter is associated with either of the precession of magnetization in multiple magnetic phases within the Fe_3Al films, the coupled precession of magnetic domains, or both simultaneously.

1. C.G. McKamey, J.H. DeVan, P.F. Tortorelli, V.K. Sikka, *J. Mater. Res.* **6**(8), 1779 (1991).
2. D.A. Smith, A. Rai, Y. Lim, et al., *Phys. Rev. Appl.* **14**, 3 (2020).
3. H.Y. Yasuda, T. Nakajima, K. Nakano, K. Yamaoka, M. Ueda, Y. Umakoshi, *Acta Materialia* **53** (20), 5343 (2005).
4. Y. Wei, W. Zhang, B. Lv, X. Xu, S. Xi, Z. Ma, *Sci. Adv.* **7**, 4 (2021).
5. C. van der Rest, V. Dupont, J.P. Erauw, P.J. Jacques, *Intermetallics* **125**, 106890 (2020).
6. Y. Murakami, K. Niitsu, T. Tanigaki, R. Kainuma, H.S. Park, D. Shindo, *Nature Comm.* **5**, 4133 (2014).

P31

The abnormally high thermoelectric response in thin-film structures based on Strontium-Barium Niobate

A.M. Pugachev, A.A. Sokolov

Institute of Automation and Electrometry, RAS, 630090 Novosibirsk, Russia
apg@iae.nsk.su

It was found that films of barium-strontium niobate ($Sr_xBa_{1-x}Nb_2O_6$,) obtained by RF sputtering on a silicon substrate with platinum electrodes demonstrate an abnormally high thermoelectric response. The response in such films is two orders of magnitude greater than the pyroelectric response in crystals.

SBN films grown with RF spattering both on a layer of indium tin oxide (ITO) and platinum, evaporated onto a silicon substrate. The samples were made in the Institute of Automation and Electrometry Siberian Branch of the Russian Academy of Sciences and in the Rzhanov Institute of Semiconductor Physics Siberian Branch of the Russian Academy of Sciences. In this work, we used such a slow modulation of the heat flux (0.1 Hz) that the sample was warmed up uniformly in depth and, accordingly, the pyroelectric response of the system was affected only by the average pyroelectric coefficient in the thickness of the sample.

To identify the nature of the thermal response, a pre-blackened electrode was irradiated with light pulses with steep fronts. The pulses were obtained by modulation of laser radiation with rectangular electric pulses using an ML 102 electro-optical modulator.

The pyroelectric response was recorded in relatively thick (1.5 μm) polarized SBN 0.5 films. A characteristic feature of the pyroelectric response was observed - a shift in the current signal relative to the thermal periodic excitation by a quarter of the period. A similar shift was observed in relatively thick films. The current response was also typical of the pyroelectric effect – positive and negative transient processes during rapid heating and cooling. The pyroelectric coefficient was close to the value obtained for crystals ($\sim 6\times10^{-4}$ C/m$^2\cdot$°K)). Unlike relatively thick films, the thermal response on a series of thin films (near 500 nm) did not have the properties typical of the pyroelectric effect – the current pulses repeated the time shape of the rectangular excitation pulse and did not have a typical transient process, and in the “slow” experiment the current response did not shift in phase. The amplitude of the current response exceeded the corresponding response by two orders of magnitude. And the structure itself generated a constant electric voltage in the absence of illumination, like a thermocouple. A possible interpretation of this effect may lie in the presence of specific barriers on the “film – electrode” interface. The mechanism of this phenomenon requires further research and clarification.

This work was supported by Russian Science Foundation (Grant No. 25-22-20030).

P32

Time dependence of coercive voltages of FeRAM cell based on $Hf_{0.5}Zr_{0.5}O_2$

A.A. Shcherbakov, E.B. Kalika, V.V. Mikheev, A.A. Chouprik

Moscow Institute of Physics and Technology (National Research University), 141701 Dolgoprudny, Russia
artemashch@yandex.ru

Ferroelectric nonvolatile memory based on hafnium oxide nanolayers has plenty of advantages, such as high speed, low power consumption, and record endurance [1-3]. However, it also has a significant disadvantage that prevents the commercialization of this technology and brings it to the level of industrial production, specifically, the limited time of information storage. This is caused by a gradual increase in the coercive voltage (so called *imprint effect*), which causes read failure after a certain time. In addition, the real-life scenarios of a memory cell are much-more complex than a simple write-store-read cycle. Coercive voltages evolve over the whole lifetime of the memory cell and read failure can occur in subsequent stages.

In this work, we propose a predictive model for calculating the evolution of coercive voltages under any scenario of memory-cell lifetime [4]. In particular, it takes into account multiple write-store-read-rewrite (both to the same state and to the opposite state) cycles, temperature fluctuations to which the memory chip is inevitably subjected, the influence of the selected operating frequency, and the procedure for recovery of the memory cell after its aging by a series of bipolar pulses, which is considered by memory designers as one of the options for increasing the retention time. The model is based on the polarization-switching dynamics described by the Landau-Khalatnikov equation and the imprint effect [5] described by the advanced imprint model of Tagantsev et al [5]. The imprint model is based on the *dead layer* concept. It consists in the idea that a dielectric layer is formed at the interface between the ferroelectric and the electrode, thus separating the polarization charge in the ferroelectric and the free electrons on the electrode interface. This separation induces a strong electric field in the dielectric layer, under the influence of which electrons pass through it and get captured by traps at the interface. The imprint model of Tagantsev et al has been refined, since it has several significant drawbacks. Firstly, the model [5] was developed only for cases in which no voltage is applied to the ferroelectric capacitor, i.e., it only considers charge injection during storage and does not consider into account injection during read and rewrite procedures, which can be significant at low operating frequencies and high operating voltages. Secondly, the original model does not take into account the change of polarization during the charge injection process, while its contribution to the total electric field in ferroelectrics is large. Thirdly, it assumes unlimited charge injection, which is not realistic. The proposed model allows to calculate the coercive voltage evolution not only during the storage process at any operating voltage, frequency and temperature, but also during the process of structure recovery by a series of bipolar pulses. The influence of parameters such as the thickness and dielectric constant of the dead layer on the charge injection and emission process at delay and polarization switching, as well as on the shape of the *P-V* curve and frequency characteristics, has been investigated. Simulation of several real-life scenarios of the ferroelectric $Hf_{0.5}Zr_{0.5}O_2$-based capacitors and comparison of an appropriate experimental data with the simulation results were also carried out.

The work was supported by the Ministry of Science and Higher Education (Agreement № 075-03-2025-662, Project FSMG-2025-0025).

1. T.S. Boscke, J. Muller, D. Brauhaus, U. Schroder, U. Bottger, *Appl. Phys. Lett.* **99**, 102903 (2011).

2. T. Francois, L. Grenouillet, J. Coignus, P. Blaise, C. Carabasse, N. Vaxelaire, T. Magis, F. Aussenac, V. Loup, C. Pellissier, *In IEDM Tech. Dig.*, 15.7.1 (2019).

3. J. Okuno, T. Kunihiro, K. Konishi, M. Materano, T. Ali, K. Kuehnel, K. Seidel, T. Mikolajick, U. Schroeder, M. Tsukamoto, T. Umebayashi, *IEEE J. Electron Devices Soc.* **10**, 29 (2022).

4. A. Shcherbakov, E. Kalika, V. Mikheev, A. Chouprik, *Phys. Rev. Appl.* **22**, 064083 (2024).

5. K. Tagantsev, I. Stolichnov, N. Setter, J.S. Cross, *J. Appl. Phys*. **96**, 6616 (2004).

P33

Micro-structure and polarization reversal in PVDF-TrFE films

V.V. Yuzhakov[1], V.S. Shubin[1], D.O. Alikin[1], A.D. Ushakov[1], M.V. Silibin[2], A.V. Sysa[2,3]

[1]*School of Natural Sciences and Mathematics, Ural Federal University, 620000 Ekaterinburg, Russia denis.alikin@urfu.ru*

[2]*Institute of Advanced Materials and Technologies, National Research University of Electronic Technology, 124498 Zelenograd, Moscow, Russia*

[3]*Scientific-Manufacturing Complex «Technological Centre», 124498 Zelenograd, Moscow, Russia*

Ferroelectric polymers such as poly(vinylidene fluoride) (PVDF) and its copolymer with trifluoroethylene, P(VDF-TrFE), exhibit remarkable mechanical flexibility, strong dielectric properties, and pronounced piezoelectricity, making them highly suitable for applications in miniaturized capacitors, high-performance actuators, and contact switches [1,2]. Although the polarization mechanisms of PVDF-based materials have been extensively studied, the dynamics of domain structures and their role in polarization reversal – critical for optimizing ferroelectric and piezoelectric performance – remain insufficiently understood.

In this work, we examine P(VDF-TrFE) films with a VDF/TrFE molar ratio of 70/30, synthesized via polymerization from a dimethylsulfoxide/acetone solution. Two film variants were prepared: one subjected to pre-polarization via corona discharge ("corona poling") [3] and another analyzed in its as-deposited state. Chromium top electrodes were subsequently deposited by magnetron sputtering. Comparative studies of phase composition, ferroelectric hysteresis loops, domain structures, and piezoelectric responses were conducted under identical conditions. Notably, the corona-poled film exhibited a substantially enhanced piezoresponse, underscoring the efficiency of corona poling in optimizing the piezoelectric performance of P(VDF-TrFE). To elucidate the origin of these macroscopic differences, we analyzed domain configurations and local piezoelectric behavior using piezoresponse force microscopy.

Furthermore, we evaluate the influence of the bias field, revealing its reduced magnitude in pre-polarized samples. This effect is attributed to defect redistribution during thermal cycling and charge injection during polarization, which collectively modify the internal electric field distribution.

The research funding from the Ministry of Science and Higher Education of the Russian Federation (Ural Federal University Program of Development within the Priority-2030 Program) is gratefully acknowledged. M.V. Silibin acknowledges the State assignment 2023-2025, number FSMR-2023-0003. The equipment of the Ural Center for Shared Use "Modern nanotechnology" Ural Federal University (Reg.№ 2968) was used.

1. N. Murayama, et al., *Ultrasonics* **14**, 1 (1976).
2. J. Belovickis, et al., *Phys. Status Solidi B* **255**, 1700196 (2018).
3.. R.A. Hill, et al., *Appl. Phys. Lett.* **65** (14), 1733 (1994).

P34

Effect of Er_2O_3 ceramic nanoparticles on the optical properties of PVDF membranes

T.S. Soliman[1,2], S.A. Vshivkov[1], Sh.I. Elkalashy[1,3]

[1]*Ural Federal University, 620000 Ekaterinburg, Russia*
tarek.attia@fsc.bu.edu.eg

[2]*Benha University, 13518 Benha, Egypt*

[3]*Egyptian Atomic Energy Authority, 13759 Cairo, Egypt*

Polyvinylidene fluoride (PVDF) is a well-known polymer recognized for its exceptional chemical stability, mechanical strength, heat resistance, piezoelectric properties, and flexibility. These characteristics have led to extensive research exploring their potential in various applications. PVDF is considered a viable alternative to ceramics due to its unique advantages, including its ability to easily form membranes, flexibility, lightweight nature, and durability. Composed of the repeating monomer unit $CH_2=CF_2$, PVDF is classified as a semicrystalline polymer and exists in five distinct forms: α, β, γ, δ, and ε.

Er_2O_3 is a thermally stable rare-earth oxide known for its excellent optical properties due to the electronic configurations of Er^{3+} ions and a wide bandgap of 5.4 eV. These characteristics make it suitable for lasers, optical amplifiers, and devices. Recently, Er_2O_3 nanoparticles have been incorporated into polyvinyl alcohol matrices to improve mechanical, electrical, and optical parameters. However, the effects of Er_2O_3 nanoparticles on linear and nonlinear optical properties and their impact on PVDF structure remain underexplored, revealing a research gap. This study aims to investigate the structural and optical characteristics of Er_2O_3-doped PVDF membranes, focusing on developing materials for flexible optoelectronics, which is crucial for advancing materials technology in applications requiring optical and mechanical flexibility.

PVDF was dissolved in dimethylformamide (DMF) and different concentrations of Er_2O_3 were added to the PVDF solution and distributed using a probe ultrasonic. The PVDF-Er_2O_3 films were obtained via the casting method. Then, the PVDF-Er_2O_3 films were characterized using an X-ray diffractometer (XRD) and Fourier transform infrared (FTIR) techniques. The PVDF-Er_2O_3 membranes' absorbance and transmittance data were determined using an ultraviolet-visible spectrophotometer.

The XRD and FTIR analyses confirmed that the concentration of Er_2O_3 in the PVDF membrane promotes the formation of the β-phase while suppressing the α-phase. Additionally, the optical properties of the PVDF membrane change following the enhancement of the β-phase. The UV-visible absorbance data were recorded for the Er_2O_3-doped PVDF membranes, allowing for the determination of the optical constants. The direct and indirect optical bandgaps for the pure PVDF membrane were found to be 5.44 eV and 4.58 eV, respectively, which decreased to 4.75 eV and 3.85 eV for the 8% Er_2O_3-doped PVDF membrane. The linear refractive index was calculated, showing an increase from 1.9371 for pure PVDF to 2.0386 for the 8% Er_2O_3-doped PVDF membranes. Moreover, the investigation of nonlinear optical constants – including first- and third-order optical susceptibility and nonlinear refractive index – revealed that an increase in Er_2O_3 concentration enhances the optical and structural properties of the PVDF matrix.

P35

Properties of annealed Ni thin films prepared by atomic layer deposition

V.A. Yakushev[1], A.S. Vishnevskiy[1], D.A. Abdullaev[2], K.A. Vorotilov[1]

[1]*MIREA - Russian Technological University (RTU MIREA), 119454 Moscow, Russia*

[2]*Institute of Nanotechnology of Microelectronics of the Russian Academy of Sciences (INME RAS), 119334 Moscow, Russia*

yakushev@mirea.ru

Over the past decade, nickel (Ni) thin films have attracted a great deal of attention due to their promising applications in electronics and related fields. One critical area of focus is the multilevel metallization systems for sub-3 nm integrated circuits. Scaling challenges require a reduction in the resistivity of nanoscale conductors. Nickel (Ni) is one of the candidates for use in advanced chips due to its low average electron free path length of 5.87 nm [1]. Additionally, nickel oxide films are highly attractive materials for various applications, including electrochromic devices, thin-film transistors, gas sensors, etc. [2]. Atomic layer deposition (ALD) is now the key method in semiconductor manufacturing technology because it can produce precise, nanometre-thick conformal coatings on structures with a high aspect ratio [3]. The mechanism of the film growth process is based on the sequential chemical reactions between the pulsed gas precursor and the substrate. In this case, impurities play an important role. Impurities in metal films can degrade their properties by being centers of dissipation of the charge flowing through them. These impurities can occur due to an incomplete chemical reaction or adsorption of a by-product. On the other hand, the nanometer scale of metal films, due to the dimensional effect and, therefore, an increased tendency to oxidation, complicates the assessment of their quality using traditional resistivity measurement method. These factors make it necessary to look for other methods of investigation of thin metal films.

The aim of this study is to investigate the physicochemical properties of vacuum- and air-annealed nickel (Ni) thin films produced using the atomic layer deposition (ALD) method. Nickel(II) acetylacetonate ($Ni(acac)_2$) and methanol were used as precursors to obtain the Ni films [4]. Deposition of 3000 cycles resulted in films with a thickness of ~60 nm. These films were then annealed in various atmospheres at different temperatures. The research methods used were FTIR, spectral ellipsometry, X-ray diffraction, and scanning electron microscopy.

It has been found that the ALD process using $Ni(acac)_2$ and methanol as precursors at a temperature of 300 °C can be used to deposit metallic Ni films with an average grain size ~ 9 nm. Annealing in either oxygen or a vacuum significantly reduces the amount of carbon impurities in the film. Specifically, annealing in oxygen at 800 °C leads to the formation of polycrystalline nickel oxide films with an average grain size ~ 56 nm.

This work was performed using the equipment of the Shared Science and Training Center for Collective Use RTU MIREA and was supported by the Ministry of Science and Higher Education of the Russian Federation within the framework of agreement No. 075-15-2021-689 dated 01.09.2021.

This work was supported by the Ministry of Science and Higher Education of the Russian Federation (project No. FSFZ-2023-0005).

1. D. Gall, *J. Appl. Phys.* **119**, 85101 (2016).

2. S.S. Narender, V.V.S. Varma, C.S. Srikar, J. Ruchitha, P.A. Varma, B.V.S. Praveen, *Chem. Eng. Technol.* **45**, 397 (2022).

3. J.A. Oke, T.C. Jen, *Int. J. Adv. Manuf. Technol.* **126**, 4811 (2023).

4. M. Sarr, N. Bahlawane, D. Arl, M. Dossot, E. McRae, D. Lenoble, *J. Phys. Chem. C* **118**, 23385 (2014).

P36

Diphenylalanine peptide nanotubes for bio-based optical and photonic applications

V.S. Bystrov[1], E.V. Paramonova[1], P.S. Zelenovskiy[2]

[1]*Institute of Mathematical Problems of Biology – branch of Keldysh Institute of Applied Mathematics, RAS, 142290 Pushchino, Moscow region, Russia*
vsbys@mail.ru

[2]*School of Natural Sciences and Mathematics, Ural Federal University, 620000 Ekaterinburg, Russia*

Bio-based nanomaterials are considered as a sustainable alternative for traditional quartz-based optical components due to their precise nanostructuring, unique optical properties, and eco-friendly nature [1]. Recently, peptide nanotubes (PNTs) made of diphenylalanine dipeptide (H-Phe-Phe-OH, FF) have attracted considerable interest as a basic element for various optical applications, including photosensors and photodetectors, due to their wide bandgap and non-linear optical properties combined with significant ferroelectric and piezoelectric activities [2,3]. Recently, we have studied photoelectronic properties of FF PNTs [4], which are important for their use in various photosensors and, particularly, as substrates for Surface-enhanced Raman spectroscopy (SERS) [5,6]. In this work, the use of FF PNTs as a SERS substrate and the polarization-dependent photodetectors is studied by computer modeling and semi-empirical quantum calculations.

For a system of interacting FF PNT and analyte molecules Methylene blue (MB) and Thymine, the calculations revealed significant changes in the total energy of the system Etot, energies of the HOMO and LUMO electronic levels, and the band gap Eg. For large distances between the PNT and MB molecules, it has been found that HOMO level is localized on the FF PNT, whereas it switches to the MB molecule at close distances. The accompanying change of Eg by c.a. 0.54 eV makes possible to detect MB molecules at FF PNT-based SERS substrate. The estimated enhancement of the SERS signal was found about 8 times, and the vibrational modes of the MB analyte molecule have been calculated. The band gap Eg of ~ 4 eV makes FF PNTs suitable for detecting light in the solar-blind ultraviolet range (SBUV) and thus for creating SBUV-sensors [4]. Additionally, Eg changes under an applied electric field [4], and thus can be finely tuned by the deposition on the ferroelectric polymers, such as PVDF-TrFE, which expands the capabilities of such sensors.

FF PNTs made of the dipeptides of different chirality, L-FF or D-FF, are capable for detection of linear and circularly polarized light (CPL), which is highly important for modern photonics. Such PNTs exhibit the circular dichroism (CD) of opposite signs and rotate the polarization plane in opposite directions [2,3]. The main question now, is how to realize a reverse motion and differentiate the polarization of the incident light wave with linear and CPL. CPL attracts considerable attention from the researchers due to its unique electromagnetic vector, which possesses potential practical applications in optical imaging, biometrics, and other interdisciplinary areas [7]. Currently, CPL detection is focused on various technical problems, such the combination of circularly polarized optical active materials with device structures to meet the detection needs [8]. All these issues are relevant and can be applied to such studies based on FF PNTs. This is a new promising direction of research in this important area of practical photonic application of the PNTs of the different chirality in the various area of the photonics.

1. S. Núñez-Sánchez, M. Lopez-Garcia, *Photoniques* **110**, 36 (2021).
2. P.S. Zelenovskiy, A.S. Nuraeva, S. Kopyl, et al., *Cryst. Growth Des.* **19**, 6414 (2019).
3. V. Bystrov, J. Coutinho, P. Zelenovskiy, et al., *Nanomaterials* **10**(10), 1999 (2020).
4. V. Bystrov, E. Paramonova, P. Zelenovskii, et.al., *Symmetry* **15**, 504 **(**2023).
5. X.X. Han, R.S. Rodriguez, C.L. Haynes, et al., *Nat. Rev. Methods Primers* **1**, 87 (2021).
6. S. Almohammed, A. Fularz, M.B. Kanoun, et al., *ACS Appl. Materials & Interfaces* **14**, 12504 (2022).
7. Y. Liu, P. Xing P. *Adv. Mater.* **35**, 2300968 (2023).
8. S. Wu, J. Deng, X. Wang, et al., *Nat. Commun.* **15**, 8743 (2024).

P37

Effect of oxygen plasma pretreatment on surface properties of lithium niobate and the proton exchange process

I.V. Petukhov, V.I. Kichigin, A.V. Sosunov, A.A. Kozlov, A.S. Yakimov

Perm State University, 614990 Perm, Russia
Petukhov-309@yandex.ru

Currently, lithium niobate crystals are one of the most widely used materials in integrated optics and optoelectronics due to their electro-optical and nonlinear optical properties. For manufacturing various integrated optical devices, the proton exchange method is used, which is usually carried out in a benzoic acid melt. Due to replacing of lithium by hydrogen ions in the surface layer of the crystal, planar and channel waveguides can be formed. The fabrication process of waveguides includes several technological operations, in which the lithium niobate surface can be subjected to various types of treatment, including oxygen plasma treatment.

In this work, the effect of oxygen plasma treatment of lithium niobate surface on the properties of the crystal surface and the proton exchange process was studied. Samples of lithium niobate (X-cut) produced by Fomos-materials (Russia) were used. Proton exchange was carried out at 190°C during 2 hours in a benzoic acid melt. Annealing was carried out in air at 370°C.

The oxygen plasma treatment of the samples was carried out on the ETNA-100PT plasma-chemical etching unit. The pressure in the chamber was equal to 1 mbar, inductor power was 80 W, the bias power on the sample was 110 W, the bias voltage on the sample was 71-72 V, the oxygen flow was 70 cm^3/min. The treatment duration varied in the range of 5-15 min.

Oxygen plasma treatment significantly slows down the proton exchange process. This results in a decrease in $\Delta n_e(0)$ (Table 1) and in a decrease in the intensity of the peaks of proton exchange phases. This follows from the results of IR spectroscopy and X-ray diffraction. Moreover, deformations caused by the formation of these phases were reduced.

Table 1. Increment of the refractive index on the waveguide surface $\Delta n_e(0)$ and the waveguide depth (δ) without and with oxygen plasma pretreatment of the surface.

Treatment	Annealing, h	$\Delta n_e(0)$	δ, μm
-	-	0.1135	1.50
	6	0.0289	7.15
Oxygen plasma	-	0.1077	1.38
	6	0.0229	7.82

It can be assumed that a possible reason for the slowdown in proton exchange is the deterioration of wetting of the lithium niobate surface by the benzoic acid melt after plasma treatment. However, measurements of the contact angle of wetting (Kruss DCF 25 E tensiometer) of the lithium niobate surface in air (130°C) with molten benzoic acid showed that wetting does not deteriorate significantly – slight increase from 8.9±1.1 to 11.4±1.4°.

The change in surface composition was more significant. XPS results indicate that plasma treatment leads to the decrease in surface oxygen content. The concentration of niobium on the surface also decreases and the concentration of lithium ions increases. In this case, the decrease in niobium concentration is approximately two times less than the decrease in oxygen concentration, and the total increase in lithium concentration approximately corresponds to the decrease in oxygen concentration. Increasing the duration of plasma treatment leads to even more pronounced changes in concentration on the crystal surface.

It can be assumed that oxygen plasma treatment knocks out oxygen ions from the surface. Removing oxygen from the surface can lead to the formation of oxygen vacancies, which are positively charged. Calculations show that the probable sites of adsorption of benzoic acid molecules are oxygen ions, the concentration of which decreases as a result of treatment. Benzoic acid in the melt is predominantly in a non-dissociated state [1, 2]. Also, an increase in the concentration of lithium ions on the surface of the crystal reduces the concentration of lithium vacancies, which suppresses the dissociative adsorption of benzoic acid molecules and the transition of protons to the subsurface layer of the crystal. Measurement of the contact angles using standard liquids (water, glycerol, dimethyl sulfoxide) and subsequent processing of the obtained results [3] showed that exposure to oxygen plasma causes a decrease in the basic component and an increase in the acidic component of the polar component of the surface energy. This should prevent the adsorption of benzoic acid on the surface of lithium niobate via the hydrogen atom, which causes inhibition of proton exchange.

Thus, in contrast to the effect of argon plasma, which enhances the process of proton exchange in a thin surface layer due to a significant increase in the concentration of defects in it [4], treatment with oxygen plasma inhibits the process of proton exchange due to the suppressing dissociative adsorption of benzoic acid and the transition of protons into the crystal lattice of lithium niobate.

This work was funded by Ministry of Education and Science of the Perm Region, Grant number C-26/37. X-Ray photoelectron spectroscopy measurements of the Ural Center for Shared Use “Modern nanotechnology” UrFU were used.

1. V.I. Kichigin, I.V. Petukhov, S.S. Mushinsky, V.I. Karmanov, D.I. Shevtsov, *Rus. J. Appl. Chem.* **84**, 2060 (2011).

2. V.I. Kichigin, I.V. Petukhov, A.R. Kornilicyn, S.S. Mushinsky, *Condensed Matter and Interphases* **24**(3), 315 (2022).

3. I.A. Starostina, O.V. Stoyanov, N.V. Makhrova, R.Y. Deberdeev, *Doklady Physical Chemistry* **436**, 8 (2011).

4. A.V. Sosunov, I.V. Petukhov, V.I. Kichigin, R.S. Ponomarev, A.A. Mololkin, M. Kuneva, *Ferroelectrics* **618**(5), 1300 (2024).

P38

Oxygen plasma surface-activated lithium niobate for controlling protons diffusion rate

D.N. Masalkin[1], A.V. Sosunov[1], I.V. Petukhov[1], A.A. Kozlov[1], A.R. Kornilicyn[1], M. Kuneva[2]

[1]*Perm State University, 614990 Perm, Russia*
masdn@mail.ru

[2]*Bulgarian Academy of Sciences, 1784 Sofia, Bulgaria*

Lithium niobate (LN) is widely used in the field of photonics and microelectronics. LN is a ferroelectric with high spontaneous polarization, the surfaces of which have a huge and largely unexplored potential [1]. Thin films of LN exhibit remarkable application potential and have attracted significant interest from scientists across various disciplines [2]. Therefore, surface and surface activation/modification play a significant role in technological operations.

The aim of the present research is to study the activation of the LN surface by O_2-plasma and its effect on proton diffusion.

Intensity of the niobium strongly depends on chamber pressure, unlike oxygen. The maximal decrease in Nb occurs at a chamber pressure of 0.1 mbar. The peak at ≈3500 cm^{-1} related to the absorption of OH groups in LN. Surface activation by O_2-plasma and subsequent direct proton exchange (PE) in LN leads to a change in the OH group spectral maximum and in the O─O band at 1747 cm^{-1}. The results are identical for both pristine LN and the LN treated in O_2-plasma at pressure 1.0 mbar. At an O_2-plasma pressure of 0.1 mbar, the intensity of the peak at 1747 cm^{-1} increases, and the intensity of the OH peak is minimal. This means an increase in the oxygen concentration on the LN surface. At a pressure of 0.01 mbar, an intermediate value is observed. The decrease in the integral intensity of the OH groups band is related to the decrease in proton concentration and hence, to the lattice deformations.

The diffusion coefficients were calculated from experimental data on the depth of substitution of Li^+ ions for protons H^+, depending on the plasma activation of the surface of LN. When the pressure decreases from 1.0 to 0.1 mbar, the diffusion coefficient jumps sharply to almost double and decreases slightly at 0.01 mbar.

The structural changes occurring during PE in O_2-plasma surface-activated LN crystals were studied by XRD. From the obtained values of ε and refractive index n_e, the phase composition was determined according to the structure-phase diagram for LN. It is found that surface activation leads to a decrease in lattice deformations. Typical direct PE leads to the simultaneous formation of highly strained and disordered β_1 and β_1 phases. The β_2 phase is characterized by the presence of interstitial protons, which makes such structures very unstable. However, activation of the LN surface leads to the formation of a less stressed, intermediate $\varkappa_2$-phase.

Also, it was found that a higher diffusion coefficient and a decrease in elastic deformations also lead to a sharp decrease in the refractive index on the LN surface during PE at the transition pressure from 1.0 to 0.1 mbar.

Proton diffusion coefficient is highly sensitive to the relation [Nb/O] on the surface. Surface activation is accompanied by a decrease in lattice deformations after PE. Li vacancies do not significantly affect the PE process. For the first time, it was possible to form an intermediate $\varkappa_2$-phase by direct PE at low temperatures. The first explanation of the adsorption of benzoic acid on the surface of LN has been proposed. There is a high potential for application of surface activation in thin-film technology. It provides a tool for building a “lab on chip” based on LN and an ability to control the etching rate of thin films.

This work was funded by Ministry of Education and Science of the Perm Region № С-26/37.

1. S. Sanna, W.G. Schmidt, *J. Phys. Condens. Matter* **29**, 413001 (2017).

2. A. Boes, L. Chang, M. Yu, C. Langrock, M. Yu, M. Zhang, Q. Lin, M. Loncar, M. Fejer, J. Bowers, A. Mitchell, *Science* **379**, eabj4396 (2023).

P39

Perovskite films in solar cells

E.D. Greshnyakov, V.Ya. Shur

School of Natural Sciences and Mathematics, Ural Federal University, 620000 Ekaterinburg, Russia
evgeny.greshnyakov@urfu.ru

Solar radiation occupies a leading position in electricity generation among alternative energy sources. Traditionally used silicon-based solar cells have an energy conversion efficiency of up to 30%, however, their large-scale application is constrained by the high cost of production. Photovoltaic devices that convert sunlight into electricity are an integral part of solar cell production technologies. Thus, the development of new cost-effective photovoltaic devices is of significant interest to industry.

Since the end of the first decade of the 21st century, research into photovoltaic cells for converting solar radiation into energy based on perovskites, compounds with a pseudocubic structure and the general formula ABX_3, has been rapidly growing. The most promising areas include organic photovoltaics and thin film technologies, which are distinguished by their availability and ease of production.

High efficiency of separation and movement of charge carriers in hybrid halide perovskites allows creating a new class of solar cells. Research in this direction of change shows that devices containing polycrystalline light-harvesting components of hybrid halide perovskites increase the energy conversion efficiency to 26.3% [1]. A tandem of perovskite compounds with silicon wafers provides the achieved energy conversion efficiency at the level of 33.89% [2].

However, hybrid perovskites are quite sensitive to oxygen, humidity, intense illumination and high temperature, which negatively affects their stability, and at the same time leads to their short service life in solar cells compared to silicon analogues. Modern research is aimed at finding ways to increase the service life of hybrid halide perovskites.

An important task is to study the influence of domain structure on the photovoltaic properties of hybrid halides perovskites. There is currently a discussion about the nature of the emergence of domain structure in hybrid halides perovskites.

Currently, there is a discussion about the nature of the emergence of the domain structure in hybrid halides perovskites. Both ferroelectric and ferroelastic nature of the emergence of the domain structure are reported. This review is devoted to the study of domain structure in perovskite materials used in solar cells.

1. Y. Yang, H. Chen, C. Liu, et al., *Science* **386**, 898 (2024).
2. J. Liu, Y. He, L. Ding, et al., *Nature* **635**, 596 (2024).

P40

Growth in electric field of domain created by femtosecond laser irradiation in the bulk of SBN crystal

V.A. Shikhova[1], A.R. Akhmatkhanov[1], B.I. Lisjikh[1], M.S. Nebogatikov[1], L.I. Ivleva[2], V.Ya. Shur[1]

[1]*School of Natural Sciences and Mathematics, Ural Federal University, 620002 Ekaterinburg, Russia*
vera@urfu.ru

[2]*Prokhorov General Physics Institute, Russian Academy of Sciences, 119991 Moscow, Russia*

At the present time the focused near infrared (NIR) femtosecond laser irradiation is used for creation of the domain structures with a given geometry in the bulk of the ferroelectric crystals [1]. Moreover, the following switching of the laser induced domains by uniform pyroelectric field was used for creation of the through domain structures [2].

The evolution of the isolated domains created in the bulk by tightly focused NIR femtosecond laser irradiation was studied under the action of uniform electric field in strontium barium niobate ($Sr_{0.61}Ba_{0.39}Nb_2O_6$) single crystals doped by Ni (0.05 wt.% Ni_2O_3). The samples were cut with a deviation from the polar axis of about three degrees. The initial domain structure representing the matrix of domains in the bulk of the single domain sample was created in three steps: (1) thermal depolarization, (2) laser irradiation, (3) removing of the nanodomain structure. Cherenkov-type second harmonic generation microscopy has been used for domain imaging in the bulk of the crystals.

The matrix of the spindle-shaped domains surrounded by nanodomains was formed as a result of laser irradiation. Subsequent application of external homogeneous negative field pulse using liquid electrodes led to complete removing of the nanodomains. All created domains were strictly oriented along the direction of the laser beam. We could not detect any microtracks created by laser irradiation by optical microscopy methods. It was shown that the application of positive field pulse with amplitude above 180 V/mm led to growth of new domains from the deepest ends of the created domains in the matrix towards Z- polar surface. The new domains grew in the polar direction which deviates from the orientation of the laser induced domains.

The field dependence of the fraction of new domains that appeared in the matrix allowed to characterize the distribution of the threshold fields. Gaussian fitting of obtained data allowed us to extract the average threshold field about (215 ± 5) V/mm and the HWHM about (37 ± 3) V/mm. The field dependence of the growth velocity of new domains followed the linear law with the domain growth mobility $(5.7 \pm 0.3)\cdot 10^3$ μm^2/(s·V).

Thus, the domain with unique shape, which represents two united cylindrical parts was created in the SBN crystal bulk as a result of two subsequent procedures: (1) laser irradiation of the sample with nanodomain structure in the direction deviated from the polar direction and (2) application of the uniform external electric field after removing of nanodomains. The growth direction of the first domain part is governed by orientation of the laser beam and the second domain part - by orientation of the polar axis.

Obtained results are important for developing domain engineering methods in ferroelectrics based on domain nucleation by the focused NIR femtosecond laser irradiation and its growth under application of homogeneous electric field.

The research was made possible by Russian Science Foundation (Grant No. 24-12-00302). The equipment of the Ural Center for Shared Use “Modern nanotechnology” Ural Federal University (Reg. № 2968) was used.

1. Y. Sheng, X. Chen, T. Xu, S. Liu, R. Zhao, W. Krolikowski, *Photonics* **11** (5), 447 (2024).

2. B.I. Lisjikh, M.S. Kosobokov, A.V. Efimov, D.K. Kuznetsov, V.Ya. Shur, *Ferroelectrics* **604**, 46 (2023).